Nature vs. Nurture: Neuronal Diversification in the Olfactory Epithelium

A thesis submitted by

Julie Hewitt Coleman

In partial fulfillment of the requirements for the degree of

Doctor of Philosophy

in

Neuroscience

TUFTS UNIVERSITY

Sackler School of Graduate Biomedical Sciences

August 2016

ADVISOR: JAMES E. SCHWOB, M.D. PH.D.

ABSTRACT

Stem cells in the olfactory epithelium (OE) can completely regenerate the entire olfactory neuroepithelium in adult animals, representing a unique, robust system of adult neurogenesis. These stem cells are classified into two populations: multipotent horizontal basal cells (HBC_{MPPs}) – the quiescent, reserve stem population, and globose basal cells (GBCs) – the actively proliferating stem population. GBCs can be sub-classified into stages of progenitor capacity and neuronal commitment from multipotent progenitors (GBC_{MPPs}) to immediate neuronal precursors (GBC_{INPs}). During the transition from a GBC_{INP} to a mature olfactory sensory neuron (OSN), each neuron selects a single olfactory receptor (OR) allele for expression, out of over 1000 different OR genes.

Despite our knowledge of the basic cell-stage progression during neuronal maturation in the OE, little is known about stem cell plasticity in respect to the process of OSN diversification and OR gene selection. In this thesis work, through a series of transplantation experiments, I found that GBC progenitors are spatially plastic in respect to both olfactory receptors (ORs) and two regionally expressed neuronal markers, NADPH:quinone oxidoreductase (NQO1) and olfactory cell adhesion molecule (OCAM). These data demonstrate that spatial cues influence neuronal diversification in the OE.

To further describe OSN diversification, I characterized the effect of cell-stage specific loss of lysine specific demethylase 1 (LSD1). LSD1 is a prime candidate for OR gene regulation as it demethylates at both histone 3, lysine 4 (H3K4) and histone 3, lysine 9 (H3K9), each of which are found on the actively transcribed OR allele or the silenced OR alleles, respectively. I found that LSD1 is required for neuronal maturation during a distinct time window between activating HBC_{MPPs} and GBC_{INPs}.

Taken together, this thesis work clarifies the processes of neuronal maturation and diversification in the olfactory epithelium and advances our understanding of LSD1-dependent neuronal maturation and stem cell plasticity within the OE.

ACKNOWLEDGEMENTS

I must first and foremost thank my graduate thesis advisor, Jim Schwob. Jim has been an excellent mentor, providing me the correct balance of guidance and exploration in my scientific endeavors. He has been extremely supportive of my life both in and out of lab: if I described an experiment I wanted to do, Jim would find the resources; if I told him I needed to spend time with my family, he would agree. I am very grateful to have done my graduate studies under such a prominent leader in the olfactory field – the very field that drew me to graduate school.

I would also like to thank my thesis committee, Grace Gill, Brent Cochran, and Alan Kopin for their continued council, suggestions, and support. I am very thankful to them for assisting me through the twists and turns of graduate school. Thank you to my outside examiner and collaborator Bob Lane, for hosting me in your lab at the beginning of my graduate career, and for now coming to participate in the culmination of my graduate studies.

The work in this thesis could not have been done without the guidance and support of members of the Schwob lab. The staples of the lab, Woochan Jang and Eric Holbrook assisted me in learning the ropes; Po Tse has provided unparalleled support with cryosectioning; and past lab members, Nikolai Schnittke and Melissa Gilbert, taught me some of the most important techniques I used in the lab, including transplantations and *in situ* hybridizations. Lab members along the ride with me, Dan Herrick, Jesse Peterson, and Brian Lin, have provided scientific guidance and general camaraderie throughout our PhD experience. I am most thankful to Brian and Jesse for their continued enthusiasm, general support, and overall cheer and entertainment in the lab. I cannot imagine ever meeting someone as generous with their time and knowledge as Brian Lin; I will be forever grateful to have had him as a co-worker for the past 5 years. I am thankful to know that the lab will continue in excellence with four new graduate students: Kevin Child, Vera Gaun, Camila Barrios-Camacho, and Matt Zunitch. My advice to you: work hard, have fun, and please enjoy your PhDs! To the various MBS, MD, PREP, and summer students: we always enjoy meeting you, teaching you, and learning from you.

I must also thank many of the friends I've made in graduate school along the way: Jennifer Shih and Micaella Panessiti were fast friends – girls I knew I would be friends with the day we met. Bina Julian has been a constant support, always smiling and cheering me on. Recent friends through the Tufts Biomedical Business Club, Alex Taracanova and Jen Nwankwo are girls I can't believe I missed out on for 3 years. I have never met someone who believed in me and supported me as fast or as wholeheartedly as

Jen Nwankwo; for this, I am truly grateful.

Friends outside of graduate school helped to keep me cheery and distracted through the trenches of failed experiments; I am thankful for many chats, walks, dinners, and laughs with Holly Jacobson. I am thankful to Michaela Calnan for being an excellent roommate during my first two years of graduate school; the two hardest years when I adjusted to city living. I cannot begin to thank the group of friends who I've spent the most time with during these years, Andrew's highschool friends: Nate Semprebon, Nick Servidio, Ezra Tanzer, Dan Martin, and Blair Sullivan. Through laughs, music, games, and celebrations, I cannot imagine a better group of friends to have spent the past years with. I must also thank friends who supported me from afar: Hannah Peckler and Alexa Staley, for always inquiring about my studies, keeping me optimistic, and seeing the bigger picture.

And of course, there is my very best friend, my husband, Andrew Coleman. Andrew makes everything possible. He picks me up when I get low and reminds me that life, love, and science are about the journey, and, if we are in this journey together, we are inevitably happy. Andrew has supported me gracefully both in and outside of lab, loading qPCR plates for me, editing my thesis, and cooking me dinner. I cannot say enough about this humble, talented, caring man.

Lastly, I would like to thank my family: My sister for always being excited by science and genuinely caring about my thesis work; My mother for her unwavering love, support and guidance; And my father for instilling a love of science and curiosity in me that will carry on throughout my career. I dedicate this thesis work to my parents, in love and recognition for everything they have done for me.

TABLE OF CONTENTS

LIST OF TABLES

LIST OF FIGURES

LIST OF ABBREVIATIONS

CoREST	REST corepressor 1
$CreER^{T2}$	cre-estrogen receptor T2 fusion
DPI	days post injection
EdU	5-ethyl-2-deoyuridine
FACS	fluorescence-activated cell sorting
GAP43	growth-associated protein 43
GBC	globose basal cell
GFP	green fluorescent protein
H3K4	histone 3, lysine 4
H3K9	histone 3, lysine 9
HBC	horizontal basal cell
HDAC	histone deactylase
HDACi	histone deactylase inhibitor
INP	immediate neuronal precursor
ISH	*in situ* hybridization
K5	keratin 5
KO	knock out
LSD1	lysine specific demethylase 1
MeBr	methylbromide
MPP	multipotent progenitor
Neurog1	neurogenin 1
NQO1	NADPH:quinone oxidoreductase
OB	olfactory bulb
OBX	olfactory bulbectomy
OCAM	olfactory cell adhesion molecule
OE	olfactory epithelium
OMP	olfactory marker protein
OR	olfactory receptor
OSN	olfactory sensory neuron
pan-TdT	CAG-TdTomato mice
RA	retinoic acid
RALDH	retinaldehyde dehydrogenase
Sus	sustentacular cell
TAM	tamaxifen
TA-N	transit amplifying-neuronally committed
TdT	tandem dimer tomato

Chapter 1. Introduction

The Olfactory Epithelium and its Neurons

1.1 Introduction to the olfactory system

Humans detect and discriminate thousands of chemical odorants, each providing sensory information that can stimulate pleasing, aversive, and emotional responses (Pichon et al., 2015). In lower mammals, olfaction plays critical roles in suckling, scavenging, mating, and predator avoidance (Logan et al., 2012; Zou et al., 2015). Phylogenetically the oldest sensory system (Hoover, 2010), olfaction is crucial to nutrition and diet, and loss of smell has detrimental effects on both quality of life and survival (Pinto et al., 2014; Rawal et al., 2016).

To achieve its function in odorant discrimination, the olfactory system possesses two distinguishing properties: (1) its primary neurons are in direct contact with the external environment and (2) it has over 1000 different olfactory receptors (ORs) that distinctly bind different chemical odorants with varying affinities (Cuschieri and Bannister, 1975a; Buck and Axel, 1991; Saito et al., 2009). These two unique aspects of the olfactory system result in specific consequences and challenges:

(1) Because these neurons are exposed to the environment, they are vulnerable to toxins and subject to high rates of turnover; for this reason, the olfactory epithelium (OE) contains stem cells with the ability to regenerate neurons throughout adulthood (Moulton, 1974; Graziadei and Monti Graziadei, 1979).

(2) In a mastery of order, each olfactory sensory neuron (OSN) expresses only one OR allele out of ~2000, allowing for activation of OSNs by specific odorants (Buck and Axel, 1991; Shykind et al., 2004).

This thesis investigates the neurogenic potential of stem cells within the OE, and the processes of neuronal maturation and diversification in the adult mouse OE. In the following sections, I provide background on the cell types of the OE, take a closer look at the regeneration process – paying special attention to spatial patterning within the OE – and cover the research to-date on OR gene selection.

1.2 Structure and Cells of the Olfactory Epithelium

The olfactory epithelium (OE) lines the posterodorsal nasal septum and the tips, shafts, and cul-de-sacs of the nasal turbinates, located on either side of the medial septum (Figure 1). The winding structure of the turbinates allows for maximal exposure of the olfactory receptors (ORs) to the air. The epithelium itself is pseudo-stratified with apical supporting cells (sustentacular cells), a thick neuronal layer, and basal stem cells (Figure 2) (Cuschieri and Bannister, 1975a; Graziadei and Monti Graziadei, 1979).

To understand the olfactory sensory neurons (OSNs), we must understand the cells that give rise to these neurons, and those that surround and support them. Here, I will describe the cell types of the OE starting from the basal lamina and moving apically.

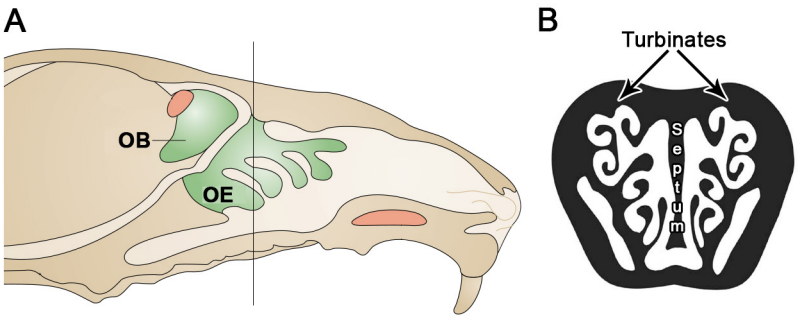

Figure 1. Basic Olfactory Anatomy
(A) Diagram of a sagittal cross-section of the mouse head. The olfactory epithelium (OE) is in the posterodorsal nasal cavity and neurons from the OE project to the olfactory bulb (OB). Components of the vomeronasal system are shown in red. (Adapted from Mombaerts, 2004) **(B)** Coronal cross-section (black line in A); the OE lines the two sets of turbinates and the medial septum. (Adapted from Harkema, Carey, & Wagner, 2006)

Basal Cells: Horizontal Basal Cells (HBCs) and Globose Basal Cells (GBCs)

There are two basal cell populations in the OE that are differentiated from one another based on morphological characteristics, cytokeratin and antibody staining, and progenitor capacity (Graziadei and Monti Graziadei, 1979; Schwartz Levey et al., 1991; Holbrook et al., 1995; Huard and Schwob, 1995). These basal cells are called horizontal basal cells (HBCs) and globose basal cells (GBCs) after their morphological appearance.

HBCs were originally identified as flattened, dark, and electron dense cells that lie directly atop the basal lamina (Figure 2A) (Cuschieri and Bannister, 1975a; Graziadei and Monti Graziadei, 1979). Further structural characterization revealed that HBCs adhere to the basal lamina via hemidesmosomes and that OSN axon bundles run between these hemidesmosomes, providing a possible context for HBCs and OSNs to signal to one another (Holbrook et al., 1995).

Early hypotheses posited that HBCs could be a stem cell population in the OE based on their morphology and location (Graziadei and Monti Graziadei, 1979). However, studies investigating the neurogenic potential of HBCs found that these cells remained quiescent following the removal of the olfactory bulb (bulbectomy or, OBX), whereas the adjacent globose basal cells (GBCs; discussed below) proliferated to replace the neurons that die as a result of OBX (Schwartz Levey et al., 1991). Nonetheless, many held on to the idea that HBCs could be a reserve stem cell population. The concept of reserve and active stem cells coexisting together has recently received much attention in the stem cell field and has proven to be the case in proliferative niches such as the hair follicle, the intestinal crypts, and the endosteum (Li and Clevers, 2010).

In the OE, the hypothesis that HBCs are a reserve stem cell population was eventually verified with the advent of genetic lineage tracing (Leung et al., 2007). Using a beta-galactosidase genetic lineage trace, Randall Reed's group demonstrated that HBCs can generate both neuronal and non-neuronal cells after harsh lesion to the OE that depletes both OSNs and non-neuronal cells (Leung et al., 2007). Further studies by our group demonstrated that transplanted activated-HBCs give rise to all cell types of the OE (Schnittke et al., 2015). It is now appreciated that HBCs are a quiescent, reserve stem-cell population in the OE activated to divide only upon severe injury (injury models are discussed in-depth in Section 1.3).

Immunohistochemically, HBCs express many typical basal cell markers including cytokeratins 5 and 14 (K5 and K14), intercellular adhesion molecule 1 (ICAM-1 or

CD54), the epidermal growth factor receptor (EGFR), the sugar moieties recognized by the lectin Bandeirea (Griffonia) simplicifolai-I (BS-1), and the transcription factors Sox2, Pax6 and p63 (Calof and Chikaraishi, 1989; Mahanthappa and Schwarting, 1993; Holbrook et al., 1995; Carter et al., 2004; Guo et al., 2010; Packard et al., 2011b).

GBCs are immediately apical to the HBCs and reside below (basal to) the immature neurons (Figure 2A). Generally, GBCs do not touch the basal lamina, although occasional contacts have been observed (Holbrook et al., 1995). GBCs were quickly characterized as stem/progenitor cells based on tritiated thymidine retention and mitotic activity (Moulton, 1974; Graziadei and Monti Graziadei, 1979; Hinds et al., 1984). Morphologically less complex than the HBCs, GBCs are small, electron-light, round cells (Cuschieri and Bannister, 1975a; Graziadei and Monti Graziadei, 1979).

Despite their morphological simplicity, GBCs are extremely heterogeneous and can be subdivided into distinct stages of multipotency and neuronal commitment based on the transcription factors they express – specifically, basic helix-loop-helix (bHLH) transcription factors. GBC-multipotent progenitors (GBC_{MPP}) express Sox2 and Pax6, GBC-transit-amplifying, neuronally fated progenitors ($GBC_{TA\text{-}N}$) express Ascl1 (a.k.a. Mash1), and GBC-immediate neuronal precursors (GBC_{INP}) express Neurogenin1 (Neurog1) and NeuroD1 (Gordon et al., 1995; Cau et al., 1997, 2002; Manglapus et al., 2004; Guo et al., 2010; Packard et al., 2011a). Additionally, the transcription factor Hes1 labels non-neuronally committed GBCs and may function against Ascl1 to form a bi-directional fate switch (Manglapus et al., 2004). All of these stages of GBCs can be mitotically active, labeling for Ki67 and PCNA. However, our lab recently characterized a subpopulation of label-retaining (LR) GBCs that express $p27^{Kip1}$, a cell-cycle arrest gene (Schwartz Levey et al., 1991; Guo et al., 2010; Jang et al., 2014). Following epithelial injury, all GBCs are Ki67 (+) suggesting that the LR-GBCs are activated in response to injury and that there is an additional quiescent stem cell population in addition to HBCs in the OE (Jang et al., 2014).

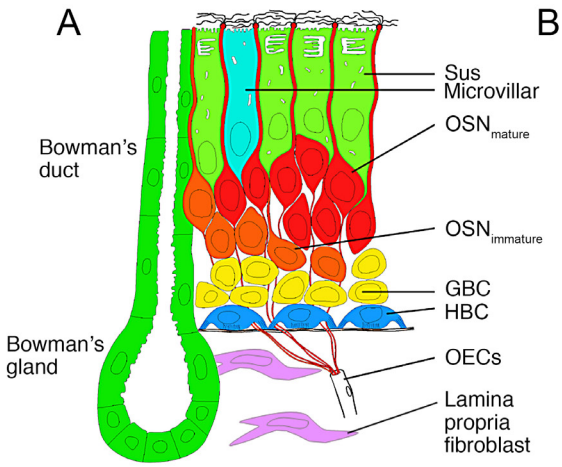

B

Primary Antibody	Cell Type
CK18	Sus cells
Sox9, ECAD	D/G cells
TrpM5	Microvillar cells
OMP	OSN mature
PGP9.5, Tuj1	OSN mature and immature
GAP43, NCAM	OSM immature
Neurogenenin, NeuroD1	GBC_{INP}
Ascl1/Mash1	GBC_{TA}
Sox2, Pax6	GBC_{MPP}
CK14, K5	HBCs
Thy1.2	LP Fibroblast
Hes5	OECs

Figure 2. Cell types of the OE
(A) From basal to apical: Horizontal basal cells (HBCs), globose basal cells (GBCs), immature olfactory sensory neurons (OSNs), mature OSNs, and sustentacular cells (Sus). Microvillar cells are interspersed between Sus cells and Bowman's duct/gland units span the entire epithelium. Below the basal lamina, olfactory ensheathing cells (OECs) insulate OSN axons. **(B)** Table of commonly used cell type markers.

Neurons: Immature and Mature Olfactory Sensory Neurons (OSNs)

The olfactory sensory neurons (OSNs) are the most populous cell type in the OE making up ~80% of the epithelium. Immature OSNs are located directly above the GBCs and mature OSNs are apical to the immature OSNs (Figure 2A). Morphologically, both immature and mature OSNs are bipolar with single dendrites that traverse between the apical sustentacular (Sus) cells (Figure 2A). Differentiating between the two, mature OSNs have extensive cilia that spread atop the Sus cells, whereas the immature neurons have not yet developed their cilia arborization (Cuschieri and Bannister, 1975a; Graziadei and Monti Graziadei, 1979; Verhaagen et al., 1989). Mature OSN dendritic cilia contain olfactory receptors (ORs) that are the functional site of odorant binding and are responsible for the initiation of odorant perception (Cuschieri and Bannister, 1975a; Firestein, 2001). To transmit this sensory information, OSN axons traverse the interstitial spaces between other OSNs, GBCs, and HBCs, trek through the basal lamina into the lamina propria where they coalesce with other axons and ultimately project through the cribriform plate to synapse with mitral and tufted cells at glomeruli in olfactory bulb

(Klenoff and Greer, 1998; Treloar et al., 2002; Mombaerts, 2006). From the olfactory bulb, mitral and tufted cells enter the lateral olfactory tract and project to several brain regions including the piriform cortex and the cortical amygdala (Haberly and Price, 1977; Sosulski et al., 2011).

Immature and mature OSNs can be differentiated from one another based on protein expression. Immature neurons express the growth associated protein-43 (GAP-43), neuron-specific beta-III tubulin (Tuj1, also known as TUBB3), protein gene product 9.5 (PGP9.5, also known as UCHL1), and neural cell adhesion molecule (NCAM) (Calof and Chikaraishi, 1989; Verhaagen et al., 1989; Roskams et al., 1998). Mature OSNs can also express Tuj1, NCAM, and PGP9.5 (albeit at lower levels) and exclusively express the olfactory marker protein (OMP), adenylyl cyclase-III (AdCy3), the olfactory-specific G-protein (G_{olf}) and other G-protein associated signaling molecules (Farbman and Marcolis, 1980; Jones and Reed, 1988; Bakalyar and Reed, 1990). In addition to these common OSN markers, certain proteins are expressed in neurons located in specific regions of the OE. For example, mature OSNs in the dorsomedial OE express the enzyme NADPH:quinone oxidoreductase (NQO1) and both immature and mature OSNs in the ventraolateral OE express the mammalian homologue of fasciclin II (mamFasII/OCAM/RNCAM/NCAM2) (Schwob and Gottlieb, 1986; Gussing and Bohm, 2004). Furthermore, ORs are expressed in patterns across the OE, a subject that is discussed in full detail in section 1.5 (Ressler et al., 1993; Vassar et al., 1993; Iwema et al., 2004). Importantly, ORs are abundantly expressed in mature OSNs and can be present at low levels in immature neurons (Iwema and Schwob, 2003; Magklara et al., 2011; Hanchate et al., 2015; Tan et al., 2015).

Supporting cells: Sustentacular (Sus) Cells and Microvillar Cells (MVCs)

Both Sus and MVCs are microvillar-capped cells with nuclei at the most apical cell layer of the epithelium (Figure 2A). These cells act as a buffer between the external

environment and the cell bodies of the OSNs, offering protection from harmful toxins. Much more is known about Sus cells than MVCs; however, characterizations of MVC populations are beginning to emerge.

Sus Cells can be distinguished based on their morphology: they are tall columnar epithelial cells with large nuclei at the apex of the OE, abundant smooth endoplasmic reticulum, a flat brush border of cilia at their apex, and thin foot processes that extend to the basal lamina, giving them an overall "goblet" shape (Morrison and Costanzo, 1990). Sus cells make a tight border at the apex of the OE, using cadherin junctions to protect OSNs, while still allowing dendrites to squeeze between the cells (Akins et al., 2007). In addition to physical protection and support, Sus cells have several enzymes that act to "detoxify" (metabolize) incoming toxins; these enzymes include members of the cytochrome-P450 family and glutathione S-transferases (Dahl et al., 1982; Banger et al., 1994; Thornton-Manning et al., 1997). Furthermore, Sus cells can be phagocytic during periods of acute or prolonged neuronal death (Suzuki et al., 1996).

Immunological identifiers of Sus cells include the structural molecules cytokeratins 8 and 18 (CK8/18) and E-cadherin, the transcription factors Sox2, Pax6, and Hes1, and the enzymes glutathioine S-transferase and cytochrome p450 (Dahl et al., 1982; Suzuki and Takeda, 1991; Banger et al., 1994; Thornton-Manning et al., 1997; Cau et al., 2000; Manglapus et al., 2004; Akins et al., 2007; Guo et al., 2010).

MVCs make up the second class of supporting cells in the OE. These cells differ structurally from Sus cells in that they (generally) have a microvillar "tuft" at their apex, have less smooth endoplasmic reticulum, and can have thick or thin foot processes that extend to the basal lamina. MVCs are interspersed between Sus cells (not abundantly; they make up ~5% of the cells in the OE) with slightly lower or higher nuclei than the surrounding Sus nuclei and are described as "flask shaped" (Miller et al., 1995; Asan and Drenckhahn, 2005; Hansen and Finger, 2008). There are no unifying markers of MVCs; instead, there appear to be several different subsets of MVCs based on the proteins they

express and their potential for electrical activity (Asan and Drenckhahn, 2005). Different subsets of MVCs have been found to express Ankyrin, CK18 and villin (Asan and Drenckhahn, 2005), Na+ and K+-ATPase (Asan and Drenckhahn, 2005), IP3 receptor type 3 (Hegg et al., 2010), and the TRPM5 channel and the ErbB3 receptor (Hansen and Finger, 2008; Gilbert et al., 2015). The function of varying MVC populations is an area of active research and falls outside the scope of this thesis.

Bowman's Duct and Gland Cells (D/G)

The Bowman's duct and gland cells are responsible for secreting mucopolysaccarides (mucous) onto the surface of the OE and are scattered throughout the epithelium. The gland is an acinar structure located beneath the basal membrane in the lamina propria (Figure 2A). Extending from the acinus are duct units, generally composed of 2-3 stacked cells connecting the gland to the apical surface of the OE; mucous and serous secreting cells are found in both the acinus and duct (Cuschieri and Bannister, 1974, 1975a). When secreted mucous reaches the surface of the OE via the ducts, it facilitates odor diffusion and provides an additional barrier from environmental toxins (Getchell and Getchell, 1991; Brittebo, 1997). In fact, the mucous contains several antibacterial and antimicrobial immune defense factors such as immunoglobulins, lactoferrin, and lysozymes (Getchell and Getchell, 1991).

It has been hypothesized that D/G cells have stem-cell characteristics; in harsh lesions of the OE, the D/G units can be the only surviving cells and have been shown to give rise to Sus cells (Schwob et al., 1995; Huard et al., 1998). Research into this topic is ongoing and might provide insight into a potential third stem cell population in the OE.

Similar to Sus cells, D/G cells express cytochrome p-450, CK8, CK18, ECAD, and the transcription factor Pax6 (Voigt et al., 1985; Getchell and Getchell, 1991; Brittebo, 1997; Guo et al., 2010). A unique marker of D/G cells in the OE is the transcription factor Sox9, a marker of several mesenchymal stem cell populations, again

pointing towards stem-like features of this cell type (Holbrook et al., 2011).

Cell types of the Lamina Propria (LP)

As previously mentioned, the acini of the Bowman's gland are located beneath the basal membrane of the OE in the lamina propria (LP), as are OSN axons that enter and traverse through the LP. Surrounding OSN axon bundles are olfactory ensheathing cells (OECs) that have a similar function to the peripheral Schwann cells in ensheathing non-myelinated axons (Vincent et al., 2005; Mackay-Sim and St John, 2011). OECs have a diverse molecular phenotype and can express GFAP, $p75^{NTR}$ and BLBP at varying levels along the olfactory tract (Vincent et al., 2005). Of most interest, OECs have long been thought to be an ideal glial cell to assist in nerve regeneration in the spinal cord based on their ability to support axon regeneration (Ramón-Cueto and Nieto-Sampedro, 1994; Li et al., 1998; Mackay-Sim and St John, 2011).

Other cells types of the LP include macrophages, fibroblasts and the putative meschenchymal stem cells (MSCs). Macrophages function to clear out cellular debris and may play a role in neuronal survival (Borders et al., 2007; Vukovic et al., 2010) and LP fibroblasts secrete growth factors that influence epithelial differentiation (Mumm et al., 1996; LaMantia et al., 2000; Gilbert et al., 2015). OE MSCs are poorly characterized to date, but may represent an additional stem cell of the olfactory system (Murrell et al., 2005; Rui et al., 2015). Among the previously discussed cell types are blood vessels and autonomic and trigeminal nerve endings thought to stimulate D/G secretion (Getchell and Getchell, 1992).

Other olfactory structures

In addition to the OE, there are three other olfactory sensory structures involved in olfactory chemosensation. The vomeronasal epithelium is structurally similar to the OE and is located in the vomeronasal organ (VNO) at the base of the nasal septum (Figure 1) (Døving and Trotier, 1998). Neurons from the VNO project to the accessory olfactory

bulb (AOB) at the posterior dorsal side of the main olfactory bulb and are thought to play a role in pheromone detection, influencing reproductive and social behaviors (Dulac and Axel, 1995; Halpern and Martínez-Marcos, 2003; Tirindelli et al., 2009). The septal organ (SO) is located on either side of the septum, posterior to the nasopalatine duct (connecting the oral and nasal cavities), has similar cellular anatomy to the OE, and has neurons that project to glomeruli in the posterior ventromedial main olfactory bulb (Ma et al., 2003; Weiler and Farbman, 2003). Due to its close proximity to the nasopalatine duct and its distribution in many mammalian species, the SO may play a role in early detection of innate biological cues such as licking behavior (Tirindelli et al., 2009). Lastly, the Grueneberg ganglion is found bilaterally in the anterodorsal area of the nasal cavity (Grüneberg, 1973). Only two cell types have been identified in the Grueneberg ganglion: glial cells and ciliated neurons (Brechbühl et al., 2008). The Grueneberg neurons project to ~10 glomeruli in the main olfactory bulb called the "necklace glomeruli" (Fuss et al., 2005). It is debated that Grueneberg neurons are involved in maternal pheromone detection and alarm pheromone detection (Fuss et al., 2005; Brechbühl et al., 2008; Tirindelli et al., 2009).

1.3 Development and Regeneration of the Olfactory Epithelium

In order to understand the regeneration of the OE following injury, we must first understand and appreciate the original generation of the epithelium, beginning with embryonic development.

Embryonic Development

The first identifiable structures that give rise to the OE are the olfactory placodes. These placodes are patches of thickened ectoderm on the rostrolateral aspects of the head that can be detected in mice at embryonic day 9 (E9) (Figure 3) (Cuschieri and Bannister, 1975b). Transcription factors thought to be involved in olfactory placode

induction include Dlx5, Oct-1, Sox2 and Pax6 (Donner et al., 2007; Bhattacharyya and Bronner-Fraser, 2008). By E10, the olfactory placode sinks below the ectoderm to form the olfactory pits, which will eventually become the nasal cavities; by E11, the pits form secondary recesses and their rims unite, creating nostrils (Cuschieri and Bannister, 1975b; Treloar et al., 2010).

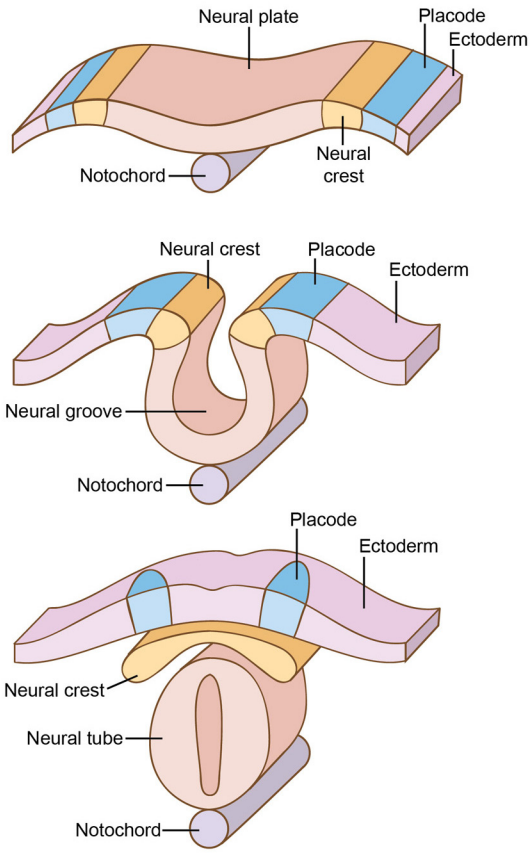

Figure 3. Embryonic development of the OE
The olfactory placodes are patches of thickened ectoderm that emerge at embryonic day 9; these placodes give rise to the olfactory pits which eventually form the nasal cavities. (Adapated from Feinberg & Mallatt, 2013)

Olfactory neurons can be detected as early as E9; importantly, OSN emergence depends on mesenchymal/epithelial interactions. Specifically, retinoic acid (RA), FGF8, sonic hedgehog (SHH) and bone morphogenic proteins (BMPs) secreted from the mesenchyme play critical roles in olfactory differentiation, patterning, and morphogenesis (LaMantia et al., 1993, 2000; Shou et al., 2000). By E11.5, ORs are expressed in OSNs, a time point preceding contact with the olfactory bulb (Sullivan et al., 1995). Beginning at E12, OSNs extend axons that traverse through the basal lamina of the OE, enter the underlying mesenchyme, and join a population of migratory cells in the "migratory mass" (thought to be composed of OEC precursors and cells migrating to other brain regions) in their journey to the rostral portion of the telencephalon where the olfactory bulb will develop (Valverde et al., 1992). This "migratory mass" utilizes guidance cues in the

mesenchyme and chemotrophic cues from the telencephalon to find its way and is the precursor of the olfactory nerve (Valverde et al., 1992).

As indicated above, the olfactory bulb (OB) develops later than the OE and from a different structure completely. The OB can first be identified at E12.5 as an invagination of the rostral telencephalon (Hinds, 1968). OB induction is stimulated by axonal contacts (from OSN axons in the migratory mass) with the rostral tip of the telencephalon (Treloar et al., 1999). OSN axons do not fully enter the bulb until E15 and instead remain in the peripheral olfactory nerve; it is hypothesized that this delay is critical for axonal sorting and aggregation in order for proper bulb targeting once glomerulogenesis begins (Treloar et al., 1999, 2002). Finally, at E18, the axon enter the dendritic zone and form protoglomeruli by E20, which become morphologically distinct as glomeruli by P0 (Treloar et al., 1999).

Returning to the development of the OE, it is important to understand the emergence of the OE cell types (discussed in Section 1.2). In contrast to the mature OE, the embryonic epithelium contains apical (as opposed to basal) GBC progenitors that give rise to the OSNs around E11.5-E12.5 (Smart, 1971). During E14.5-E17, the progenitor cells migrate to the basal lamina, and Sus and D/G cells develop (Cuschieri and Bannister, 1975a). HBCs are the last cell type generated (similarly migrating from apical to basal) appearing at E17.5 as characterized by p63 (+)/K14 (+) cells located atop the basal lamina (Holbrook et al., 1995; Packard et al., 2011b).

Natural neuronal turnover in the adult

Pioneering work in the 1960s and 70s established that cells near the base of the adult OE can incorporate thymidine analogues and differentiate into neurons; furthermore, a portion of these traced neurons eventually disappear (Moulton et al., 1970; Graziadei and Metcalf, 1971; Graziadei, 1973; Moulton, 1974; Graziadei and Monti Graziadei, 1978, 1979). These observations laid the foundation for two important features

of the adult OE: (1) basal cells have the capacity to generate OSNs in adulthood and (2) OSNs naturally die, perhaps promoting generation of more neurons. Indeed, using retrovirally derived vectors, investigators have demonstrated that the globose basal cells (GBCs) give rise to neurons in uninjured animals (Schwob et al., 1994).

In reference to the second feature – that OSNs naturally turn over – it was first hypothesized that neurons in the OE have fixed, finite lifespans. Investigators surmised that the rate of proliferation in the basal layers could be used to estimate the length of neuronal life, which they posited to be about one month (Graziadei and Monti Graziadei, 1979). However, this interpretation has proven to be faulty. In fact, immature OSNs turn over at much higher rates than mature OSNs, and the lifespan of mature OSNs is still unknown – although, some suggest that OSN lifespan could be up to one year (Hinds et al., 1984; Carr and Farbman, 1993; Deckner et al., 1997). In an experiment attempting to define OSN lifespan, it was found that OSNs labeled by retrograde transport of a stable marker from the bulb persisted for longer than one month, suggesting that mature OSNs making glomerular contacts survive for longer than a month (Mackay-Sim and Kittel, 1991).

Lesion models demonstrating the regenerative capacity of the OE

In addition to its ability to maintain homeostasis during slow OSN turnover, the OE is also competent at recovering from more severe injury. In this vein, our laboratory utilizes several rodent lesion models to study olfactory neurogenesis, primarily olfactory bulbectomy (OBX) and exposure to the olfactotoxic gas Methylbromide (MeBr). These two models have been used extensively in the olfactory field and have provided numerous insights into the stages of adult neurogenesis in the OE. I will discuss each model separately and mention similar lesion models as they pertain to each.

Olfactory bulbectomy (OBX) involves the surgical removal of one or both of the olfactory bulbs. Because the OSNs rely on the bulb for trophic support via their

axons, OBX causes the axons to degenerate and leads to mature OSN death (Schwob et al., 1992). In attempt to restore the neuronal population, GBCs undergo massive proliferation, producing an abundance of GAP-43 (+) immature OSNs (Schwartz Levey et al., 1991; Carr and Farbman, 1993; Schwob et al., 1994). These neurons persist until they reach the bulb, cannot form glomeruli, and degenerate. Thus, OBX results in sustained proliferation, increased numbers of immature OSNs, and continual OSN death. Importantly, removal of the olfactory bulb does not activate the second, quiescent population of stem cells, the horizontal basal cells (HBCs) (Schwartz Levey et al., 1991; Schwob et al., 1994). A similar lesion model, the olfactory nerve transection, also results in stimulation of the GBCs, although new OSNs can eventually re-create the olfactory nerve and contact the olfactory bulb (Costanzo, 1985; Caggiano et al., 1994). Thus, this lesion model differs from the OBX in that massive proliferation and neuronal death is not sustained.

Methyl bromide (MeBr) gas is olfactotoxic and destroys the entire epithelium, sparing only the basal cells – both globose and horizontal (Figure 4) (Hurtt et al., 1987, 1988; Schwob et al., 1995). Specifically, MeBr gas is metabolized into toxic free radicals by Sus cells which consequently destroy differentiated cells in the OE (Eustis et al.,

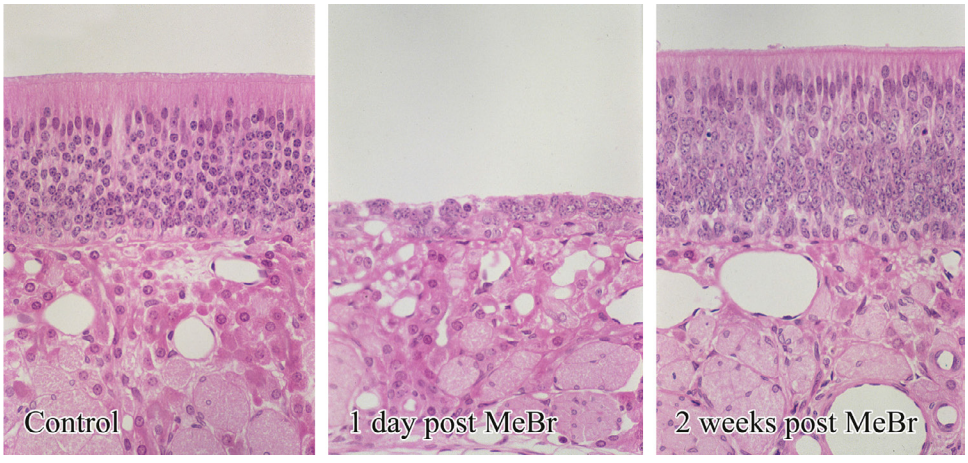

Figure 4. Methylbromide (MeBr) lesion model
MeBr lesion destroys the mature cell populations of the OE, leaving intact on the basal stem cells; after weeks, the entire tissue is regenerated. Shown is H&E staining of control, 1 day post MeBr, and 3 weeks post MeBr in rat OE.

1988; Hurtt et al., 1988). In response to the concomitant loss of OSNs, Sus cells, and duct cells, both GBCs and HBCs are activated to replace the mature cell population (Figure 4). Importantly, through many studies utilizing MeBr-lesion, genetic lineage-tracing, and transplantation, it has been shown that both GBCs and HBCs can give rise to all differentiated cell types of the OE upon severe injury to the epithelium (Jang et al., 2003; Chen et al., 2004; Leung et al., 2007).

Proceeding systematically through the events in the OE after MeBr lesion, rapid cell loss (95% of the neurons and supporting cells) occurs at 24 hours post MeBr (Schwob et al., 1995). Within 2 days, there is massive proliferation of the basal cells, and by 4 days neurons appear (Schwob et al., 1995; Leung et al., 2007). Around the middle of the second week, OMP (+) OSNs are detectable, simultaneous with glomerular reinnervation (Schwob et al., 1999). Similarly, Sus cells reappear by 2 days and form a congruent layer by 10 days post lesion. By 8 weeks, the OE has stabilized and resembles the state of the pre-injured epithelium, with remarkable regeneration of spatial patterning within the epithelium (discussed further in section 1.5) (Schwob et al., 1995; Iwema et al., 2004).

Of great importance, the MeBr lesion model allows for an almost complete, temporally synchronized characterization of the maturation process of stem cells to differentiated cells in the OE (Figure 5). As demonstrated by staining at different days post MeBr lesion (and backed up by an array of studies), neuronal differentiation proceeds from Sox2 (+)/Pax6 (+) multipotent progenitors (MPPs), to Ascl1 (+) transit amplifying-neuronally committed cells (TA-N), to Neurog1 (+) and NeuroD1 (+) immediate neuronal progenitors (INP), to immature and mature OSNs (Cau et al., 1997, 2002; Manglapus et al., 2004; Guo et al., 2010; Packard et al., 2011a). Sus cell differentiation occurs with exclusive expression of Hes1 and suppression of Ascl1 expression (Figure 5) (Cau et al., 2000; Manglapus et al., 2004).

As previously mentioned, the HBCs are activated to divide by MeBr lesion; this

activation occurs through the down-regulation of p63, releasing HBCs from dormancy (Packard et al., 2011b). At 3 days post lesion, HBCs expressing both CK14 and p63 appear at the most basal level and p63 (-)/CK14 (+) HBCs continue to differentiate into the GBC lineage. By 5 days post lesion, p63 (-)/CK14 (+) are rare and the p63 (+)/CK14 (+) HBCs are restored (Packard et al., 2011b).

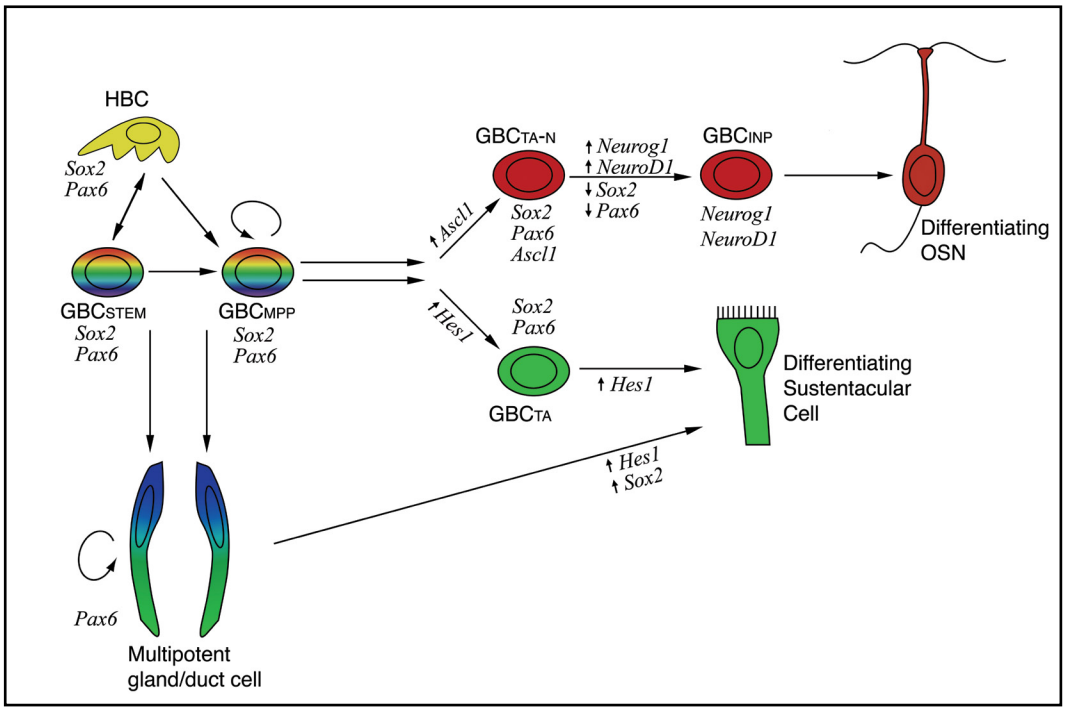

Figure 5. Maturation from stem to differentiated cells in the OE
The regenerative capacity of HBCs, GBCs, and D/G cells is shown with cell type-specific regeneration highlighted by TF expression/regulation.

Finally, it should be noted that Bowman's duct cells have shown proliferative capacity following MeBr lesion. This proliferation is apparent at 2 days post lesion; from 3-14 days post lesion, the ducts progenitors can produce CK18 (+) Sus cells (Schwob et al., 1995).

There are several lesion models that mimic the MeBr paradigm including chemical toxins such as methimazole, zinc sulfate, and dichlobenil. Methimazole is administered intraperitoneally (IP) and, similar to MeBr lesion, results in cytochrome p-450-mediated cell death, sparing the basal cells and destroying the differentiated

cells of the OE (Bergman et al., 2002). Unlike MeBr lesion, methimazole-lesioned OE regeneration takes significantly longer, with basal cells activation at 3-4 days (Brittebo, 1995; Bergman et al., 2002). Additionally, the regenerative pattern is non-uniform and is thus slightly harder to rely upon for comparison across lesions (Brittebo, 1995). Zinc sulfate is administered via nasal irrigation and is similarly delayed in regeneration and impaired in reproducibility (Matulionis, 1975; Burd, 1993). A unique aspect of zinc suflate OE destruction is that axons never reconnect with the bulb (Matulionis, 1975; Burd, 1993). Dichlobenil is administered IP and results in necrosis throughout the dorsomedial OE with very little recovery even up to 6 months post treatment and instead results in respiratory metaplasia (Bergman et al., 2002). Respiratory metaplasia is common in aging humans; therefore dichlobenil administration could be a useful tool in studying olfactory sensory loss in humans (Holbrook et al., 2005).

1.4 Lineage Commitment

Olfactory lesion models combined with genetic tracing provide excellent tools to investigate lineage commitment in the OE. In this section, I will revisit neuronal lineage commitment in the OE and will review exceptions to lineage commitment in other systems.

OE neuronal lineage commitment

The detailed progression of GBCs expressing different transcription factors along their way to neuronal commitment (Figure 5, Figure 6) was originally based on genetic epistasis experiments and cell recovery following epithelial injury. The first defined GBC population were the Ascl1 (+) (a.k.a. Mash1) GBCs. In mice lacking Ascl1, olfactory neuronal progenitors were never formed and neurons never developed; however supporting cells were present, suggesting that Ascl1 is specifically required for neuronal differentiation (Guillemot et al., 1993; Gordon et al., 1995). Further studies utilizing

Ascl1 knock out (KO) mice and *Neurog1* KO mice identified that *Ascl1* is required to initiate neuronal differentiation and that it precedes *Neurog1* expression, which itself is not required for olfactory progenitor survival, but is necessary for OSN differentiation (Cau et al., 1997, 2002).

Following these epistasis experiments, our lab systematically characterized the appearance of transcription factors following MeBr lesion and similarly described the neurogenic progression from Ascl1 (+) GBCs to Neurog1 (+)/NeuroD1 (+) GBCs (Manglapus et al., 2004). Subsequent analysis of the transcription factors Sox2 and Pax6 found that these factors can be expressed in cells prior to Ascl1 (+) GBCs, although they can also overlap with Ascl1 and a small portion of the Neurog1/NeuroD1 GBCs (Figure 6) (Guo et al., 2010). Importantly, all the GBC stages contain actively cycling cells as demonstrated by Ki67 staining, tritiated thymidine incorporation, and BrdU/EdU incorporation (Moulton, 1974; Guo et al., 2010; Jang et al., 2014).

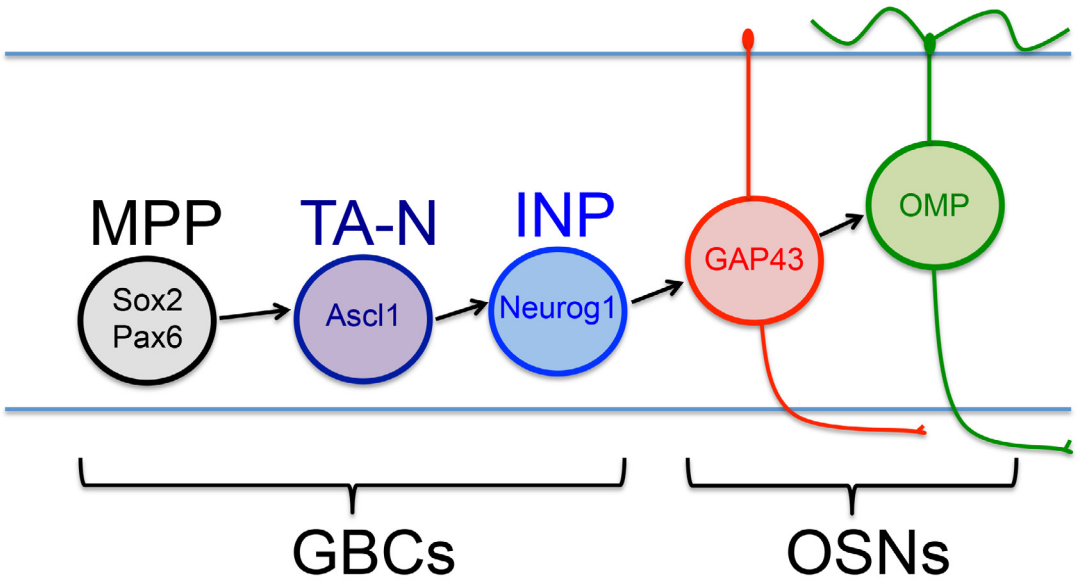

Figure 6. The progressive expression of transcription factors from GBCs to OSNs. Multipotent progenitors (MPPs) express Sox2 and Pax6, transit-amplifying neuronally committed (TA-N) GBCs express Ascl1, and immediate neuronal precursors (INPs) express Neurogenin1 (Neurog1). Immature OSNs express GAP43 while mature OSN express OMP.

There are two experimental models to directly test progenitor capacity: 1) genetic lineage tracing and 2) transplantation of isolated cell populations. Using genetic lineage tracing, our lab has shown that all OSNs derive from NeuroD1 (+) GBC precursors (in the OE, VNO, SO, and Grueneberg ganglion) and that NeuroD1 (+) cells only give rise to OSNs (Packard et al., 2011a). Utilizing transplantation techniques, our lab verified that bulk GBCs can give rise to all cells types of the OE (Chen et al., 2004). Recent studies in our lab using both lineage tracing and transplantation have confirmed that Sox2 (+) GBCs are multipotent in the OE and the Neurog1 (+) GBCs give rise only to neurons (data included in this thesis, Chapter 3).

Exceptions to lineage commitment in other systems

As with most biological phenomena, there are exceptions to "terminal" differentiation. This fact was impressed upon the scientific community with the seminal work of Shinya Yamanaka when his group published on the conversion of differentiated human fibroblast cells into pluripotent stem cells (Takahashi et al., 2007). These experiments opened the large and growing field of human and mammalian induced pluripotent stem cells (iPSCs). Given our ability to reprogram terminally differentiated cells *ex vivo*, the question has now become: is dedifferentiation possible *in vivo*? One could hypothesize that there must be the potential of dedifferentiative capacity in normal systems, otherwise how else would the machinery exist *ex vivo*? As such, several researchers have begun digging for examples of *in vivo* dedifferentiation.

One of the first reports of apparent *in vivo* dedifferentiation came from two studies investigating liver regeneration. Using transplantation and genetic lineage tracing, two groups found that fully differentiated hepatocytes can give rise to differentiated biliary epithelial cells upon liver injury (Michalopoulos et al., 2005; Yanger et al., 2013). However, with a closer look at the conversion of hepatocytes to biliary epithelial cells, no intermediate cell stages were identified; therefore hepatocytes are capable

of transdifferentiation – the process by which cells are interconverted between two terminally differentiated states – as opposed to dedifferenatiation – the process by which a terminally differentiated cell acquires less differentiated properties (Stanger, 2015).

At the same time the liver lineage tracing experiments were performed, a different group investigated the role of differentiated airway epithelial cells in tissue repair. They found that upon airway injury, epithelial cells gave rise to basal stem cells, this time demonstrating true *in vivo* dedifferentiation (Tata et al., 2013; Zhao et al., 2014). Most recently, *in vivo* dedifferentiation has been shown in the intestinal crypts where enterocyte progenitors can revert to stem cells upon Lgr5 (+) stem cell ablation (Tetteh et al., 2016).

Potential for plasticity within the OE

Given the plasticity of terminally differentiated cells in the liver, airway epithelium, and intestinal crypts, it is possible that lineage committed GBCs, or even terminally differentiated OSNs could dedifferentiate or transdifferentiate upon epithelial injury. This concept inadvertently became a topic in my dissertation work and will be revisited in the results section.

1.5 Olfactory Receptors

Olfactory receptors (ORs) make up the largest gene family in mammals and are arguably the most fascinating genes of the OE (Glusman et al., 2001; Zozulya et al., 2001; Zhang and Firestein, 2002). In the following sections, I will touch upon several aspects of ORs including their structure, functions, and expression patterns.

Structure and Genetics

The OR multigene family was discovered in 1991 in the Nobel Prize-winning work of Linda Buck and Richard Axel (Buck and Axel, 1991). Prior to this discovery,

seminal work in the OE established that ORs were located in OSN cilia and that adenylyl cyclase (AdCy), cyclic AMP, G-proteins, and inositol trisphophate (IP3) signaling all played a role in OR sensory transmission, suggesting that ORs were members of the 7-transmembrane receptor family (G-protein coupled receptors, GPCRs) (Pace et al.; Bronshteín and Minor, 1977; Sklar et al., 1986; Jones and Reed, 1988; Boekhoff and Breer, 1990; Breer et al., 1990). The notion that odor stimulation occurred through GPCRs was a critical observation that enabled Buck and Axel to amplify hundreds of ORs using degenerate GPCR PCR primers (Buck and Axel, 1991). Astoundingly, humans have ~900 OR genes and mice have ~1500 OR genes (Lander et al., 2001; Zhang and Firestein, 2002; Clowney et al., 2011). However, a large portion of these genes are non-functional pseudogenes; in humans ~50% of ORs are pseudogenes and in mice ~25% are pseudogenes (Zhang and Firestein, 2002; Malnic et al., 2004; Clowney et al., 2011). It is unknown why OR pseudogenes have persisted at such high percentages.

The OR GPCR contains both conserved and variable regions: conserved regions are found in transmembrane domains 1, 2, 3, 6, 7, and variable regions involved in ligand binding include transmembrane domains 3,4, and 5 (domain 3 contains both conserved and variable regions) (Buck and Axel, 1991; Kobilka, 1992). Olfactory GPCRs are unique in containing an unusually long second extracellular loop that is hypothesized to play a role in ligand binding (Mombaerts, 1999; Man et al., 2004).

OR genes are distributed in 17 clusters across all chromosomes except for 12 and Y in mice and 20 and Y in humans (Glusman et al., 2001; Zhang and Firestein, 2002). There are two distinct classes of vertebrate ORs: Class 1 ORs (~160) are more evolutionarily ancient, are found in fish, and are located on Chromosome 7; Class 2 ORs (~1300) make up 90% of mammalian ORs and are spread across the chromosomes with a bias towards six chromosomes that make up 73% of the ORs: Chromosomes 1, 6, 9, 11, 14, and 19 (in humans) (Glusman et al., 2001; Alioto and Ngai, 2005; Zhang et al., 2007a). Importantly, OR genes do not contain introns and are generally around 900 base

pairs in length (Buck and Axel, 1991). OR sequences can be very similar to one another; sequences sharing more than 40% protein sequence identity are classified as family members and those with greater than 60% protein sequence identity make up subfamilies (Lancet and Ben-Arie, 1993).

Signaling

As previously mentioned, ORs are G-protein coupled receptors (GPCRs) located in OSN cilia that are in direct contact with the external environment. When chemical odorants bind to the variable regions of the ORs, a conformation change in the receptor induces the G protein, $G\alpha_{olf}$, to dissociate from Gβ and Gγ and activate adenylyl cyclase 3 (AdCy3) (Figure 7) (Jones and Reed, 1988; Belluscio et al., 1998; Wong et al., 2000). Once activated, AdCy3 converts ATP into the second messenger cAMP, which then binds to a cyclic nucleotide-gated channel (CNG) similar to those found in photoreceptors (Brunet et al., 1996). The CNG facilitates an influx of sodium and calcium ions into the pre-synaptic terminal, eventually depolarizing the neuron below threshold and stimulating an action potential (Firestein et al., 1991). This action potential propagates through the

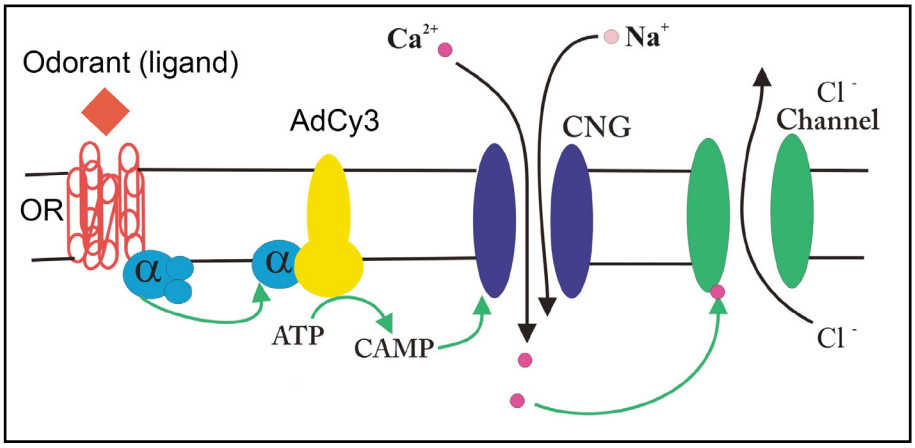

Figure 7. Olfactory receptor signal transduction
Odorants bind to olfactory receptors (ORs) causing a conformation change that allows $G\alpha_{olf}$ to dissociate from the G-protien complex and activate adenylyl cyclase-3 (AdCy3). AdCy3 converts ATP to cAMP, which then opens cyclic nucleotide-gated channels (CNG) allowing a depolarizing influx of calcium and sodium into the neuron.

neurons and ends in glutamate release onto mitral and tufted cells in glomeruli of the olfactory bulb (Berkowicz et al., 1994). It should be noted that some ORs signal through a PLC/IP3 mediated mechanism as opposed to cAMP (Boekhoff and Breer, 1990; Breer et al., 1990).

Ligand Matching and the Combinatorial Code

The task of matching chemical odorants to specific receptors (ligand to receptor) has been a daunting task in the olfactory field, with surprisingly slow progress. A major hindrance to the de-orphanizing pursuit has been the difficulty of achieving surface OR expression in heterologous systems. Side-stepping this issue, the first de-orphaned receptor, OR I7, was endogenously overexpressed in mice using a recombinant adenovirus. Electoolfactograms (EOGs) were recorded from dissected OE during exposure to various odorants and it was found that I7 responds to heptanol, octanol, nonanol, and decanol, all strong fruity odors (Zhao, 1998). Remarkably, the I7 receptor discriminates between hexanol (C_6) and heptanol (C_7), giving no response to hexanol (Zhao, 1998). Although this method of endogenous expression was successful in identifying ligands for the I7 receptor, it is not a reasonable approach for de-ophanizing thousands of ORs.

Working to develop more high-throughput screens for identifying OR-ligand interactions, investigators discovered that fusing the first 20 residues of human rhodopsin to the N-terminal end of an OR allows for surface expression of ORs in heterologous cells (Krautwurst et al., 1998). Similarly, co-expression of ORs with olfactory chaperones RTP1 and REEP results in surface OR expression (Matsunami et al., 2009). More recently, a novel assay using S100a5-tauGFP mice, which express GFP in actively stimulated OSNs, has been used to de-orphan ORs and provides a promising high-throughput technique to speed up the pursuit of receptor-ligand pairings (McClintock et al., 2014).

Using the methods described, OR receptive fields have been tested by many groups and all have pointed to a "combinatorial code" model of olfactory perception (Malnic et al., 1999; Araneda et al., 2000; Kajiya et al., 2001; Abaffy et al., 2006; Repicky and Luetje, 2009; Saito et al., 2009). The basis of this combinatorial code is that each OR responds to a number of chemical odorants with varying magnitudes; therefore the identity of a single odorant is determined by the subset of ORs it activates and the degree to which is activates these ORs (Saito et al., 2009). This combinatorial code allows for detection and discrimination between thousands of different odors and was actually proposed early on in olfactory studies by E.D. Adrian based on his observations that different odors produced different spatio-temporal activation in the olfactory bulb (Adrian, 1950).

Singular OR Expression

Given the discussion above regarding the combinatorial code of olfactory perception, one may postulate that each olfactory neuron expresses only one OR – suggesting that the activation of one OSN relies on the receptive field of a single OR (Bozza et al., 2002). This concept has been demonstrated, debated, re-established, and revisited many times over.

Following the initial discovery of the OR gene family, OR *in situ* hybridization experiments revealed that ORs are expressed in patterns across the epithelium and that no one neuron was positive for two ORs in the RNA probe pool (Ressler et al., 1993; Vassar et al., 1993). However, this did not rule out the case that OSNs could express multiple ORs due to the sheer number of possible OR combinations. Nonetheless, researchers favored the idea of singular OR expression and sought to validate the emerging "one-neuron, one-receptor" rule. In support of this idea, Richard Axel's group demonstrated that ORs are monoallelically expressed in OSNs (Chess et al., 1994). Building upon this observation, it was found that non-allelic OR transgenes with identical coding

regions were never expressed together in one OSN, suggesting that OR expression is both monoallelic and mutually exclusive (Serizawa et al., 2000; Ishii et al., 2001). Remarkably, if the β2-adrenergic receptor is placed as a transgene under control of an OR promoter, it is also expressed monoallelically and ostensibly monogenically (Feinstein et al., 2004). However, while these experiments demonstrate monoallelic OR expression, they do not conclusively demonstrate monogenic OR expression.

The idea that OR expression is singular in each OSN raises the daunting question as to how a monoallelic and monogenic state can be achieved. One attractive explanation is that OR genes undergo DNA rearrangements similar to the generation of T-cell receptor diversity (Hozumi et al., 1976). This hypothesis was disproven in two sets of experiments taking the nuclei of post-mitotic OSNs, injecting them into oocytes, and demonstrating that the resulting mice have the entire repertoire of ORs – thus refuting the idea that the post-mitotic OSN had irreversible changes to its DNA during OR selection (Eggan et al., 2004; Li et al., 2004).

At the same time that the DNA re-arrangement hypothesis was tested, other groups started looking at the "one neuron, one receptor" rule from the opposite end: feedback regulation. Many hypothesized that once a functional OR was expressed, it inhibited the expression of additional ORs. To tackle this question, Sakano's group created a YAC-MOR28 transgene lacking the MOR28 coding sequence and found that OSNs positive for the mutant construct (tagged with GFP) co-expressed other ORs, suggesting that OR protein is necessary for singular OR expression (Serizawa et al., 2003). Importantly, the mutant construct contained a specific locus control region (LCR) named the "H region" that is necessary for MOR28 expression, allowing the MOR28 mutant to be expressed in identical fashion to endogenous MOR28 (Serizawa et al., 2003). As a control, a functional MOR28 transgene expressed with the appropriate LCR showed no overlap with the endogenous MOR28 allele or other ORs (Serizawa et al., 2003).

Building upon Sakano's experiments, Randall Reed's group showed that the presence of untranslatable OR mRNA is insufficient to exclude expression of other ORs, further demonstrating that presence of OR protein is essential in maintaining (or perhaps even establishing) monogenic OR expression (Lewcock and Reed, 2004). Furthermore, Axel's group observed that immature OSNs can switch between ORs before settling on one OR and that this switching is especially prevalent in OSNs that initially choose to express an OR pseudogene, suggesting that functional ORs are necessary for singular OR expression (Shykind et al., 2004). More recently, it was discovered that high levels of OR transcription and translation are necessary to ensure singular OR expression (Abdus-Saboor et al., 2016).

The fact that functional OR protein is necessary for maintenance of one OR per neuron suggests that negative feedback could be activity dependent. However, in OSNs with $G\alpha_{olf}$ signaling deficiencies, only one receptor is expressed, and in OSNs with hyperactive G-protein signaling, multiple OR can be expressed (Imai et al., 2006). It may be the case that feedback from the Gβ and Gγ proteins are important for OR silencing; this hypothesis has shown promise in zebrafish OE, but has yet to be verified in the mammalian system (Ferreira et al., 2014).

The identification of the olfactory LCR, the "H region", by Sakano's group (Serizawa et al., 2003) led many to believe that this enhancer could be involved in singular OR expression. Further investigation into the H enhancer found that it could act as both a cis- and trans-chromosomal regulator, increasing the number of OR genes the enhancer interacts with and suggesting that it may act as a master regulator of all OR genes (Lomvardas et al., 2006). However, subsequent studies revealed that H enhancer deletion only affected the expression of the more proximal OR genes on chromosome 14 (*MOR28*, *MOR10*, *MOR83*, and *MOR29A*) (Fuss et al., 2007).

Zooming in closer on the OR coding region, many have hypothesized that the OR promoter region plays a role in singular OR expression. This is based on observations

that the OR promoter sequence is required for OR transgene expression and that it can be used to express non-OR transgenes (such as the β2-adrenergic receptor), influencing the transgene to demonstrate monoallelic and monogenic expression (Vassalli et al., 2002; Feinstein et al., 2004; Rothman et al., 2005). Thus, many groups have investigated the exact components of OR promoter sequences in pursuit of conserved regions that may be important for singular OR expression.

There are two conserved regulatory sequences found in OR promoters: Olf1/Early B-cell factor sites (O/E sites), which are usually between 50-150 basepairs upstream of the transcriptional start site, and homeodomain sites, which are found further upstream (Vassalli et al., 2002; Hoppe et al., 2003; Michaloski et al., 2006; Clowney et al., 2011). Deletion of these sites reduces the expression of OR transgenes and introducing multiple copies of the domains increases the frequency of transgene expression (Rothman et al., 2005; Vassalli et al., 2011). Two homeodomain transcription factors, Lhx2 and Emx2 have been heavily studied in the OE and each influence OR expression. In *Lhx2* knock-out mice, the majority of maturing OSNs halt at the immature neuronal stage, however a small portion of OSNs mature to express Class I ORs in the dorsal OE (Hirota and Mombaerts, 2004; Hirota et al., 2007). Conversely, neurons reach full maturity in *Emx2* knock-out mice, but there is an overall decrease in both Class I and Class II OR expression. The decreases in OR expression are due to fewer OSNs expressing each OR; however, a handful of ORs are expressed in more OSNs than usual (perhaps as a form of compensation) (McIntyre et al., 2008). Ultimately both Lhx2 and Emx2 are essential in stimulating OR transcription, but do not appear to play a role in monogenic OR expression (Hirota et al., 2007; McIntyre et al., 2008). Years of investigation have demonstrated that OR promoters are bound by a small number of common transcription factors (the most studied being Lhx2 and Emx2), a situation that does not lend itself to transcription factors, or combinations of transcription factors, playing a determining role in singular OR expression.

In considering the basic phenomenon of monogenic OR expression, one must imagine a scenario where ~999 genes (as a low estimate) are silenced. With increasing awareness of epigenetic silencing and activation in biological sciences, it is no surprise that OE researchers began to hypothesize that chromatin silencing could play a role in singular OR expression. In fact, many investigators (including our group) have frustratingly observed that several transgenic reporters that work elsewhere in the mouse are silenced in the OE, suggesting a more prevalent degree of silencing occurring in the OE than in other tissues.

Using chromatin immunopreciptation (ChIP), Lomvardas' group found that OR clusters in the mouse OE are coated with tissue-specific heterochromatic markers H3K9me3 and H4K20me3 (Magklara et al., 2011). Furthermore, this OR heterochromatization is apparent in neurons, Sus cells, and Neurgo1-eGFP (+) GBCs, but not HBCs, leading the group to hypothesize that widespread OR silencing occurs early on in GBCs – before a GBC is even fated to become a neuron. Importantly, they observed that expressed OR alleles are not marked with H3K9me3 and instead have the transcriptional activating methylation marker, H3K4me3 (Magklara et al., 2011). Thus, the model emerged where large scale epigenetic OR silencing is established early on, followed by stochastic release of repression and concomitant activation of a single OR allele.

Subsequent to the discovery of epigenetic OR silencing, it was found that Lamin B Receptor (LBR)-dependent spatial sequestering of OR genes plays a role in monogenic OR expression, that the unfolded protein response (UPR) may be a negative feedback mechanism in singular OR expression, and that Lysine Specific Demethylase1 (LSD1) plays a crucial role in singular OR expression (Clowney et al., 2012; Krolewski et al., 2013; Lyons et al., 2013, 2014). As LSD1 is highly pertinent to my thesis work, the role of LSD1 in the OE is discussed in depth in a subsequent section of the introduction (Section 1.7).

Although there has been extensive research into how monogenic OR expression could occur, ranging from epigenetics, promoter sequences, transcription factors, feedback mechanisms, and DNA-rearrangements, the very fact that ORs are actually singularly expressed in OSNs has still not been demonstrated conclusively. Recently, four separate groups of researchers tackled this question using single-cell RNA-seq to examine every OR mRNA expressed in single neurons (Hanchate et al., 2015; Saraiva et al., 2015; Tan et al., 2015; Scholz et al., 2016). The studies all report that a dominant OR is expressed in mature OSNs, that some mature OSNs express multiple ORs at low levels, and that multiple ORs can be detected in immature OSNs. One study found that up to 20 additional ORs (at very low levels) can be detected in mature OSNs predominantly expressing *Olfr73* (Scholz et al., 2016). Two of the other studies reported detection of multiple ORs in mature OSNs: 6 out of 25 mature OSNs sequenced (24%) (Hanchate et al., 2015), and 3 out of 68 mature OSNs (4.4%) (Tan et al., 2015). Based on this newly published data, the dogma of "one neuron, one receptor" must be qualified: while many mature OSNs predominantly express one OR, they may express multiple ORs at lower levels; immature OSNs frequently express greater than one OR. Further investigation into monogenic OR expression utilizing single-cell RNA-seq will be essential to clarify percentages of mature OSNs expressing multiple ORs.

OR expression timing and patterning

Timing: OR mRNA can first be detected in the developing OE and the migratory mass at embryonic day 11.5 (E11.5) by chromogenic *in situ* hybridization (Sullivan et al., 1995; Schwarzenbacher et al., 2004); conversely, in the cribriform mesenchyme, OR mRNA is detectable at E10 by isotopic *in situ* hybridization (Nef et al., 1992). A recent study using gene-specific OR primers was able to amplify OR cDNA as early as E9 (Rodriguez-Gil et al., 2010); to date, this is the earliest report of OR presence in the developing olfactory system. Interestingly, at E9, OSN somata are present but have not

yet developed axons, suggesting that OR transcription could begin as early as neuronal birth and predate neuronal contact with olfactory bulb (Sullivan et al., 1995; Rodriguez-Gil et al., 2010). In fact, ORs are expressed in mice lacking bulbs, demonstrating that OR expression is independent of axonal contact with the bulb (Sullivan et al., 1995).

An additional metric to specify the timing of OR expression is to compare the onset of OR expression to the timing of cell division using thymidine incorporation assays. By this approach, OR mRNA and protein are first detectable around 4 days after basal cell division, 24 hours after OSN axons have reached the bulb, but prior to glomerularization (Rodriguez-Gil et al., 2015). Furthermore OR expression lags behind the appearance of GAP-43 expression by 3 days, independent of OR class or chromosome location (Rodriguez-Gil et al., 2015).

A third strategy for defining the onset of OR expression is comparing the timing of OR expression to markers of neuronal maturation. In this respect, our lab has demonstrated that OR mRNA and protein are present in both immature GAP-43 (+) OSNs and in mature OMP (+) OSNs in the adult OE (Iwema and Schwob, 2003). Other groups have identified OR transcripts in Neurog1-eGFP (+) immediate neuronal precursors (INPs) purified by FACS followed by microarray analysis; however, these cells may be immature OSNs due to the perdurance of GFP after Neurog1 transcription ceases (Magklara et al., 2011). More recently, single-cell RNA-seq experiments have further validated OR mRNA expression in immature OSNs (Hanchate et al., 2015; Saraiva et al., 2015; Tan et al., 2015; Scholz et al., 2016).

Although OR mRNA and protein <u>expression</u> occurs in immature OSNs, OR <u>choice</u> (i.e., the selection of an OR allele) may occur at an earlier developmental timepoint such as in GBC_{INPs}. Potentially mitigating this idea is the fact that OR switching occurs in immature OSNs and that mRNA from multiple ORs is present in immature OSNs by single-cell RNA-seq, suggesting that if a choice has been made, it is not permanent at this point (Lewcock and Reed, 2004; Shykind et al., 2004; Hanchate

et al., 2015; Saraiva et al., 2015; Tan et al., 2015; Scholz et al., 2016). In fact, electo-olfactograms (EOGs) have shown that immature OSNs have wide receptive fields and become selective during the transition from immature to mature OMP (+) OSNs (Gesteland et al., 1982). Taking this information together, it is possible that the final choice of a single OR for high expression occurs close to the transition from immature to mature OSN.

Patterning: In addition to their unique (almost) singular expression within OSNs, ORs have distinct expression patterns across the OE that emerge as early as E13 (Sullivan et al., 1995; Rodriguez-Gil et al., 2010). OR patterning was originally described as "zonal", with ORs falling into 1 of 4 zones along the dorsal-ventral axis of the OE (Ressler et al., 1993; Vassar et al., 1993). However, closer examination demonstrated that many ORs straddle "zone" borders; thus, OR expression patterns are more accurately described as stripes that shift and overlap along the dorsomedial/ventrolateral axis of

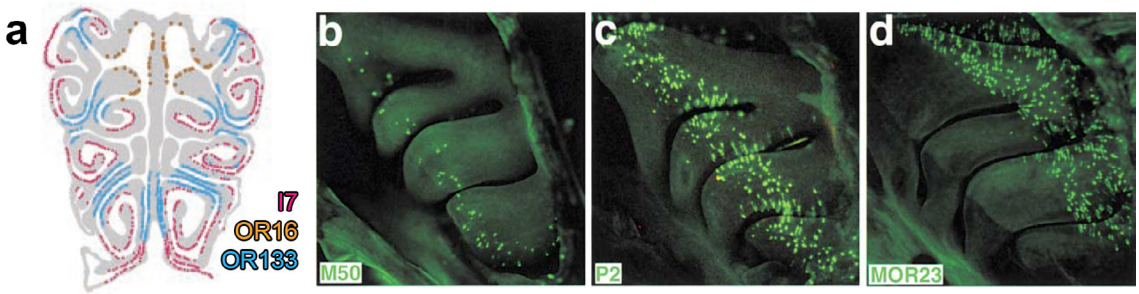

Figure 8. Olfactory receptors are expressed in stripes across the olfactory epithelium. **(A)** Coronal section demonstrating regional location of three ORs: I7, 16, and 133 (Adapted from Iwema et al., 2004). **(B-D)** Whole mount preparations demonstrating regional locations of three ORs: M50, P2, and MOR23 (Adapted from Vassalli et al., 2002)

the OE (Figure 8) (Iwema et al., 2004; Miyamichi, 2005). One known exception to the "stripes" is the MOR262 subfamily (OR37 subfamily), which is expressed in a "patch" in the center of the turbinates (Strotmann et al., 1994; Iwema et al., 2004). Class I ORs are restricted to the dorsal OE, while Class II ORs are expressed across the entire epithelium (Miyamichi, 2005; Tsuboi et al., 2006).

There have been many hypotheses as to how OR spatial patterning is established and maintained. Early on, it was thought that promoter sequences played a role in spatial OR expression. Indeed Class I ORs have more O/E sites within their promoter region than Class II ORs, and the two atypical, ventrally expressed Class I ORs have similar promoter sequences to Class II ORs (Hoppe et al., 2006). Additionally, the promoter sequences of the MOR262 "patch" subfamily have six conserved promoter motifs that differ from the rest of the Class II ORs, suggesting that their promoter sequence may play a role in their unique expression pattern (Hoppe et al., 2003, 2006). However, if promoter sequences influence the expression patterns of all Class II ORs, there would have to be a wide variety of OR promoter sequences; in fact, Class II ORs promoters are highly conserved (Michaloski et al., 2006; Clowney et al., 2011). Nonetheless, in experiments specifically looking at the *M71* promoter, it was found that mutations in either the O/E or homeodomain sites resulted in the ventralization of OR expression again suggesting that promoter regions play at least some role in OR patterning (Rothman et al., 2005). It has also been proposed that locus control regions (LCRs) such as the H-region could play a role in OR patterning; however, of the seven OR genes regulated by the H-region, three are expressed in the ventral OE while four are expressed dorsally (Serizawa et al., 2003; Fuss et al., 2007; Nishizumi et al., 2007).

Remarkably, reporter transgenes downstream of OR promoters demonstrate OR spatial patterning across the epithelium (Lewcock and Reed, 2004; Rothman et al., 2005; Zhang et al., 2007b). Furthermore, the β2-adrenergic transgene driven by an OR promoter is spatially expressed across the OE, demonstrating that OR protein is not necessary for spatial patterning (Feinstein et al., 2004), and OR minigenes (transgenes) as small as 2.2kb are patterned across the epithelium, demonstrating that local (as opposed to long-range) genomic interactions can influence spatial OR expression (Vassalli et al., 2002). However, researchers have also found that the genomic context of transgene integration and copy numbers influences expression patterns (Qasba and Reed, 1998; Rothman et

al., 2005; Zhang et al., 2007b). Despite these observations, it is still unclear whether genomic sequences upstream of the OR coding region can account for OR gene choice and patterning, though they do at least contribute.

A second hypothesis for OR pattern generation is that differential expression of transcription factors influence OR distribution. While Lhx2 and Emx2 are uniformly expressed across the OE, the transcription factor Msx1 shows graded expression across the OE and may be involved in pattern generation (Norlin et al., 2001). Other regional transcription factors have yet to be identified; however, several proteins are differentially expressed across the OE – perhaps the most interesting being the retinoic acid (RA) synthesizing enzymes, the RALDHs (Norlin et al., 2001; Peluso et al., 2012). Spatial expression of the RALDHs suggests the RA gradients could influence OR spatial patterning, an attractive model considering that graded RA expression controls spatially determined cell fate choices in many developmental and regeneration settings. This topic is given further attention in a following section (Section 1.6).

Finally, it should be noted that OR expression patterns can regenerate appropriately in adulthood. Specifically, in unilaterally-lesioned rats, the regenerated side of the OE produces a mirror image to OR patterning on the contralateral, un-injured side (Iwema et al., 2004). Thus, while the regulation of OR pattern generation may differ embryonically, it is likely that

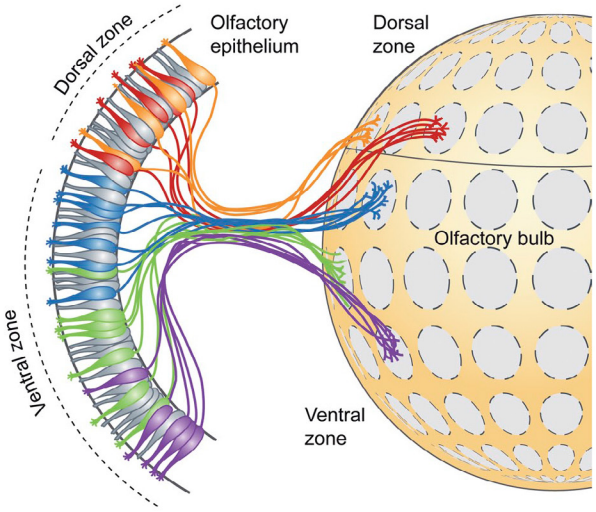

Figure 9. OSNs expressing the same OR converge together at glomeruli in the olfactory bulb in a rhinotopic fashion.
(Adapted from DeMaria & Ngai, 2010)

factors involved during original pattern generation persist into adulthood.

OR axonal guidance

Following the discovery of OR patterning in the OE, it was shortly discovered that these patterns are projected onto the olfactory bulb (OB); this OE-OB "zonal" projection is referred to as rhinotopy (Figure 9) (Ressler et al., 1994; Vassar et al., 1994). Specifically, OSNs expressing the same OR project to two glomeruli (one medial and one lateral) in each bulb respectively, and each glomeruli contains projections from OSNs all expressing the same OR (Figure 9) (Ressler et al., 1994; Vassar et al., 1994; Mombaerts et al., 1996). Furthermore, dorsal/ventral OE expression is directly reflected by dorsal/ventral bulb projections (Mori et al., 1999; Miyamichi, 2005). The conservation of a spatial map from the OE to the bulb fits into the combinatorial model of sensory transmission whereby certain sets of glomeruli are activated based on odorant binding at different ORs.

After OE/OB rhinotopy was observed, the question became: which came first? – the OE patterning, or the OB patterning? It was quickly determined that OR patterns develop before axonal targeting at the bulb, as early as E13 (Sullivan et al., 1995; Rodriguez-Gil et al., 2010). Building upon these observations, it was found that ORs themselves play a significant role in axonal anterior/posterior targeting and glomerular convergence (Mombaerts et al., 1996; Bulfone et al., 1998; Wang et al., 1998; Rodriguez-Gil et al., 2015). The OR promoters seem to play a critical role in this process as β2-adrenergic transgenes expressed under an OR locus form glomeruli, and OR minigenes (as small as 2.2kb) properly target specific glomeruli (Vassalli et al., 2002; Feinstein et al., 2004). These observations suggest that neither OR protein nor OR-specific signaling are necessary for axonal targeting at the bulb. Interestingly, odorant-independent second messenger activity may play a role in anterior/posterior bulb targeting (Nakashima et al., 2013). Furthermore, OR gene swap experiments have demonstrated the OR gene

itself is not sufficient for precise glomerular targeting as OSNs expressing a mutant OR coding sequence do not project onto the substitute OR glomerulus, but instead converge at glomeruli between the substituted coding sequence and the original mutated OR (Mombaerts et al., 1996; Wang et al., 1998). Thus, unsurprisingly, other signaling molecules play a role in OSN axonal guidance and targeting such as Slit1, Semaphorin3F, Robo2, Neuropilin2, and IGF signaling (Cho et al., 2007; Scolnick et al., 2008; Takeuchi et al., 2010).

Recently, two studies demonstrated that OR transgene expression can cause endogenous OSNs to reroute if the transgene is expressed before axonal map establishment, suggesting that there is a critical developmental time window for proper glomerular targeting (Ma et al., 2014; Tsai and Barnea, 2014). In fact, precise axon convergence at the bulb is not observed in adult mice after methylbromide injury or following olfactory nerve transection (Schwob et al., 1999; Christensen et al., 2001; Holbrook et al., 2014). Alternatively, it has also been shown that the bulb may not be required for axonal convergence: OSN axons are able to converge in mice developmentally lacking olfactory bulbs or following bulbectomy (St. John et al., 2003; Chehrehasa et al., 2006). It is apparent that the further one tests the limits of the olfactory system, far more exceptions than rules surface.

TAARs and V1Rs

Outside of canonical ORs, there are three other types of olfactory chemosensory GPCRs: the trace amine-associated receptors (TAARs), type-1 and type-2 receptors (V1Rs and V2Rs), and formyl peptide receptors, the latter of which are found only in rodents (Dulac and Axel, 1995; Liberles and Buck, 2006; Liberles et al., 2009). TAARs have been indentified in human, mice, and fish; similar to ORs, TAARs are expressed in unique subsets of OSNs patterned across the OE. The ligands identified for mouse TAARs include amines found in urine and are associated with social cues such as stress

and male/female detection (Liberles and Buck, 2006). V1Rs and V2Rs are found in the vomeronasal sensory neurons (VSNs) in the vomeronasal organ (VNO) (Dulac and Axel, 1995). These receptors detect pheromones – secreted, odorless substances recognized by the opposite sex of the same species (Dulac and Axel, 1995). Finally, rodents have five *FPR* genes expressed in the VNO, which are thought to recognize pathogen-associated odorants such as bacterial flora (Liberles et al., 2009).

OR expression outside of the OE

While ORs are mainly expressed in the OE, OR transcripts have been found in other tissues. The first place ectopic OR transcripts were identified was the human testis (Parmentier et al., 1992; Vanderhaeghen et al., 1997). Further investigation found that ORs are also found in mice testis, and that they most likely play a role in chemoreception during sperm-egg communication, thereby assisting in fertilization (Fukuda et al., 2004). Outside of the OE and testis, OR transcripts have been found in the heart, muscle, embryo, spleen, pancreas, blood, lung, kidney, and brain at varying timepoints during development (Kang and Koo, 2012). Further investigation into ectopic OR expression is necessary for a better understanding of OR function outside of the OE.

1.6 Spatial patterning across the OE

In addition to OR spatial patterning across the OE, other proteins and transcription factors show graded distribution across the epithelium. In this section, I will discuss the most described spatially expressed proteins and consider their implications for influencing OE patterning.

RB-8/MamFasII/RNCAM/NCAM2/OCAM

The first antibody that exhibited divided immunoreactivity in the OE was discovered in 1986 and purified in 1988, predating the discovery of ORs (Schwob and

Gottlieb, 1986, 1988; Yoshihara et al., 1997). This monoclonal antibody was originally designated RB-8 and was later found to probe for an immunoglobulin superfamily cell adhesion molecule referred to as the mammalian homologue of fasciclin II (mamFasII), olfactory cell adhesion molecule (OCAM), RB-8 neural cell adhesion molecule (RNCAM), and neural cell adhesion molecule 2 (NCAM2) (Schwob and Gottlieb, 1986; Paoloni-Giacobino et al., 1997; Yoshihara et al., 1997; Hamlin et al., 2004). In this thesis, I will refer to this molecule as OCAM for simplicity's sake (however, "olfactory" cell adhesion molecule is a misnomer as this protein is found abundantly outside of the OE (Paoloni-Giacobino et al., 1997; Winther et al., 2012)).

Within the OE, ventrolateral OSNs are OCAM (+) and a sharp line demarcates the OCAM (-) region of the dorsomedial OE (Schwob and Gottlieb, 1986; Yoshihara et al., 1997; Alenius and Bohm, 2003; Treloar et al., 2003). OSNs stain for OCAM with mesh-like, surface staining that can be rather faint; alternatively, the fascicles of the olfactory nerve are densely stained by OCAM antibodies (Schwob and Gottlieb, 1986). OSNs expressing OCAM send axons to the ventrolateral region of the bulb and non-expressing axons project to the dorsomedial bulb, suggesting that OCAM could provide axonal guidance to the ventrolateral OSNs and assist in rhinotopy establishment (Schwob and Gottlieb, 1986; Yoshihara et al., 1997; Alenius and Bohm, 2003; Treloar et al., 2003). However, using OCAM KO mice, it was found that OCAM is not essential for OE-OB connectivity and is instead required for the compartmental organization and segregation of axodendritic and dendrodendritic synapses within glomeruli (Walz et al., 2006).

Developmentally, OCAM is expressed prior to axonal contact with the bulb: *OCAM* mRNA is evident by both RT-PCR and *in situ* hybridization at E12.5 and the protein can be detected by immunohistochemistry at E13.5 (axons enter the bulb around E15) (Treloar et al., 1999; Hamlin et al., 2004). Surprisingly, OCAM is also transiently expressed in mitral/tufted cells in the dorsal olfactory bulb that inversely synapse with OCAM (-)/NQO1 (+) OSNs (Treloar et al., 2003). These OCAM (+) mitral/tufted cells

first appear at E18 prior to glomerularization, and persist until at least P0, but are not present in the adult OB (Treloar et al., 2003).

NADPH:quinone oxidoreductase (NQO1)

A second regionally expressed protein found in the OE is the NADPH:quinone oxidoreductase (NQO1), an enzyme that catalyzes the reduction of quinones – a class of organic compounds derived from aromatic compounds (Gussing and Bohm, 2004). *NQO1* mRNA and protein are found in OSNs of the dorsomedial OE, with a striking border defined by the NQO1/OCAM interface. Interestingly, the NQO1/OCAM border is often respected by OR expression zones, suggesting that similar developmental cues may instruct spatial gene expression in both OR choice and NQO1/OCAM choice (Figure 10)

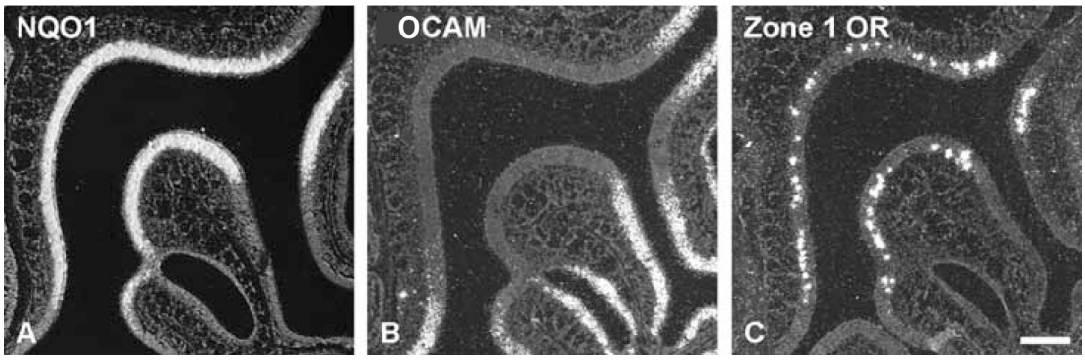

Figure 10. ORs are expressed within NQO1/OCAM boundaries.
(A) NQO1 (+) dorsomedial OE. **(B)** OCAM (+) ventrolateral OE. **(C)** An OR expressed in the NQO1 (+) region. (Adapted from Gussing & Bohm, 2004)

(Gussing and Bohm, 2004). While the exact function of NQO1 in the OE is unknown, its role in the bioactivation of quinoidal compounds suggests a connection with observed zone-specific toxicity of certain olfactory toxins (Gussing and Bohm, 2004). Conversely, the NQO1 (+) region of the OE (dorsomedial) can also show a resistance to olfactotoxins – often our lab observes "sparing" of the dorsal recess during MeBr exposure. While this may be related to NQO1 activity, it also could be due to the physical location of the dorsal recess and the process of airflow through the nasal cavity.

RA synthetic enzymes (RALDHs)

One of the most interesting dispersed proteins across the OE are the retinoic acid (RA) synthetic enzymes, the RALDHs. RALDHs and RA metabolizing enzymes control graded RA concentrations (Wang et al., 1996; Zhao et al., 1996; Niederreither et al., 2002), which have been shown to influence spatially determined cell fate choices in many developing and regenerating settings including gastrulation, limb bud formation, motor neuron differentiation, and epithelial differentiation in the intestine and trachea (Tickle et al., 1982; Niederreither et al., 2002; Appel and Eisen, 2003; Rhinn and Dollé, 2012). Therefore, differential expression of RALDHs across the OE suggests that RA could be an important signal for OSN pattern formation with respect to ORs and other spatially expressed proteins, such as NQO1 and OCAM.

During OE development, mesenchymal-epithelial interactions are crucial for morphogenesis and secreted factors from the mesenchyme play a critical role in neuronal differentiation. These secreted factors include FGF8, sonic hedgehog (SHH), BMPs, and RA (LaMantia et al., 1993, 2000; Shou et al., 2000). In the early embryo, RALDH-2 is expressed in the frontonasal mesenchyme providing a key source of RA that initiates expression of other RA-signaling molecules (such as retinoid receptors) and influences the eventual expression of RALDH-3 (Bhasin et al., 2003). RALDH-3 itself is crucial for development and survival; RALDH-3 knock-out mice die perinatally due to nasal malformations resulting in respiratory failure (Dupé et al., 2003).

In addition to RA's role in differentiation and morphogenesis, retinoic acid plays a role in developmental OE patterning. This was first demonstrated in mesenchymal/ epithelial co-cultures where mesenchyme was taken from an RA-deficient animal (*Pax6*^{sey} mice) and placed in culture with wild-type OE. Under these circumstances, the wild-type mucosa failed to organize and differentiate, but a portion of medial olfactory characteristics did develop. This suggests that medial OE differentiation is less dependent on RA signaling than the lateral OE (LaMantia et al., 2000). Furthermore, the RALDHs

and RA-response genes are differentially expressed across the developing olfactory mucosa (OM) shown by both *in situ* hybridization and RA-reporters: at E16, RALDH1, 2, and 3 are found in the ventrolateral OM and RA-responsive genes are found in a subset of OSNs in the dorsolateral OE (Whitesides et al., 1998; Niederreither et al., 2002).

In the adult OE, RALDHs continue to be differentially expressed in both the mesenchyme and epithelium (Norlin et al., 2001; Peluso et al., 2012). RALDH1 is strongly expressed in the ventrolateral Sus cells and in stromal cells of the ventrolateral lamina propria, RALDH2 shows similar, albeit lower expression in Sus cells as RALDH1, and RALDH3 is limited to stromal cells of the ventrolateral lamina propria that are adjacent to the basal lamia (Peluso et al., 2012). Additionally, the RA-binding protein CRABII is similarly found in the ventrolateral OE. Conversely, the RA metabolizing enzyme CYP26 is not differentially expressed in the OE as demonstrated by qPCR in dissected dorsal vs. ventral OE (Peluso et al., 2012). Based on these observations, the RALDHs could be important for maintaining RA gradients in the adult OE and may set up borders that influence NQO1/OCAM and OR patterning. In fact, the RALDH and OCAM borders are sharply aligned (Peluso et al., 2012).

To test the effect of RA secretion on spatial patterning, one would wish to inhibit RA production in the adult OE under a regenerative setting – a challenging task. To address this problem, our lab used a retrovirus to introduce a dominant negative form of the RA receptor in basal cells after MeBr lesion. Unfortunately, under these circumstances, OMP (+) mature OSNs do not develop, preventing any observations regarding spatial patterning (Peluso et al., 2012).

Other regionally expressed transcription factors and proteins

Aside from ORs, OCAM, NQO1, and the RALDHs, there are a handful of other identified spatially expressed proteins and transcription factors. Two regulators of G-protein signaling, RGS9 and RGSZ1 have mutually exclusive expression in

the dorsomedial and ventrolateral OE respectively (Norlin and Berghard, 2001). Additionally, the Msx1 homebox transcription factor and Neuropilin-2 are expressed in the ventrolateral OE and the BMP-type I receptor, Alk6, is found in the dorsomedial OE (Norlin et al., 2001). It is likely that more transcription factors, proteins, and secreted factors are dispersed across the OE – however, they have yet to be described.

1.7 The lysine specific demethylase 1 (LSD1)

As mentioned in section 1.5, the lysine specific demethylase 1 (LSD1) may play a crucial role in singular OR expression. In this section, I will review what is known about LSD1 function outside of the olfactory system and then will focus on what is known in the OE, as well as what is left to be investigated.

Discovery and function

Histone modifications are a type of epigenetic modification that affect chromatin structure and ultimately influence transcription (Strahl and Allis, 2000). Two types of histone alterations have been most heavily studied (although others exist): histone acetylation and histone methylation (Kouzarides, 2000, 2007; Rice and Allis, 2001;

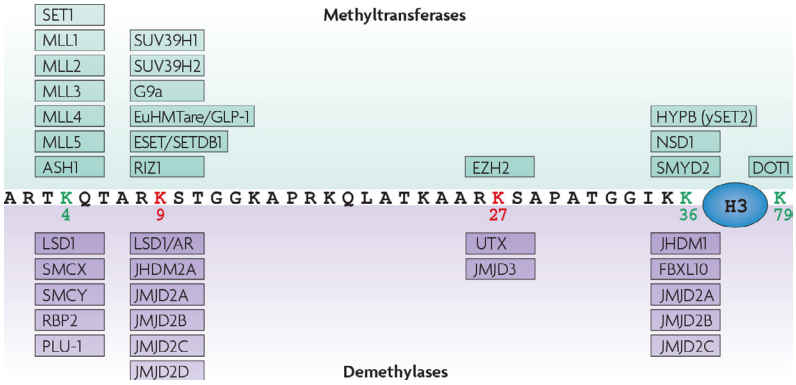

Figure 11. Dynamic regulation of histone methylation on H3. Lysines that promote transcription when methylated are in green, and residues that inhibit transcription when methylated are in red. Methytransferases are listed above and demethylases are listed below (Adapted from Shi, 2007)

Zhang and Reinberg, 2001). The fact that histones are substrates for methylation was originally discovered in 1964; subsequent to this discovery, the work of many researchers has shown that lysine residues 4, 9, 27, and 36 on histone 3 (H3) and lysine 20 on histone 4 (H4) are preferred sites for histone methylation (Murray, 1964; Strahl et al., 1999; Kouzarides, 2007). Furthermore, histone methylation can be transcriptionally activating or transcriptionally repressive (Strahl et al., 1999; Nakayama et al., 2001; Lee et al., 2005a); therefore, enzymes that add or remove histone methylations (methyltransferases and demethylases respectively) can be either activating or repressive (Figure 11).

This first histone methylation-modifying enzyme identified was the lysine specific demethylase 1 (a.k.a. LSD1, KDM1A, BHC110, AOF2) (Hakimi et al., 2002; Shi et al., 2004). LSD1 removes methyl groups from histone 3, lysine 4 (H3K4) – a transcriptional activating methylation mark (Shi et al., 2004). Thus, LSD1 was originally described as a transcriptional repressive histone-modifying enzyme. At the time of its discovery, it was understood that LSD1 functions in a co-repressor complex that can include the C-terminal binding protein (CtBP), histone deacetylase 1 or 2 (HDAC1,2), and the REST corepressor 1 (CoREST1), amongst other complex components (Hakimi et al., 2002; Shi et al., 2005). Furthermore, it was found that LSD1 specifically removes mono- and di- methylations at H3K4 (H3K4me1 and H3K4me2), but cannot demethylate H3K4 trimethylation (H3K4me3), and that LSD1's enzymatic activity at nucleosomes depends on its association with CoREST1 (Shi et al., 2004; Lee et al., 2005b).

Although LSD1 mainly demethylates at H3K4 to repress transcription, it was recently found to demethylate at H3K9me1/2, a transcriptionally repressive histone mark, thereby making LSD1 also capable of transcriptional activation (Metzger et al., 2005; Garcia-Bassets et al., 2007; Laurent et al., 2015). Binding partners necessary for LSD1 activity at H3K9 include the nuclear hormone receptors: the androgen receptor (AR) and the estrogen receptor (ER) (Metzger et al., 2005; Garcia-Bassets et al., 2007; Nair et al., 2010). Interestingly, a recent report found that a neuron-specific isoform of LSD1,

LSD1+8a, is able to demethylate H3K9me2 when in complex with supervillin (SVIL) (Laurent et al., 2015). Taking these data collectively, LSD1 substrate specificity is largely mediated by its associated proteins.

LSD1 in disease, development, and differentiation

The role of LSD1 in cancer progression has received much attention in the past years and many LSD1 inhibitors have been proposed as therapeutic agents, though they have yet to reach the clinic (Gale and Yan, 2015). LSD1 has oncogenic properties in several cancers including prostate, bladder, breast, lung, leukemia, neuroblastomas, sarcomas and hepato-carcinomas (Amente et al., 2013; Zhang et al., 2013; Phillips et al., 2014). Expression of LSD1 mRNA and protein is high in cancerous tissue, inhibiting LSD1 in cancer cells lines suppresses proliferation, migration, and invasion, and overexpressing LSD1 in cancer cell lines enhances cell growth (Hayami et al., 2011; Lv et al., 2012; Zhao et al., 2013). Similar to its normal activity, LSD1's function in cancer initiation depends on its association with other proteins and transcription factors. For example, when associated with the transcription factor SLUG (SNAI2), LSD1 plays a role in mammary cancer initiation by unlocking stem cell transitions – specifically luminal differentiation (Phillips et al., 2014).

As suggested by its role in stem cell transitions in breast cancer, LSD1 is an important player in stem cell maintenance. In fact, LSD1 is a key histone modifier in balancing self-renewal and differentiation in embryonic stem cells (ESCs) (Adamo et al., 2011). Specifically, LSD1 regulates bivalent chromatin domains – regulatory regions of developmental genes that contain both H3K4me2/3 (activating) and H3K27me3 (repressive) marks that are "poised" for activation during development (Bernstein et al., 2006; Adamo et al., 2011). Furthermore, LSD1 affects self-renewal and differentiation in human iPSCs (Yan et al., 2016).

Developmentally, LSD1 first appears in the morula and is later found in the inner

cell mass of blastocysts; in mice lacking LSD1, the egg cylinder fails to elongate and undergo gastrulation leading to lethality around embryonic days 5-7 (Wang et al., 2007, 2009; Foster et al., 2010).The loss of LSD1 causes aberrant expression of 588 genes including many transcription factors involved in anterior/posterior patterning and limb development (Foster et al., 2010). Given this information, it is not surprising that loss of LSD1 is embryonic lethal (Wang et al., 2007, 2009; Foster et al., 2010).

Outside of its role in ESC differentiation, LSD1 is necessary for terminal differentiation (from precursor cells) in many cell types including pituitary cells, adipocytes, photoreceptor cells, gastrointestinal endocrine cells, hematopoietic cells, and neurons (Saleque et al., 2007; Wang et al., 2007; Musri et al., 2010; Sun et al., 2010; Ray et al., 2014; Laurent et al., 2015; Popova et al., 2015). Again, LSD1 complex partners are critical in orchestrating LSD1-induced differentiation; for example, supervillin is necessary for LSD1 mediated activation of neuronal genes and CoREST2 is necessary for neuronal precursor (NPC) proliferation and differentiation in the cortex (Laurent et al., 2015; Wang et al., 2016). Interestingly, LSD1/CoREST1 complexes inhibit neuronal gene expression in non-neuronal cell types (Andrés et al., 1999; Ballas et al., 2001; Ceballos-Chavez et al., 2012; Sáez et al., 2015). The divergent functions of LSD1 promoting neuronal differentiation in certain cell types and inhibiting it in others reflects the dual activating/repressive capacity of the enzyme at H3K9 and H3K4 respectively.

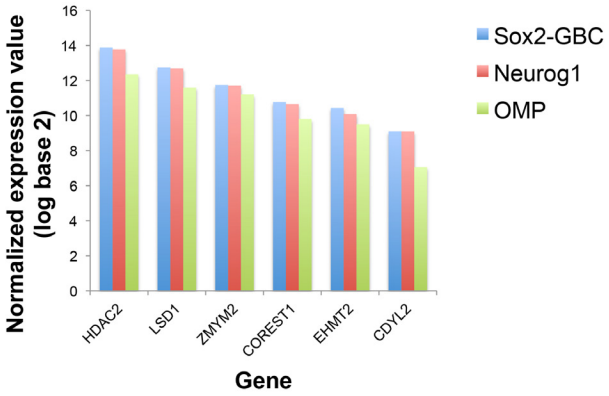

Figure 12. LSD1/CoREST complex components are regulated as differentiation proceeds. Shown are normalized mRNA expression values (microarray analysis) for samples in the neurogenic progression, showing that LSD1/CoREST complex components are upregulated in progenitor cells and decrease in expression as differentiation proceeds. (Adapted from Krolewski et al., 2013)

LSD1 expression and function in the OE

LSD1 was first found in the OE via microarray analysis: LSD1 transcript is abundant in Sox2 (+) and Neurog1 (+) GBCs and decreases in expression with neuronal maturation (Figure 12) (Krolewski et al., 2013). Further investigation using mRNA-seq and immunohistochemistry showed that LSD1 protein and mRNA are abundant in GBCs (Krolewski et al., 2013; Lyons et al., 2013). More specifically, the cell population that overlaps best with LSD1 (+) cells in the OE are the Neurog1-eGFP (+) GBCs (Krolewski et al., 2013; Lyons et al., 2013; Kilinc et al., 2016).

Given the fact the LSD1 is differentially expressed in the OE and that LSD1 can act as either transcriptionally activating or repressing, several hypotheses of LSD1's role in the OE have emerged. Most inviting is the hypothesis that LSD1 plays a pivotal role in singular OR gene choice, as LSD1 can demethylate at both H3K4me1/2 and H3K9me1/2 – both of which are found on OR alleles (Magklara et al., 2011). In fact, LSD1 is expressed in neuronal precursors at a time before OR expression (Neurog1-GBCs), and decreases in expression in mature OSNs that have chosen an OR. Therefore, LSD1 may repress OR expression in precursor cells and its down regulation may be associated with the release of an OR gene from its repressed state. Specifically, this model imagines that LSD1 is in constant competition with H3K4 methyltransferases, until the methyltransferases win at a specific OR allele, resulting in H3K4me3-dependent transcription activation.

On the flip side, several groups have hypothesized that LSD1 activates OR transcription by removing H3K9me/me2 at a specific OR allele (Lyons et al., 2013). Importantly, in this scenario, an initial demethylase is necessary to remove the first methyl group from H3K9me3 as LSD1 only demethylates at mono- and di-methylated lysines (Shi et al., 2004). This model seems unlikely given the abundance of LSD1 expression in precursor cells (as in, if LSD1 were activating only one allele, it would likely be very hard to detect in OE). However, a recent report found that LSD1

compartmentalizes in early post-mitotic cells (immature OSNs) and co-localizes with 1-3 OR loci during this timeframe, suggesting that LSD1 may in fact modify specific OR alleles at the time of OR gene choice (Kilinc et al., 2016). As LSD1-dependent OR activation has been given the most attention in the OE field, I will review the literature supporting this model.

The seminal paper on LSD1 function in the OE was published in 2013 shortly after OR gene heterochromatinization was characterized (Magklara et al., 2011). To analyze LSD1 function, Lomvardas' group knocked-out LSD1 using a *floxed-Lsd1* transgenic mouse and three cell-specific drivers (separately): *Foxg1-Cre*, *MOR28-Cre*, and *OMP-Cre* (Wang et al., 2007; Lyons et al., 2013). Foxg1 is a transcription factor expressed in ventrolateral embryonic OE that is required for OE development as well as survival (Duggan et al., 2008). Not surprisingly, LSD1 knock out under the Foxg1-Cre driver resulted in embryonic lethality at E18.5, thereby limiting the study to embryonic development. Despite this limitation, it was clear that the loss of LSD1 in Foxg1 (+) cells aborted terminal OSN differentiation (Lyons et al., 2013). When LSD1 was knocked out with the OR driver, MOR28-Cre, or the OMP-Cre driver, there was no phenotype, which was not surprising given that LSD1 is not highly expressed in mature OSNs (Lyons et al., 2013).

In looking at OR expression, the investigators found that *Foxg1-Cre/Lsd1*$^{fl/fl}$ mice did not express any ORs by *in situ* hybridization. This result formed the basis of their hypothesis: LSD1 is necessary for OR activation. While this may be true, it is hard to prove decisively given that mature OSNs do not develop in these animals. Despite this confound, one could argue that the OSNs are not maturing because they are never turning on OR expression. In support of this argument, the group demonstrated that overexpression of a specific OR in the *Foxg1-Cre/Lsd1*$^{fl/fl}$ mice rescued OSN maturation as assayed by Adenylyl cyclase 3 (AdCy3) immunoreactivity. Interestingly, when they overexpressed LSD1 in mature OSNs, they found that LSD1 inhibited OR expression

(Lyons et al., 2013). Therefore, LSD1 may activate or repress OR expression depending on its timing of expression.

Building upon this paper, Xie's group modeled LSD1 gene activation and found that OR singularity can be achieved by slow stepwise H3K9me3 demethylation followed by fast feedback to turn off LSD1 expression (Tan et al., 2013). Importantly, the model requires an original H3K9me3 demethylase and the presence of H3K9 methyltransferases that opposes the action of LSD1. In regard to the former, an H3K9me3 demethylase that removes the initial methyl group at OR loci has yet to be described. In regard to the latter, further work has identified that knocking out the G9a histone methyltransferase and the G9a-like protein (GLP) (both of which methylate H3K9) result in increased expression of some OR genes (and a decrease in others), as well as a loss of singular OR expression (Ferreira et al., 2014; Lyons et al., 2014). Therefore G9a and GLP may be the methyltransferases that lay down the original repressive H3K9 methylation and oppose LSD1 activity.

Taking the data collectively, it is clear that OR genes are marked with repressive heterochromatin and that LSD1 KO results in a lack of neuronal maturation in the OE. It is likely that G9a and GLP are involved in OR heterochromatinization, and it may be the case that LSD1 plays a role in releasing OR repression at specific OR alleles by removing methyl groups from H3K9. However, it could also be the case that LSD1 is involved in OSN differentiation through a mechanism that does not involve OR gene selection. Further investigation into LSD1 binding partners in the OE and functional studies of LSD1 in the adult animal will help clarify its role in both OR selection and OSN terminal differentiation.

1.8 Summary and Hypotheses

This thesis investigates the processes of OSN maturation and diversification in the adult mouse OE. It is specifically focused on spatial influences on neuronal diversification and the role of LSD1 in OSN maturation. The thesis is broken into three results chapters addressing the following questions:

Chapter 3: Do transplanted progenitors mimic neuronal differentiation *in situ*? In this section, I describe the transplantation methods used throughout this thesis and lay the groundwork that the transplantation model can recapitulate the differentiative capacity of specific cell types as previously described in the literature. Remarkably, these control experiments led to the discovery that injury to the OE can induce dedifferentiation in the OSN lineage.

Chapter 4: Do spatial cues influence OSN diversification? Through a series of transplantation experiments, I demonstrate that the location of a neuronal progenitor within the OE influences gene choices that direct neuronal diversification. These experiments investigate expression of the regional markers NQO1 and OCAM and the olfactory receptors.

Chapter 5: Is LSD1 involved in OR gene choice? To address the role of LSD1 in OR gene choice, I conditionally knocked out LSD1 in three progenitor cell populations. In this section, I show that LSD1 is essential for terminal OSN differentiation during a specific time window during OSN maturation.

Chapter 6: Discussion and Future Directions. In the final chapter, I synthesize the data from this thesis and propose next steps to further clarify the complex processes of neuronal maturation and diversification within the OE.

Chapter 2.

Materials and Methods

2.1 Animals and breeding

"Wildtype" F1 mice used for transplantation, western blotting, and reference tissue for immunohistochemistry and *in situ* hybridization were bred from C57/BJ6 and 129S1/Sv1MJ mice in house or were ordered from Jackson Laboratories (stock #101043). Olfactory receptor reporter mice, *M72-IRES-tauGFP* and *P2-IRES-taulacZ*, were generously gifted by Dr. Peter Mombaerts and bred together in house (Mombaerts et al., 1996; Feinstein and Mombaerts, 2004). *Sox2-eGFP* generously provided by Dr. Mahendra Rao (Ellis et al., 2004), *Neurog1-eGFP* BAC mice generated through the GENSAT Project (Gong et al., 2003), and *OMP-GFP* mice generously provided by Dr. Peter Mombaerts (Potter et al., 2001) were each were separately bred to constitutive *CAG-TdTomoto* mice generated in house by breeding the *Ai9 R26Rfl(stop) TdTomato* strain with the germ line constitutive *Sox2-Cre* driver (stock #008454). *K5-CreER^{T2}* generously provided by Dr. Pierre Chambon and Dr. Randall Reed (Indra et al., 1999), *Ascl1-CreER^{T2}* from Jackson Laboratories (stock #012882), and *Neurog1-CreER^{T2}* generously provided by Dr. Lisa Goodrich (Koundakjian et al., 2007), were each bred in house to the Cre reporter strain *Ai9 R26Rfl(stop)TdTomato* from Jackson Laboratories (stock #007909) and – for the LSD1 knockout experiments – to *floxed LSD1* mice generously provided by Dr. Michael Rosenfeld (Wang et al., 2007). All mice were maintained on ad libitum rodent chow and water and were housed in a heat- and humidity-controlled, AALAC-accredited vivarium operating under a 12:12-h light:dark cycle. All protocols for the use of vertebrate animals were approved by the Committee for the Humane Use of Animals at Tufts University School of Medicine.

2.2 Methyl bromide lesion

Eight-week old mice were passively exposed to MeBr gas (Matheson Gas Products, East Rutherford, NJ) for 8 hours at a concentration of 170 ppm in purified air at a rate of 10L/min. Unilateral exposures were performed by plugging the left naris with

a 5-mm piece of PE10 tubing and the lumen of the tube was obstructed with a knotted 5.0 suture thread. Following lesion, mice were kept on the same feeding and housing schedule and were sacrificed at the indicated timepoints post lesion.

2.3 Olfactory bulbectomy

Mice were anesthetized with 50 µl double cocktail of 0.05 mg/ml ketamine and 0.1 mg/ml xylazine; one booster of 30 µl was given when necessary. Once animals were unresponsive to toe pinches, they were immobilized in a stereotactic head mount above a 37°C heating pad for homeostasis. A single incision was made on shaved, disinfected skin to expose the overlying frontal bone and a bone drill was used to expose the right olfactory bulb; the bulb was removed by aspiration and oxycel was placed into the empty cavity to achieve hemostasis. Lastly, the overlying skin was sutured, mice were given 1 ml of sterile saline subcutaneously, and were placed on a warm pad for recovery.

2.4 Drug preparation and administration

EdU (ThermoFisher catalog #A10044) dissolved in sterile PBS was injected subcutaneously in 10-week old mice at 50 mg/kg body weight. Animals were sacrificed at 1,2,3,5,7, and 9 days post EdU injection and EdU was detected in processed tissue (described below) via Click-iT chemistry as described by the manufacturer (ThermoFisher catalog #C10339).

Tamoxifen (Tam) purchased from Sigma (#T5648) was dissolved in sterile USP-grade corn oil at 30 mg/ml by gentle inversion at 60°C for 10 minutes; the dissolved Tam was injected intraperitoneally at 150 mg/kg into 6 week-old mice once a day for two days.

Methimazole lesion was performed with a single intraperitoneal injection of 50 mg/g methimazole in saline solution at 10 mg/ml. Following injection, mice were kept on the same feeding and housing schedule and were sacrificed at 2 weeks post lesion.

2.5 Tissue Processing

Mice were anaesthetized by intra-muscular injection of a triple cocktail of ketamine (37.5 mg/kg), xylazine (7.5 mg/kg), and acepromazine (1.25 mg/kg). Anaesthetized animals were transcardially flushed with PBS and perfused with 4% PFA (1M mono- and dibasic phosphates, ph7.4) or with 1% PLP (1% PFA, 0.1M mono- and dibasic phosphates, 90mM lysine, 0.1M sodium periodate). Following perfusion, the cranium and bones overlying the nose were removed; the remaining nasal tissue was post-fixed under vacuum for 1 hour, rinsed in PBS and decalcified in saturated EDTA overnight. Tissue was transferred to 30% sucrose overnight for cryoprotection and then embedded in OCT compound (Miles Inc., Elkhart, IN) and frozen in liquid nitrogen. 10 or 20 µm coronal sections were generated on a Leica cryostat and mounted on Ultraclear Plus charged slides (Denville Scientific) and stored at -20°C until needed.

2.6 Tissue Dissociation

Animals were anaesthetized with intra-muscular injection of triple cocktail (see above) and perfused with cold Low-Ca^{2+} Ringers solution (140mM NaCl, 5mM KCl, 10mM HEPES, 1mM EDTA, 10mM glucose, 1mM sodium pyruvate, pH7.2). The OE was dissected and placed in 3ml Low-Ca^{2+} on ice. After mincing the tissue, 3ml of 0.05% Trypsin-EDTA was added to the slurry followed by a 10-minute incubation at 37°C. The tissue was pelleted at 2000xg and the Trypsin-EDTA was discarded and replaced by an enzyme cocktail (100 U/ml collagenase, 250 U/ml hyaluronidase, 75 U/ml DNase I, 0.1 mg/ml trypsin inhibitor, 5U/ml papain; from Worthington Biochemical, Roche, and Sigma) in Regular Ringer solution (140 mM NaCl, 5mM KCl, 10mM HEPES, 1mM EDTA, 10mM glucose, 1 mM sodium pyruvate, 1mM $CaCl_2$, 1mM $MgCl_2$, pH7.2). The tissue was incubated in enzyme cocktail for 30 minutes followed by filtration through a 35µm mesh, centrifugation, and resuspension in DMEM for transplantation with 50 µl suspended cells per host animal. For experiments with the HDAC inhibitor: 10 µM

Oxamflatin (Santa Cruz cat #205960) was spiked into the cell suspension and incubated at 37℃ for 1.5 hours.

2.7 Fluorescence activated cell sorting (FACS)

Olfactory epithelium was dissociated as described above except the cells were resuspended in 1X HBSS containing 25 mM HEPES, 10 mM EDTA, and 0.5% BSA. Cells were sorted on a Legacy MoFlo (ne. Cytomation, now owned by Beckman Coulter) on the clonal setting. Cells were collected into 1.5 ml tubes for bulk sorts or in PCR tubes for single cell analysis.

2.8 Transplantation

Transplantation was performed as previously described (Schnittke et al. 2015). In brief: Host animals were exposed to MeBr gas 24 hours prior to transplantation; on the day of transplantation, host animals were anaesthetized with 50 µl 0.05 mg/ml ketamine and 0.1 mg/ml xylazine double cocktail and maintained with 10 µl Ketamine/ Acepromazine double cocktail: 13.33 mg/ml ketamine and .66 mg/ml Acepromazine. Once under full anesthesia, the anterior neck was shaved and disinfected and a tracheotomy was performed. The palate was raised with a 3cm piece of PE-100 tubing to close the nasopharyngeal passage and 50µl of resuspended cells (dissociated from donor animals as described above) were flushed into the naris through PE-10 tubing. Mice were positioned at a 45° angle, alternating sides every 30 minutes for 3 hours. After this time, the solution was removed from the nasal cavity, the tracheotomy was sutured, the mice were given subcutaneous saline injections and were placed on a recovery warm pad. Three or four weeks later the animals were sacrificed.

2.9 Single-cell RT-PCR and OR identification

Single OMP-GFP (+)/CAG-TdT (+) cells were isolated from transplant host

animals by FACS. Cells were sorted directly into 50µl lysis buffer (DNase/RNase-free water [Invitrogen cat #10977], 0.005% NP-40 [Roche cat #1332473, 0.02% RNase Inhibitor [ThermoFisher cat #10777019]) in 0.5µl tubes and placed into a 65°C incubator for 2 minutes. In no-RT control experiments, the cell lysis was split into 2, 25µl aliquots, which were brought back to 50µl with water. From this point, I used Clontech's SMARTer Pico PCR cDNA Synthesis Kit (cat #634928) for single-cell RT-PCR (for the no-RT experiments, I added water instead of the reverse transcriptase). The resulting cDNA was used for many PCR experiments, including PCR for β-actin, TdTomato, OMP, Tuj1, GAP43, Sox2, and olfactory receptors (ORs). In this study I used the degenerate OR primer pair P26/P27 (Malnic et al., 1999). OR PCR products were TOPO cloned (Invitrogen TOPO TA cloning kit, cat #450640) into TOP10 cells (Invitrogen cat #C4040-03) and plated on LB-ampicillin plates for blue/white screening. White colonies were selected for minipreps and sequencing.

2.10 Quantitative RT-PCR

RNA was made from dissociated, FACS isolated cells using the Quick-RNA MicroPrep Kit from Zymo Research as described by the manufacturer (catalog #R1050); cDNA was generated using PrimeScript RT Master Mix from Clontech as described by the manufacturer (catalog #RR036A). SYBR Green qPCR mastermix (Qiagen, catalog #330529) was used for qPCR amplification on a BioRad CFX96 Real Time System with a C1000 Thermal Cycler.

2.11 RNA-sequencing

Two fluorescent reporter mouse lines were used for FACS isolation of single cells of interest: OMP-GFP/pan-TdT (from dorsal to ventral transplant experiments) and OMP-GFP (3 weeks post bulbectomy). FACS isolated cells were captured on a 5-10 um mRNA Seq IFC (Fluidigm, 100-5759) and visually inspected to positively identify single

cell capture prior to lysis and cDNA synthesis according to manufacturer's instructions. Three RNA spike-ins were added to the lysis buffer for further batch effect correction. cDNA was quantified using Invitrogen's Quant-iT high sensitivity DNA Assay kit (Q33120) prior to library construction using Illumina Nextera XT Library Prep Kit (FC-131-1024), following manufacturer's instructions and Fluidigm modifications. Single cell libraries were tagged with unique barcodes using Nextera XT Index Kit V2 B,C,D (FC-131-2002, FC-131-2003, FC-131-2004), and pooled prior to Agencourt AMPure XP Bead cleanup. The library was quantified using Quant-iT and size distribution determined using a Fragment Analyzer (Advanced Analytical Technologies, Inc) prior to sequencing at ~3M 100bp paired end reads per cell on an Illumina HiSeq2500 running in High Output v4 mode. Demultiplexed reads were FASTQC trimmed prior to mapping using RSEM on the Tufts High Performance Computing Cluster. Batch effects were removed using Bayesian methods implemented in the R package ComBat. This was followed by hierarchical clustering and visualization of clusters using the dimension reducing algorithm t-SNE, implemented in the R package Rtsne. Determination of the cutoff points for OMP and GAP43 expression was performed using the R package OptimalCutpoints, using the Youden Index Method (Youden, 1950; Schisterman et al., 2005; López-Ratón et al., 2014). The results of these calculations matched the results from visual and K-means clustering methods. For OR expression cutoffs, a similar method was used, however the multinomial logistic regression was used instead as multiple cutoffs were calculated, one of baseline noise as an initial filter, and the other for true high expression of a specific OR. The final result of this is a cutoff of 1139 transcripts per million (TPM) for OMP, 47 for GAP43, and 357 for ORs to be counted as "positive."

2.12 Western blotting and immunoprecipitation

Dissected whole-OE was flash frozen in liquid nitrogen, suspended in lysis buffer (1M Tris pH 7.5, 0.5M EDTA, 1X protease and phosphatase inhibitors [ThermoFisher

cat #79440], 20% Triton X-100, 0.5M NA_3VO_4, 2M NaCl) at 60 µl/mg of tissue, and sonicated until the tissue was homogenized. Membranes were removed by spinning at 14,000 rpm and a bicinchoninic acid assay (BCA) protein assay was used to determine protein concentrations; stocks of 2 mg/ml were made up in 1X LDS sample buffer (ThermoFisher cat #B0008) and 1X reducing agent (ThermoFisher cat #B0009) and frozen at -80°C until used for Western blotting. Samples were denatured at 95°C for 5 minutes and loaded at 40µg/lane for gel electrophoresis and PVDF transfer using the Bolt Mini Blot Module (ThermoFisher cat #B1000). The membranes were blocked in 1X TBST (20mM Tris, 0.15 NaCl, 0.1% Tween-20) with 5% Carnation Instant Non-fat Dry Milk for one hour at room temperature. Primary antibodies were incubated overnight at 4°C at the following concentrations: CoREST, 1:500 (NeuroMab cat #75-039); LSD1, 1:20,000 (Abcam cat #ab62582); NQO1, 1:1000 (Abcam 80588); OCAM, 1:6,000 [Rabbit RB-8 antiserum(Schwob and Gottlieb, 1988)]; beta-actin 1:1,000 (ThermoFisher cat #MA5-15739). The following day, membranes were washed in 1X TBST/5% milk 6 times for 5 minutes and secondary HRP conjugated antibodies (Jackson ImmunoResearch) were incubated at 1:1000 for 1 hour at room temperature. After two, 30 minutes washes, the membrane was incubated in ECL substrate (ThermoFisher cat #34080) and developed.

For immunoprecipitation, I used RIPA buffer for lysis (150 mM NaCl, 1% NP-40, 0.5% sodium deoxycholate, 0.1% SDS< 50 mM Tris, pH 8.0). Following sonication and BCA protein quantification, the protein was diluted to 1mg/300µl and LSD1 primary antibody was incubated in the lysate at 1:100 overnight at 4°C with rotation. The NAb Protein G spin kit was used for immunoprecipitation as described by the manufacturer (ThermoFisher cat#89949). During Western blotting, primary antibodies were used at 1:5,000 and 1:500 for LSD1 and CoREST respectively; secondary HRP conjugates were used at 1:2,000. Gel electrophoresis, transfer, and development were performed as described above.

2.13 Horizontal Basal Cell Cultures

Olfactory epithelium was dissected in a clean hood and placed in culture dissociation media (Pneumacult Ex, Stemcell Tech cat #05008; 1X Gem21, Gemini Bio cat #400-161; 1X N2 Neuroplex Supplement, Gemini Bio cat #400-163; 1X collagenase/hyaluronidase, Stemcell Tech cat #07912). The tissue was minced, vortexed, and placed on a rotator at 37°C for 1 hour. Cells were pelleted and resuspended in 5 ml 0.25% Trypsin-EDTA (Stemcell Tech cat #07901) with trituration, followed by the addition of 10 ml 1X HBSS containing 25 mM HEPES, 10 mM EDTA, and trypsin inhibitor (MP Biomedicals cat #101113). After a second round of pelleting, 1 ml Dispase (StemCell Tech cat #07912) and 100µL DNase1 (StemCell Tech cat #07900) were added to the pellet with tituration. Again, 10 ml HBSS was added and the cells were filtered through a 40 micron mesh. Cells were pelleted a final time and resuspended in plating media (Pneumacult Ex, 1X Gem21, 1X N2 Neuroplex Supplement, 100ng/ml RSPO-1 [Sinobiological, human recombinant]; 50 ng/ml Noggin [Sinobiological, human recombinant]; 10 mm ROCK inhibitor [Sigma cat #Y27632]). A more detailed description of the HBC culture model is in preparation for publication (Peterson et. al, *in preparation*). Cultured HBCs were treated with 10 µM HDAC inhibitor Oxamflation (Santa Cruz cat #205960) for 6 hours followed by a brief wash in PBS, fixation, and staining for acetyl-Histone 3 Lysine 9 (H3K9ac) (Millipore cat #07-352).

2.14 In situ hybridization

Probe preparation: Probe templates were PCR products of OR gene-specific containing T3/T7 overhangs. *In vitro* transcription was performed using either T3 RNA Polymerase (Sigma, cat# 110311; protocol as described by manufacturer) or T7 RNA polymerase (NEB, cat # E2040; protocol as described by manufacturer).

Hybridization protocol. Slides were removed from storage at -80°C and air-dried at room temperature for 30 minutes. Tissue was rehydrated in DEPC-PBS for 4 minutes,

incubated in 1% Triton X-100 for 4 minutes, permeabilized with 0.05 mg/ml Proteinase K (Thermofisher, cat #AM2546) in 0.5M Tris-HCl/0.1M NaCl/0.1M EDTA pH8 for 4 minutes, rinsed twice with DEPC-PBS followed by DEPC-water, and air-dried at room temperature for at least 1 hour. 150 µl DIG-RNA probe was applied to each slide at 2 mg/ml in 50:50 formamide/hybridization solution (Sigma, cat #H7782) and was sealed with a parafilm coverslip. Hybridization occurred overnight in a sealed humid box (containing 50:50 formamide/5X SSC) at 55°C. The following day, slides were washed twice in 2X SSC at room temperature for 30 minutes and twice in 0.1X SSC at 70°C for 30 minutes. Prior to signal detection, slides were equilibrated in Tris Buffer (0.1M Tris-HCl, 0.15M NaCl pH7.5) for 2 minutes at room temperature and blocked in TNB (made as described by the manufacturer, PerkinElmer cat #FP1012) for 30 minutes at 37°C. Anti-DIG-AP (Jackson ImmunoResearch, cat# 200-052-156) diluted at 1:1000 in TNB was incubated on the slides for 3 hours at room temperature. Finally, following three washes in Tris Buffer (10 minutes each), slides were rinsed in predevelopment buffer (100mM Tris, 100mM NaCl, 50 mM $MgCl_2$ pH9.8) and developed in 1:1 predevelopment buffer (adjusted to have the same final concentrations listed above)/10% PVA, 0.1X BCIP (50 mg/ml in DMF), 0.1X NBT (100 mg/ml in 70% DMF) overnight at 37°C.

2.15 Immunohistochemistry

Prior to immunostaining, rubber cement was applied around each section and dried onto the slide for 15 minutes on a hot plate; slides were then rinsed in PBS to remove OCT. Sections were subjected to antibody-specific pretreatments including: 5 minute incubation in 0.005% Trypsin-EDTA, 5 minute incubation in 3% hydrogen peroxide in methanol, 10 minute incubation in 0.01M citrate buffer (pH 6.0) in a commercial food steamer, and 30 minute incubation in 0.01M citrate buffer at 84°C. Sections were blocked with 10% donkey serum/5% non-fat dry milk/4% BSA/0.1% TritonX-100 in PBS and incubated overnight at 4°C in primary antibody. The next

day, staining was visualized using an array of methods as indicated in Table 1 and as described: (1) Secondary amplification (directly conjugated): Primary antibodies were washed off with 3x5 minute PBS rinses and secondary antibodies were incubated for one hour at room temperature at 1:100. (2) Tertiary amplification: Primary antibodies were washed off and biotinylated secondaries were incubated for one hour at room temperature at 1:100, followed by 3x5 minute PBS washes. Flour-conjugated streptavidin was incubated at 1:100 for one hour at room temperature. (3) Tyramide signal amplification (TSA): Biotinylated secondaries were used as described above; however after washing, horseradish peroxidase conjugated streptavidin (HRP-SA from Jackson ImmunoResearch #016-030-084) diluted in 1% casein in Tris buffer was used at 1:400 for one hour at room temperature. After washing, FITC-teramide diluted in 0.1M Borate, 0.003% hydrogen peroxide, was applied for 9 minutes at room temperature.

Following amplification, slides were placed in DAPI for 10 minutes, mounted in N-propyl gallate, and coverslipped. Slide edges were sealed with a thin layer of commercial-grade nail polish and stored at -20°C until imaging.

Primary antibodies used and specific detections methods are described in Table 1. The following secondary antibodies were used: AlexaFlour 488-donkey antichicken IgG, Cy3-donkey antichicken IgG, Cy3-donkey antigoat IgG, Cy3-donkey antimouse IgG, Cy3-donkey antirabbit IgG, AlexaFlour 647-donkey antigoat IgG, AlexaFlour 647-donkey antimouse IgG, AlexaFlour 647-donkey antirabbit IgG, Biotin-donkey antichicken IgG, Biotin-donkey antigoat IgG, Biotin-donkey antimouse IgG, and Biotin-donkey antirabbit IgG, HRP-donkey antimouse IgG, HRP-donkey antirabbit IgG; all were used at 1:100 for immunohistochemistry or 1:1000 for Western blotting. Additionally, Cy3 conjugated streptavidin was used at 1:100. All secondary and tertiary antibodies were obtained from Jackson ImmunoReasearch where they were tested for minimal crossreactivity.

2.16 Imaging and Quantification

Images were taken with a Spot RT2 color digital camera attached to a Nikon 800E epiflourescent microscope, a Zeiss 510 confocal microscope, a Zeiss LSM 800, and a Keyence BZ-E710 fluorescence microscope for mosaic images. Images were first processed using Fiji software to adjust color palette, balance and contrast applied to the entire image prior to figure assembly in Adobe Photoshop CS5.1 where images were cropped and set.

For Sox2/Neurog1 transplants, quantification was done on the Nikon 800E epifluorescent microscope with a dual red/green filter set to allow direct observation and simultaneous counting of Tdtomato (red) lineage traced cells with markers of choice stained to green. Consecutive 20 μm sections from the anterior to posterior OE were stained and counted systematically to identify all clones where a clone is defined as being a tight group of cells which do not have other labeled cells within ten cell bodies in any of the x, y, or z (consecutive slides) directions. Statistical analysis and graphs were done using either Sigmaplot or R software with a minimum cutoff of $p<0.05$ for statistical significance. In graphs, mean values and standard deviation are reported.

For the NQO1/OCAM transplantation experiments, quantification was done on the Zeiss 510 confocal microscope in multi-track mode to allow for simultaneous scanning of TdT, NQO1, and OCAM. All TdT (+) OSNs were counted for each host animal from 20 micron sections across the entire anterior to posterior OE. TdT (+) OSNs counted were either NQO1 (+) or OCAM (+) and the % of each was calculated from the total OSNs (TdT/NQO1 + TdT/OCAM cells). Results were graphed using Prism software; %NQO1 (+) and %OCAM (+) cells were averaged across animals and error bars represent standard error of the mean. For HDACi transplant experiments: Chi-square with Yate's correction was performed to determine significance between groups using Prism software.

EdU incorporation quantifications were done on a Nikon 800E epifluorescent

microscope with a dual red/green filter set to allow direct observation and simultaneous counting of single- and double-labeled cells. For P2/EdU co-labeling experiments, eight evenly spaced sections through the anterior to posterior epithelium were counted; for the rest of the EdU co-staining experiments, four evenly spaced sections were analyzed. All cell counts were made in the P2-expressing regions of the OE excluding counts of OR28 (+) and M72 (+) cells which were taken in OR28 and M72 expressing regions respectively. All double positive cells were normalized to the total number of EdU (+) cells counted per region and in the case of the ORs, we normalized to both EdU (+) and OR (+) cells counted per region. For graphical representation, we summed the total cells counted within each animal and averaged counts from three animals, shown as a line graph with a standard error based on biological replicates at each timepoint.

For quantifying neuronal maturation following LSD1 knockout, I again counted four evenly spaced sections from the anterior to posterior OE. Due to a reduced efficiency of recombination, TdT-positivity did not always signify LSD1 knockout in these animals, in other words, some TdT (+) cells in *Lsd1*$^{fl/fl}$ animals stained positive for LSD1 protein, but the extent of incomplete recombination varied from region of the epithelium to region. Consistently, the dorsolateral OE was characterized by efficient knockout of LSD1. As a consequence, we selected this area for purposes of quantification. Counts of OMP (+)/TdT (+) cells were normalized to the total number of OMP (+)/TdT (+) and Tuj (+)/TdT (+) cells (total neurons) for all animals. For graphical representation, I summed counts within animals and plotted the average and SEM of the three animals. Prism software was used to perform one-way ANOVAs and if significant, a post-hoc Tukey's multiple comparison was performed to determine p-values between groups.

Table 1. Antibodies and staining protocols used in this thesis

Primary Antibody	Source/vendor (catalog #)	Protocol	Cell types(s) Marked
Ch α-beta-gal	Abcam (ab9361)	Pre-Tx: 5 min 0.005% trypsin-EDTA (1:750) DC	All beta-gal (+) cells
Rb α-CK14	Proteintech (10143-1-AP)	Pre-Tx: 5 min 3% H202 in methanol + 10 min steam (1:1000) DC	HBCs
Ms α-CoREST	NeuroMab (75-039)	Pre-Tx: 5 min 3% H202 in methanol + 10 min steam (1:500) FITC-TSA	GBCs and immature OSNs
Rb α-GAP-43	Abcam (ab75810)	Pre-Tx: 5 min 3% H202 in methanol (1:1000) FITC-TSA	Immature OSNs
Ch α-GFP	Abcam (ab13970)	(1:250) DC	All GFP (+) cells
Rb α-H3K9ac	Millipore (07-352)	(1:5000) Tertiary	Acetyl-histone H3
Ms α-HDAC2	Abcam (12169)	Pre-Tx: 5 min 3% H202 in methanol + 10 min steam (1:100) DC	GBCs and immature OSNs
Ms α-Ki67	Becton Dickinson (556003)	Pre-Tx: 5 min 3% H202 in methanol + 10 min steam (1:100) Tertiary	Proliferating cells
Rb α-LSD1	Abcam (ab62582)	Pre-Tx: 5 min 3% H202 in methanol + 10 min steam (1:20,000) FITC-TSA	GBCs and immature OSNs
Gt α-mCherry	Sicgen (AB0040-500)	Pre-Tx: 5 min 3% H202 in methanol + 10 min steam	All TdT (+) cells
Rb α-MOR28	Gilad Barnea PhD, Brown University	Pre-Tx: 5 min 3% H202 in methanol + 10 min steam (1:5,000) Tertiary	OSNs expressing MOR28

Rb α-NQO1	Abcam (ab80588)	Pre-Tx: 5 min 3% H202 in methanol + 30 mins 84°C (1:200) DC	Mature OSNs in the dorsal OE
Gt α-OCAM	R&D Systems (AF778)	Pre-Tx: 5 min 3% H202 in methanol + 30 mins 84°C (1:200) FITC-TSA	OSNs in the ventral OE
Gt α-OMP	SantaCruz (sc-49070)	Pre-Tx: 5 min 3% H202 in methanol for + 10 min steam (1:200) DC	Mature OSNs
Ms α-Pax6	DSHB (AB-528427)	Pre-Tx: 5 min 3% H202 in methanol for + 10 min steam (1:25) TSA	GBCs and Sus Cells
Rb α-PGP9.5	Proteintech (11064-1-AP)	Pre-Tx: 5 min 3% H202 in methanol for + 10 min steam (1:200) DC	Immature and mature OSNs
Rb α-RFP	Rockland (600-401-379)	Pre-Tx: 5 min 3% H202 in methanol + 10 min steam (1:200) DC	All TdT (+) cells
Ch α-RFP	Rockland (600-901-379)	Pre-Tx: 5 min 3% H202 in methanol + 30 mins 84°C (1:200) DC	All TdT (+) cells
Gt α-Sox2	SantaCruz (sc-17320)	Pre-Tx: 5 min 3% H202 in methanol + 10 min steam (1:200) TSA	GBCs and Sus Cells
Rb α-Sox9	Millipore (AB5535)	Pre-Tx: 5 min 3% H202 in methanol + 10 min steam (1:100) DC	Duct/Gland Cells
Rb α-TRPM5	Alomone Labs (ACC-045)	Pre-Tx: 5 min 3% H202 in methanol + 10 min steam (1:400) TSA	Microvillar Cells

Ms α-Tuj1	Biolegend (801202)	Pre-Tx: 5 min 3% H202 in methanol + 10 min steam (1:100) DC	Immature OSNs
Rb α-V-Glut	Synaptic Systems (135-402)	Pre-Tx: 5 min 3% H202 in methanol (1:8,000) Tertiary	Post-synaptic Mitral cells

Table Key: Antibody hosts: Ch, Chicken; D, donkey; Gt, goat; Ms, mouse; Rb, rabbit. Antibody visualization: a variety of secondary fluorophores were used at 1:100 for direct conjugation (DC), including Cy3, 488, and 647 (Jackson ImmunoReaseach); for Tertiary amplification: biotinylated secondary antibody (bDα-x) was followed by incubation in fluor-stratavidin (fluor-SA); for FITC teramide signal amplification (FITC-TSA): biotinylated secondaries were followed by incubation in horseradish peroxidase conjugated streptavidin (SA-HRP, Jackson ImmunoResearch) followed by incubation in FITC-teramide diluted in 0.1M borate, 0.003% hydrogen peroxide. Pretreatments (Pre-Tx): 30 mins 84°C: slides were incubated in 0.01M citrate, pH6 at 84°C for 30 min; steam: sections were covered with 0.01M citrate, pH6 and steamed in a commercial food steamer for 10 min.

Chapter 3. Results

The Dedifferentiative Capacity of Neuronally Committed Globose Basal Cells

Adapted from:

Lin B, Coleman JH, Herrick DB, Peterson J, Schwob JE. Endogenous Reprogramming of Neuronally Committed Cells After Injury. Manuscript in preparation.

Contributions:

Immunohistochemistry quantifications and qPCR were performed by Brian Lin; all other data were a combined effort between Lin & Coleman.

Rationale:

The first half of my thesis work relies on an OE stem cell transplantation assay used previously in our lab (Chen et al., 2004; Schnittke et al., 2015). Prior to beginning these experiments, I sought to optimize this assay and to demonstrate that transplanted progenitors recapitulate the differentiative capacities seen *in situ*.

3.1 Olfactory bulbectomy results in an expansion of Ki67 proliferative cells, Sox2-eGFP (+) GBC_{MPPs}, and Neurog1-eGFP (+) GBC_{INPs}.

Previous studies in our lab demonstrated that isolated GBCs are capable of engrafting into a lesioned host epithelium and can generate all cell types of the OE including neurons, Sus cells, and duct/gland cells (Chen et al., 2004). Conversely, differentiated Sus and duct cells were incapable of generating other cells types following transplantation and HBCs did not engraft (Chen et al., 2004). More recently, Nikolai Schnittke demonstrated that activated HBCs can engraft and give rise to all OE cells types under the transplantation paradigm (Schnittke et al., 2015). Thus, actively proliferating cells are capable of engraftment whereas quiescent or differentiated cells are not.

In order to increase the total numbers of proliferative cells for harvesting and transplantation, we performed olfactory bulbectomies (OBX) on donor animals (Schwartz Levey et al., 1991). To begin, we characterized proliferative cell expansion at distinct timepoints following bulbectomy (without transplantation). As demonstrated by Ki67 staining at 4-8 days post unilateral OBX, the proliferative cell population expands following bulb ablation (Fig. 1). Similarly, Neurog1-eGFP (+) GBC immediate neuronal precursors (GBC_{INPs}) expand beginning as early as 5 days post OBX (Fig. 2).

As an additional measure of OBX-induced GBC expansion, we used flow cytometry to quantify proportions of Neurog1-eGFP (+) GBC_{INPs} and Sox2-eGFP (+) GBC multipotent progenitors (GBC_{MPPs}) under unlesioned and OBX conditions. At five

days post OBX, the Sox2 and Neurog1 cell populations increased by ~4 fold and ~5 fold respectively (Fig. 3). Given this information, we harvested cells from donor animals at 5 days post OBX to increase the number of proliferative cells capable of engrafting into the host epithelium.

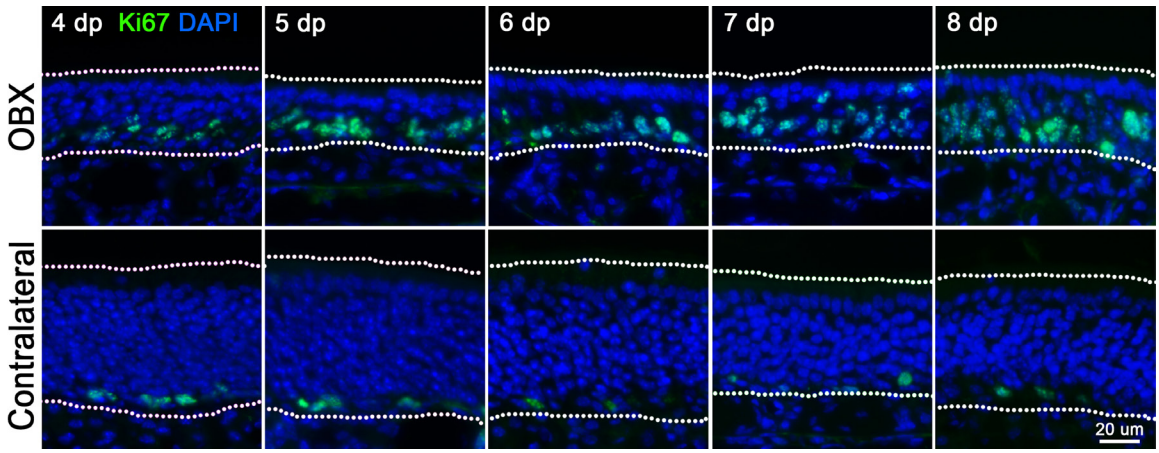

Figure 1. Ki67 (+) cells expand following OBX.
Ki67 (+) cells from 4 days post OBX to 8 days post OBX. **Top:** OBX side. **Bottom:** Contralateral unlesioned side. Dotted white line indicates the basal lamina (bottom) and apical surface (top).

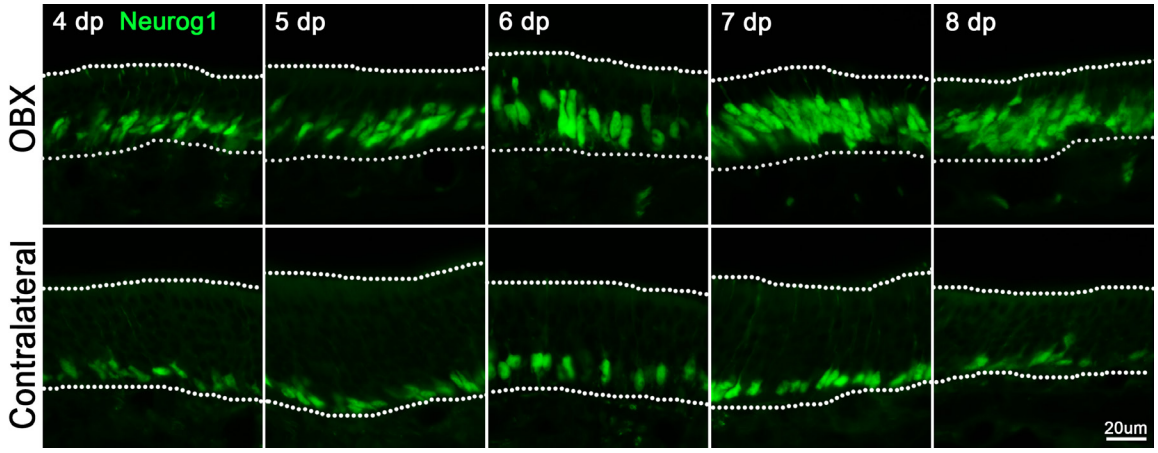

Figure 2. Neurog1 (+) GBCs expand following OBX.
Neurog1 (+) cells from 4 days post OBX to 8 days post OBX. **Top:** OBX side. **Bottom:** Contralateral unlesioned side. Dotted white line indicates the basal lamina (bottom) and apical surface (top).

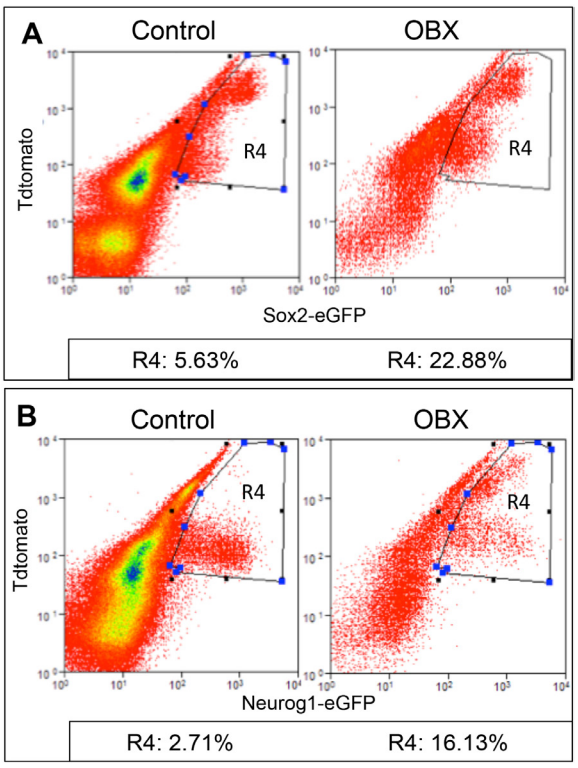

Figure 3. OBX increases total numbers of both Sox2-eGFP (+) and Neurog1-eGFP (+) GBCs.
(A) OBX increases GFP (+)/TdT (+) cells in Sox2-eGFP/Pan-TdT animals from 5.63% to 22.88% of total OE cells. **(B)** OBX increases GFP (+)/TdT (+) cells percentages in Neurog1-eGFP/Pan-TdT animals from 2.71% to 16.13% of total OE cells.

3.2 Transplanted Sox2-eGFP (+) and Neurog1-eGFP (+) GBCs from OBX donors give rise to all OE cell types

To test the differentiative capacity of progenitor cells, we transplanted sorted Sox2-eGFP (+)/pan-Tdtomato (+) (TdT) and Neurog1-eGFP (+)/pan-TdT GBCs into regenerating host epithelia (separately). The constitutive TdT was used to trace graft-derived cells in the host epithelium. Transplanted Sox2-eGFP (+) GBC_{MPPs} isolated from donor animals at 5 days post OBX gave rise to all OE cell types (Figure 4, Figure 6A), including Sus cells (Fig. 4B,C,D), neurons (Fig. 4C), microvillar cells (Fig. 4D), duct/ gland cells (Fig, 4E), and GBCs (Fig. 4E). Sus cells were identified by morphology and apical Sox2 positivity, OSNs were identified by morphology and PGP9.5 positivity, microvillar cells were identified through their teardrop morphology and TRPM5 positivity, duct/gland cells were identified by Sox9 expression, and GBCs were identified through basal Sox2 positivity. These results correlate with the multipotent progenitor capacity of Sox2-GBCs as previously described (Chen et al., 2004; Guo et al., 2010).

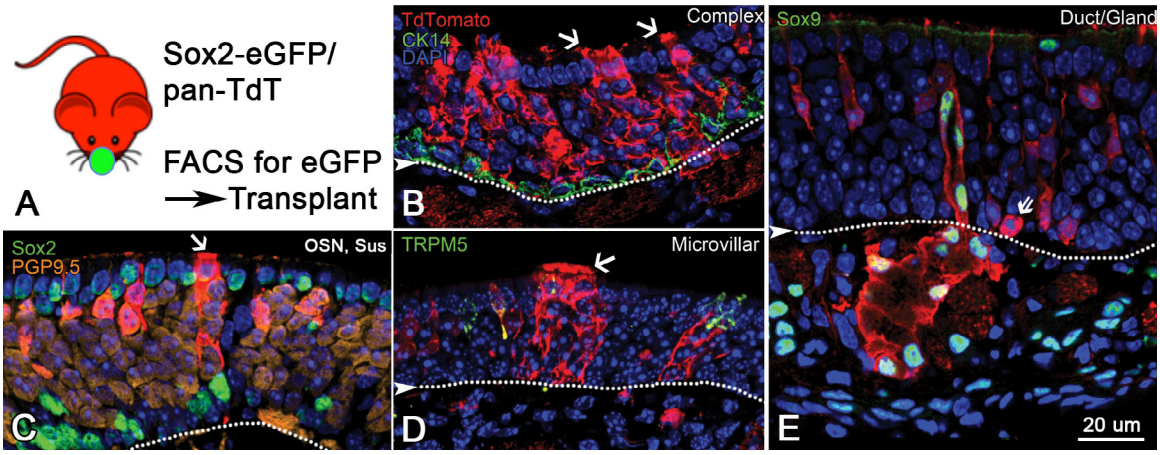

Figure 4. Transplanted Sox2-eGFP (+) GBCs from OBX donor animals give rise to all OE cell types in a host epithelium.
(A) OE from donor Sox2-eGFP/pan-TdT animals was FACS sorted for eGFP and transplanted into lesioned host OE. Engrafted cells gave rise to complex clones containing **(B)** Sus cells **(C)** OSNs and Sus cells **(D)** Sus cells and microvillar cells and **(E)** Duct/gland units and GBCs. Arrows point to Sus cells and double arrow points to a GBC. Dotted white line indicates the basal lamina.

Surprisingly, transplanted Neurog1-eGFP (+)/pan-TdT (+) GBC_{INPs} isolated from donor animals at 5 days post OBX also gave rise to all OE cell types (Fig. 5, Fig. 6A) including Sus cells (Fig. 5C,E), neurons (Fig. 5C,G), respiratory cells (Fig. 5D), GBCs (Fig. 5E), microvillar cells (Fig. 5F,G), and gland cells (Fig. 5G). This was an unexpected result as Neurog1 (+) GBCs are generally considered to be immediate neuronal precursors (INPs) that directly give rise to OSNs (Cau et al., 2002; Manglapus et al., 2004; Packard et al., 2011). To clarify whether our results reflected an artifact of the transplantation procedure itself, or if bulbectomy induced a dedifferentiative capacity of Neurog1 (+) GBCs, we performed transplants with uninjured Neurog1-eGFP donor animals. In this case, we found that transplanted Neurog1-eGFP (+) GBCs largely gave rise to OSNs (Fig. 5B, Fig. 6A), suggesting that OBX injury unlocks a dedifferentiative capacity in previously neuronally committed progenitors.

In our quantification of the cell types made by each transplant condition, we found that while OBX Neurog1-eGFP (+) GBCs have the capacity to generate all OE cell types, they are biased towards neuronal differentiation as compared to the Sox2

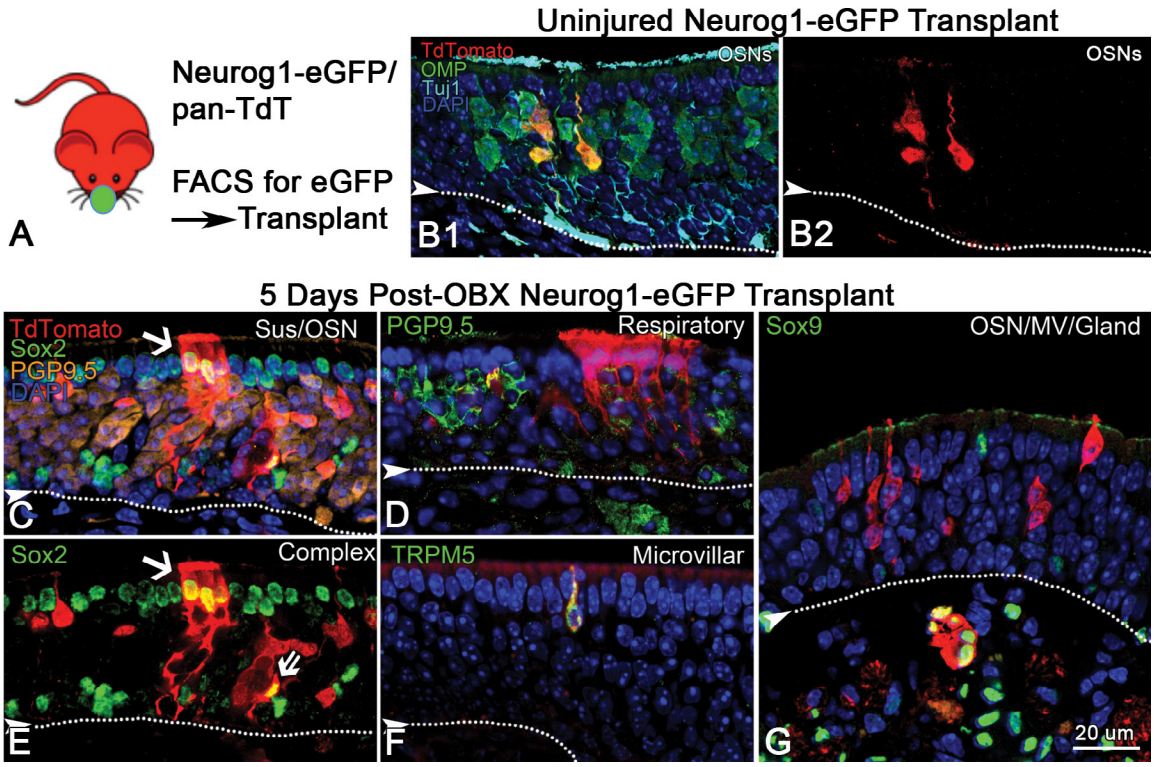

Figure 5. Transplanted Neurog1-eGFP (+) GBCs from uninjured animals give rise to neurons; transplanted Neurog1-eGFP (+) GBCs from OBX animals give rise to all OE cell types.
(A) OE from donor Neurog1-eGFP/pan-TdT animals was FACS sorted for eGFP and transplanted into lesioned host OE. **(B)** Uninjured donor cells gave rise to OSNs. **(C)** Injured donor cells gave rise to complex clones containing Sus and OSNs **(D)** Respiratory cells **(E)** Sus cells and GBCs **(F)** Microvillar cells and **(G)** OSNs, microvillar cells, and gland cells. Arrows point to Sus cells and double arrow points to a GBC. Dotted white line indicates the basal lamina.

transplants (Fig. 6A). In assessing the clone sizes of the three transplanted populations as a readout for proliferative capacity, we found that bulbectomy increased Neurog1-eGFP (+) GBC proliferation to statistically indistinguishable levels compared to the Sox2 transplants (Fig. 6B).

To ensure that our FACS specifically isolated Sox2 (+) and Neurog1 (+) GBCs (respectively), we performed post-hoc qPCR analysis on each sorted population. Figure 7A-B represents the sorting strategy used for each cell population. In each case, we selected for single cells via pulse width and side scatter, sorted out HBCs with CD54 antibody staining, and specifically selected the middle (Mid) population of TdT (+)/GFP

(+) cells (Fig. 7A,B). We collected the middle population to avoid Sox2 (+) Sus cells that express high levels of GFP (Fig. 7A), and to avoid CD54 (+) cells in the Neurog1 sort (Fig. 7B). qPCR showed that while *Sox2* levels were not enriched in the Sox2-eGFP (+) basal cells when compared to the remaining cells, it becomes significantly enriched when we first removed GFP(high) Sus cells (Fig. 7C). Surprisingly, *Sox2* was highly upregulated in Neurog1-eGFP (+) GBCs at 5 days post OBX (Fig. 7C). In reference to Neurog1 mRNA levels, we found no *Neurog1* in sorted Sox2 (+) GBCs, and an enrichment for *Neurog1* in both the OBX and uninjured Neurog1-eGFP (+) sorted GBCs (Fig. 7D).

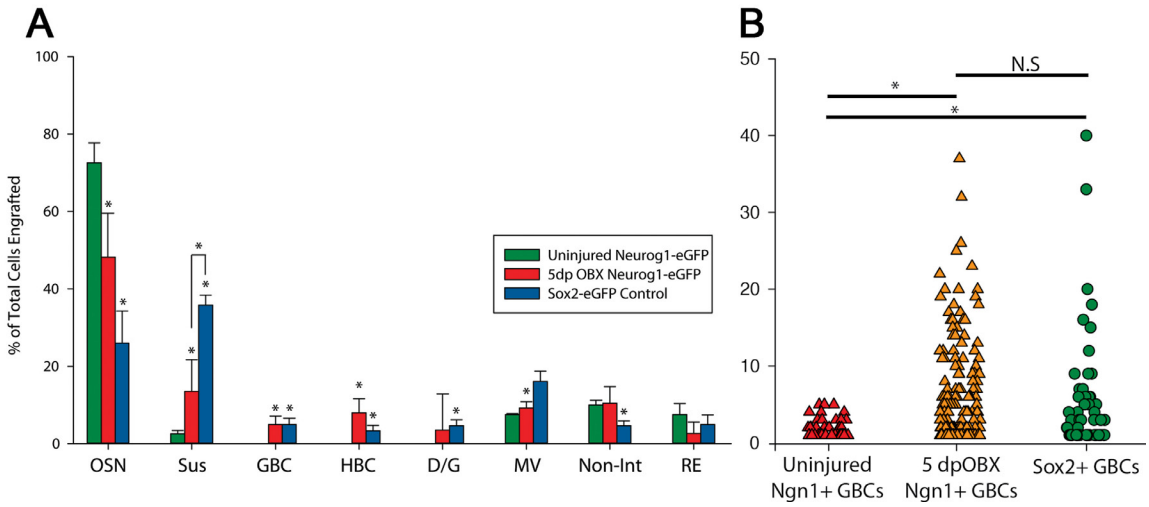

Figure 6. Quantification of graft-derived cells from Sox2-eGFP and Neurog1-eGFP transplants.
(A) Cell types produced from each transplant condition as a percentage of total cells engrafted: Sox2-eGFP (+) GBCs produce all cell types, control Neurog1-eGFP (+) GBCs primarily produce OSNs, and OBX Neurog1-eGFP (+) GBCs produce all OE cell types with a bias towards OSNs. Error bars represent SD between three animals. **(B)** Clone size for each transplant condition to assay proliferative capacity: OBX increases the proliferation of Neurog1-eGFP (+) GBCs to indistinguishable levels to those of Sox2-eGFP (+) GBCs. For both analyses, data were first tested for normality using the Shapiro-Wilk Normality test; if the data passed normality, a standard parametric ANOVA test was performed to determine the validity of performing pairwise post-hoc Holm-Sidak tests; if the data failed the normality test, a non-parametric Kruskal-Wallis One-Way ANOVA on Ranks was used instead, followed by Dunn's Method. Error bars represent SEM and asterisks indicate statisitical difference from the uninjured condition unless indicated otherwise.

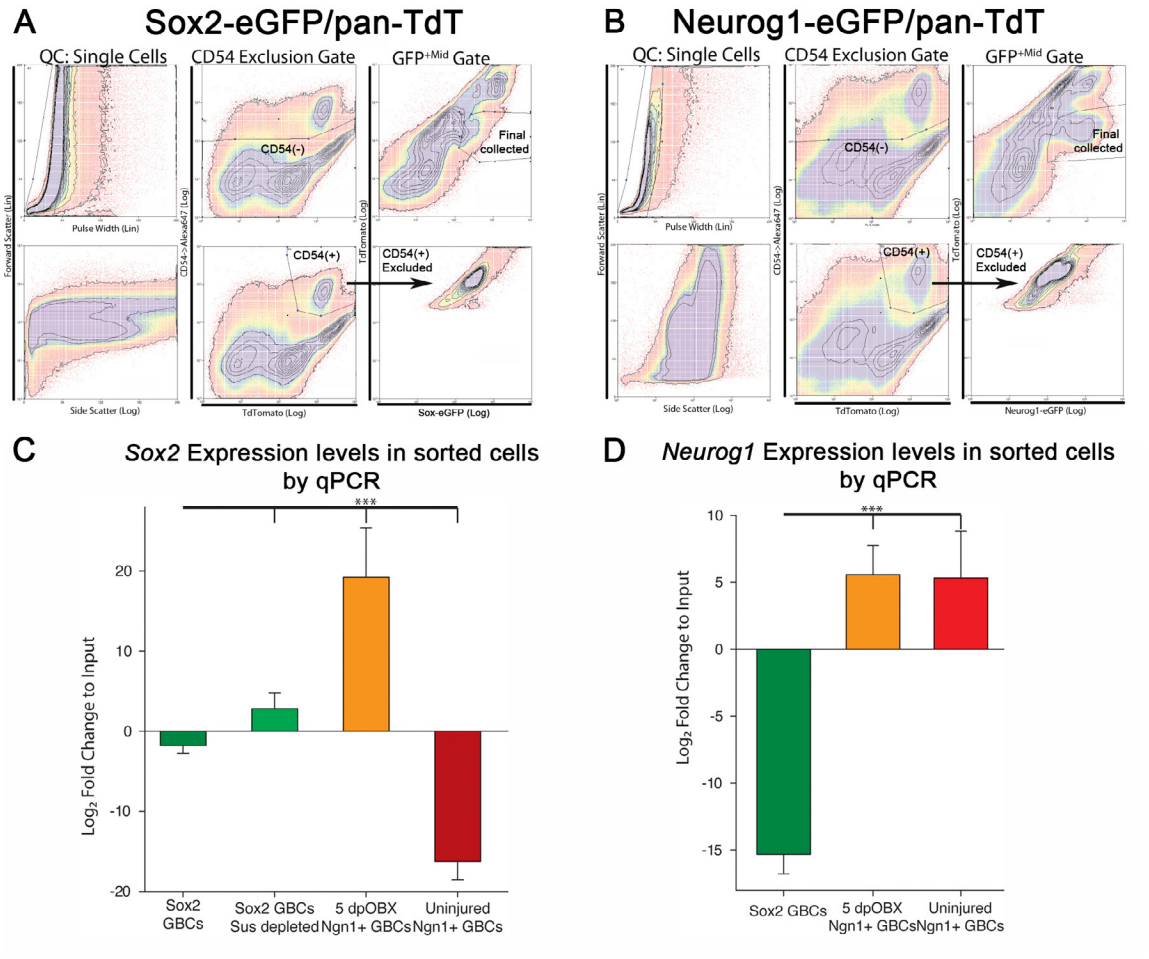

Figure 7. FACS strategy and post-hoc qPCR validation of sorted cell populations. **(A)** Sox2-eGFP/Pan-TdT sorting strategy: single cells were selected via pulse width and side scatter, HBCs were removed via CD54, and the middle (Mid) population of GFP (+)/TdT (+) cells were collected **(B)** Neurog1-eGFP/Pan-TdT sorting strategy: single cells were selected via pulse width and side scatter, HBCs were removed via CD54, and and the middle (Mid) population of GFP (+)/TdT (+) cells were collected **(C)** FACS post-hoc *Sox2* expression levels in each sorted population by qPCR: *Sox2* is enriched in Sox2 (+) GBCs when Sus cells are removed; *Sox2* is upregulated in Neurog1 (+) GBCs at 5 days post OBX. **(D)** FACS post-hoc *Neurog1* expression levels in each sorted population by qPCR: *Neurog1* is enriched in both OBX and uninjured Neurog1 (+) GBCs. Error bars represent SEM and asterisks indicate statistical difference from Sox2 GBCs via a predetermined t-test.

3.3 A portion of Neurog1-eGFP (+) GBCs express Sox2 following OBX

Given our observation of increased *Sox2* mRNA in Neurog1-eGFP (+) GBCs following OBX, we assessed Sox2 – and its co-expressed transcription factor Pax6 (Guo et al., 2010) – expression patterns in Neurog1-eGFP (+) precursors *in situ* via

immunohistochemistry. Under basal conditions, Neurog1-eGFP (+) GBCs do not co-express Sox2 or Pax6 (Fig. 8A,B,C). However, both transcription factors appear in Neurog1-eGFP (+) cells by 4 days post OBX and continue to co-localize up to 8 days post OBX (Fig. 8A,B). In our quantification of Sox2 (+)/Neurog1-eGFP (+) colocalization, we found that double positive cells peak around 4 days post OBX and begin to taper by 6 days post OBX (Fig. 8C). As Sox2 is involved in progenitor capacity in many adult epithelial populations (Arnold et al., 2011), we hypothesize that the upregulation of Sox2 in Neurog1-eGFP (+) GBCs following OBX may account for their

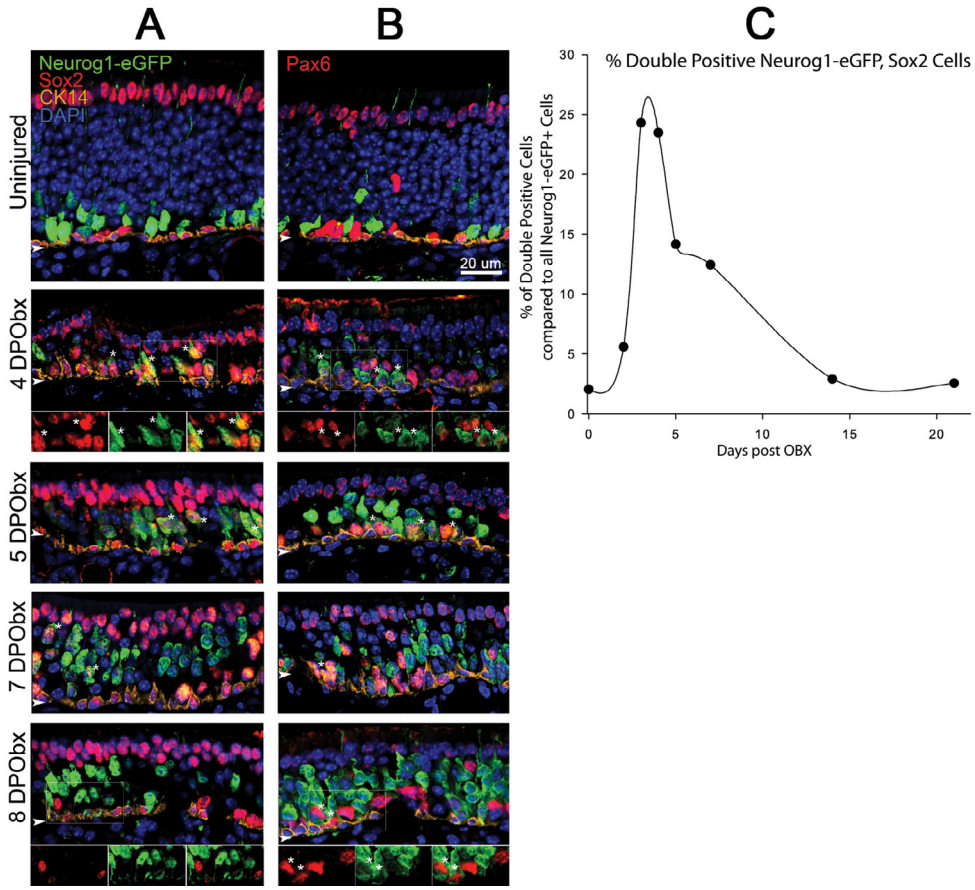

Figure 8. Neurog1-eGFP (+) GBCs express Sox2 and Pax6 following OBX. **(A)** Neurog1-eGFP/Sox2 co-staining timecourse from 4-8 days post OBX. **(B)** Neurog1-eGFP/Pax6 co-staining timecourse from 4-8 days post OBX. **(C)** Quantification of the % Neurog1-eGFP (+)/Sox2 (+) cells out of total Neurog1-eGFP (+) cells from 0–3 weeks post OBX. Four sections from the anterior to the posterior OE were counted for each timepoint; all cells were counted.

dedifferentiative and regenerative capacity. This line of research became the focus for Brian Lin and will be reported in full in his dissertation work.

Summary

OBX increases the number of proliferative cells for transplantation and unlocks a previously uncharacterized dedifferentiative capacity in Neurog1-eGFP (+) GBCs (Fig. 1-6); this capacity may depend on upregulation of Sox2 in Neurog1-eGFP (+) GBCs (Fig. 7,8). While this line of research is of high interest to our lab and the olfactory and stem cell fields, dedifferentiation complicates analysis of the transplantation assay. Thus, in the remainder of my experiments, I isolated cells from uninjured animals for transplantation. Under normal conditions, we demonstrated that transplanted progenitors mimic differentiation as described *in situ* (Fig. 4, Fig. 5B).

Chapter 4. Results

Spatial determination of neuronal diversification in the olfactory epithelium

Adapted from:

Coleman JH, Lin B, Peterson J, Lane RP, Schwob JE. Location Matters: Spatial determination of neuronal diversification in the olfactory epithelium. Manuscript in preparation.

Rationale:

Neurons in the olfactory epithelium (OE) differ from one another in the olfactory receptor (OR) they express and in the neuronal markers they express – such as the enzyme NADPH:quinone oxidoreductase (NQO1) and the olfactory cell adhesion molecule (OCAM) (Schwob and Gottlieb, 1986; Buck and Axel, 1991; Ressler et al., 1993; Vassar et al., 1993; Gussing and Bohm, 2004). Importantly, both ORs and NQO1/OCAM are regionally expressed within the OE and these patterns can be precisely regenerated following epithelial injury (Schwob and Gottlieb, 1986; Gussing and Bohm, 2004; Iwema et al., 2004; Miyamichi, 2005). These observations suggest that spatial cues within the OE may direct both OR and NQO1/OCAM gene expression and ultimately play a significant role in neuronal diversification. Nonetheless, many believe that OE stem cells are hardwired upon cell birth to become a distinct neuronal type irrespective of external factors. Thus, to directly test whether spatial cues drive neuronal diversification, I performed a series of transplantation experiments assessing stem cell spatial plasticity with respect to both NQO1/OCAM and OR expression.

4.1 Spatial cues direct neuronal diversification in respect to NQO1/OCAM expression

To determine whether spatial cues direct neuronal diversification, I transplanted stem cells from the dorsal, NQO1 (+) epithelium of TdTomato (+) (TdT) donor mice to the ventral, OCAM (+) epithelium of methyl bromide (MeBr)-lesioned host mice (Fig. 1). MeBr lesion destroys the mature cell populations of the OE, leaving intact only the proliferative stem cells (Schwob et al., 1995) and provides a regenerative setting for transplanted stem cells to engraft into (Chen et al., 2004). In mice, MeBr lesion leaves the dorsal OE largely intact, limiting engraftment to the ventral region. After allowing the host epithelium to regenerate for three weeks (Fig. 1B), providing sufficient time for neuronal maturation (Schwob et al., 1995) and pattern regeneration (Fig. 2), I stained the

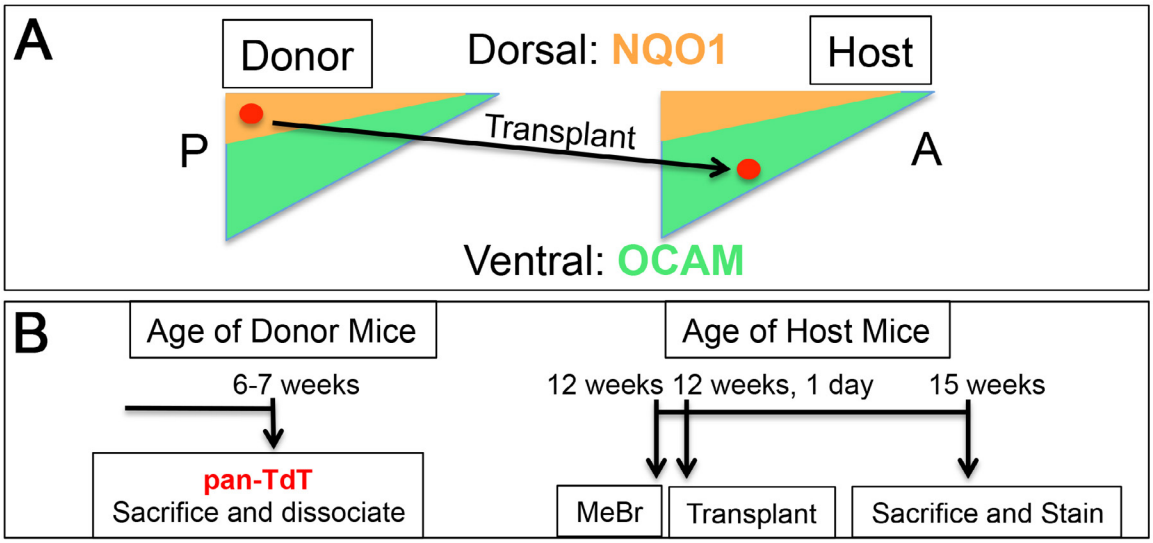

Figure 1. NQO1/OCAM transplant experimental design and animal timeline
(A) Experimental design: The dorsal epithelium was harvested from pan-TdT (+) mice and transplanted into methylbromide-lesioned host epithelium. After 3 weeks, host epithelium was harvested and stained for NQO1 and OCAM. A= Anterior; P= Posterior. **(B)** Animal timeline: Donor mice were sacrificed at 6-7 weeks; Host animals were lesioned at 12 weeks, transplanted the next day and sacrificed three weeks later.

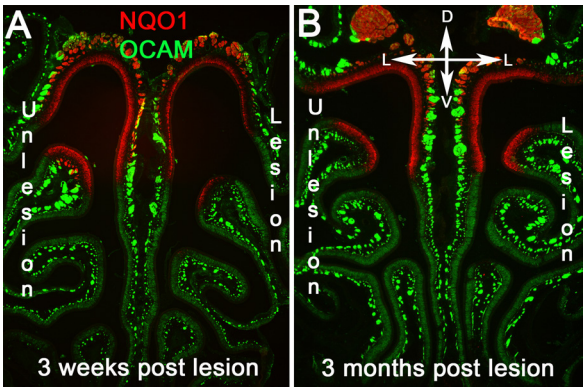

Figure 2. NQO1/OCAM borders are regenerated at 3 weeks and 3 months post MeBr lesion.
(A) NQO1/OCAM patterns are restored at three weeks post MeBr-lesion as shown by unilateral lesion. **(B)** NQO1/OCAM patterns are restored at 3 months post MeBr-lesion as shown by unilateral lesion. D= Dorsal; V= Ventral; L= lateral.

host epithelium for OCAM and NQO1 to determine if the neuronal progeny of the transplanted stem cells expressed the marker of the donor or host region. It should be noted that I transplanted dissociated OE; however, only proliferative stem cells are capable of engrafting into a regenerating OE and making OSNs (Chen et al., 2004). To be certain that I was not transplanting mature OSNs, I performed control transplant experiments with sorted OMP-GFP (+) mature OSNs and demonstrated that these cells are incapable of engraftment (Fig. 3A-D). Importantly, both NQO1 and OCAM are expressed in mature

OSNs and not transplantable progenitors, the most downstream of which is marked by Neurog1-eGFP (Fig. 3E-J).

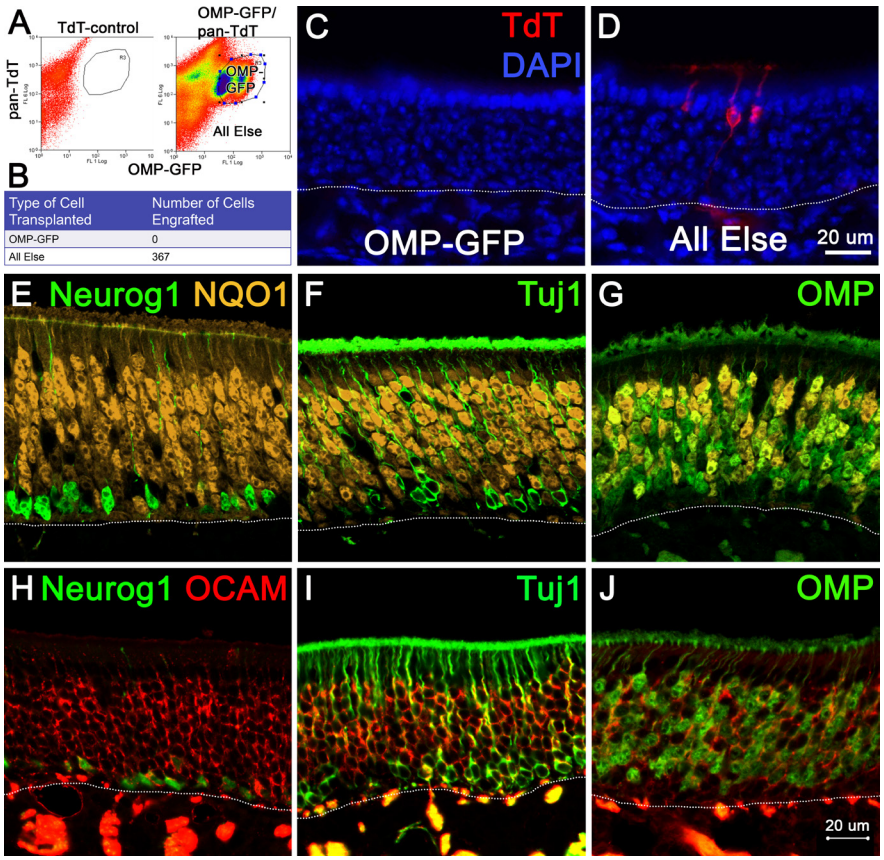

Figure 3. OSNs do not engraft; NQO1 (+) and OCAM (+) cells are OSNs.
(A) FACS strategy to isolate OMP-GFP/pan-TdT cells and "All Else" cells. **(B)** Quantification of number of cells engrafted from OMP-GFP sorted and "All Else" cells. **(C)** Host epithelium of sorted OMP-GFP transplants contain no graft-derived cells. **(D)** Host epithelium of "All Else" transplants contains graft-derived OSNs. **(E)** NQO1 (+) cells do not overlap with Neurog1-eGFP (+) cells or **(F)** Tuj1 (+) immature OSNs, but do costain for the mature neuronal maker **(G)** OMP. **(H)** OCAM (+) cells slightly overlap with Neurog1-eGFP (+) cells and **(I)** Tuj1 (+) immature OSNs, but largely costain for the mature neuronal maker **(J)** OMP. Dotted white line indicates the basal lamina.

In the dorsal to ventral transplants, an average of 85% of all graft-derived OSNs expressed the neuronal marker of the host region (OCAM) (Fig. 4A,F) and 15% expressed the neuronal marker of the donor region (NQO1) (Fig. 4B,F). As a control,

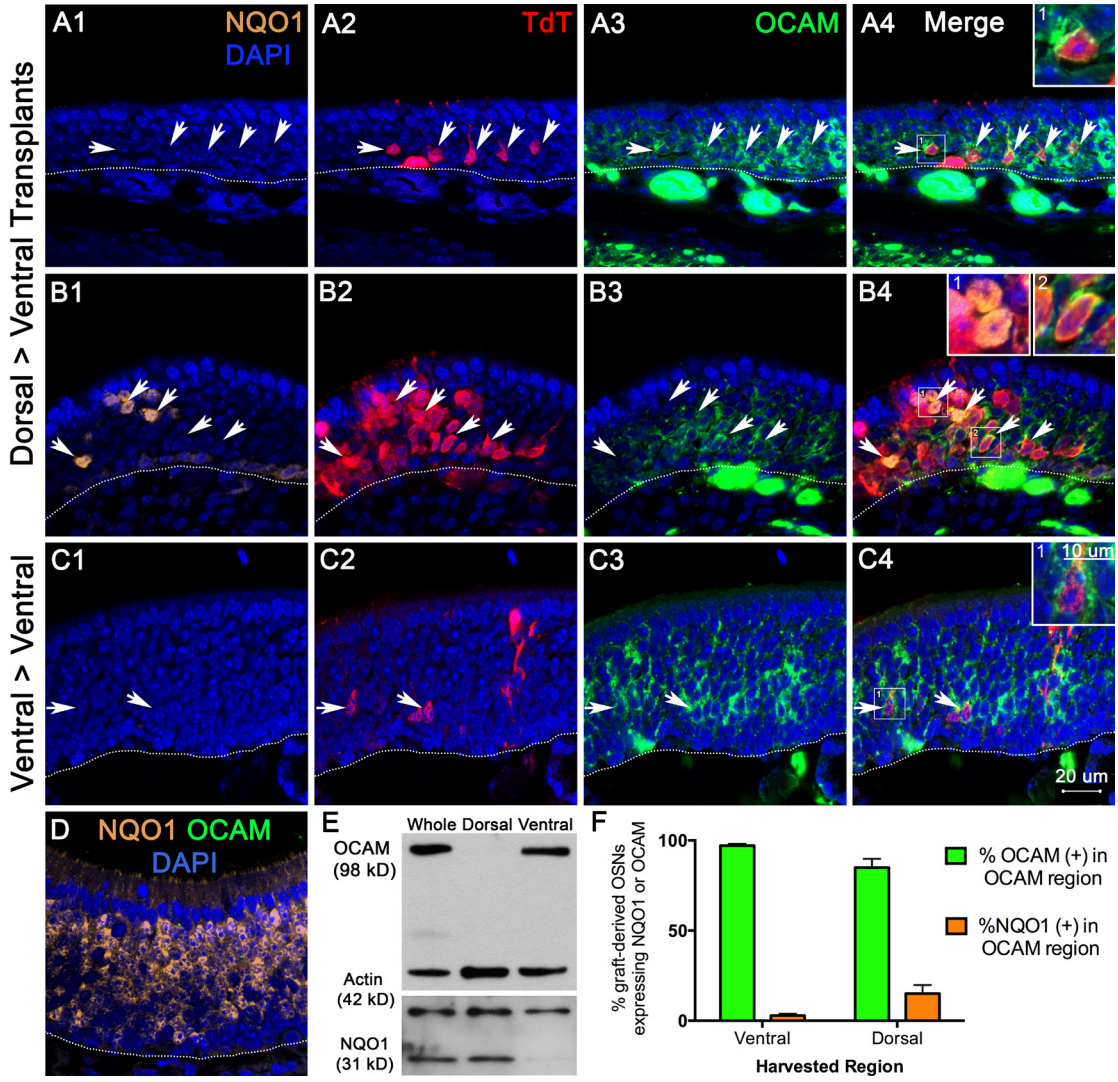

Figure 4. Spatial cues direct neuronal diversification in respect to NQO1 and OCAM expression.

(A) Example of stem cells harvested from the dorsal NQO1 (+) OE and engrafted into the OCAM (+) OE that express the ventral marker OCAM. **(B)** Example of a large, neuron-only cluster containing graft-derived OSNs expressing NQO1 and OCAM (separately). **(C)** Control transplant: ventral donor stem cells engraft into the ventral OE and mature to express OCAM. **(D)** Every section counted had robust NQO1 staining in the dorsal epithelium. **(E)** Western blot demonstrating region-specific expression in dissected tissues. **(F)** Quantification of the % of OCAM (+) or NQO1 (+) graft-derived neurons out of the total number of graft-derived neurons. Ventral to ventral: graphed is the mean of two animals (total 1534 graft-derived OSNs). Dorsal to ventral: graphed is the mean of three animals (total 1473 graft-derived OSNs); error bars represent SEM. Dotted white line indicates the basal lamina.

97% of all ventral to ventral transplants expressed OCAM after transplantation (Fig. 4C,F). In all sections quantified, I verified robust NQO1 staining in the dorsal recess

(Fig. 4D) to be certain that a lack of NQO1 staining was never due to antigen destruction or immunostaining errors. As a direct measure of the purity of my dorsal and ventral dissections, I blotted my preparations for OCAM and NQO1 (Fig. 4E). The dorsal dissections had robust NQO1 positivity and no OCAM protein; conversely, the ventral dissections were robust for OCAM positivity and had minimal NQO1 protein (Fig. 4E). Because I observed an 85:15 ratio of plastic vs. non-plastic (Fig. 4F), I assessed whether cluster location, size, or type influenced the plasticity of transplanted stem cells. I found that almost all engraftment locations contained a portion of NQO1 (+) graft-derived cells (Fig. 5A) and that both neuron-only and complex clusters from small to massive size contained NQO1 (+) cells (Fig. 5B).

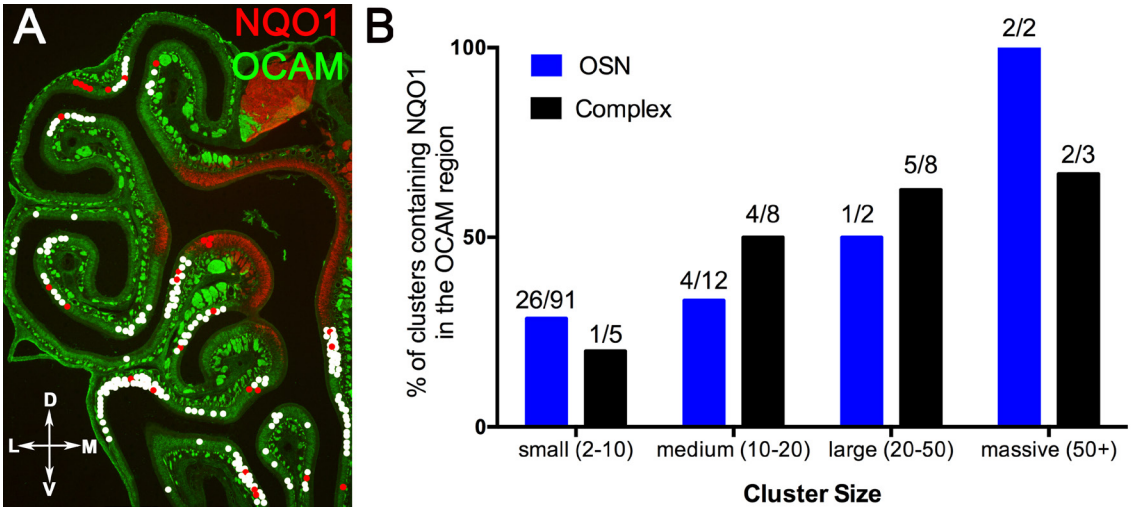

Figure 5. Engrafted clusters containing NQO1 (+) cells in the OCAM region are spread across the OE, are both neuron only and complex, and range from small to massive. **(A)** Location of graft-derived neurons in the dorsal to ventral transplants. Each dot represents 1-10 cells; white dots = OCAM (+) OSNs and red dots = NQO1 (+) OSNs. Data is summed across sections from anterior to posterior of 3 host animals. **(B)** Quantification of the % of clusters containing NQO1 (+) cells in the OCAM (+) region, binned by both cluster type (neuron only and complex) and cluster size. D= Dorsal; V= Ventral; M= Medial; L = Lateral.

Given that the majority of graft-derived neurons adapted to the ventral OCAM (+) host region, I speculated that their axons projected to the OCAM (+) region of the olfactory bulb. By looking at TdT (+) axonal projections in the olfactory bulb, I found

that the graft-derived neurons project to the bulb, entered glomeruli, and co-localized with the pre-synaptic marker, vesicular glutamate transporter 2 (V-GLUT2) (Fig. 6). Furthermore, these TdT (+) projections were found in the OCAM (+) region of the olfactory bulb (Fig. 6), again demonstrating the spatial plasticity of the transplanted stem cells. Interestingly, axons had not yet entered glomeruli in posterior sections of the olfactory bulb (Fig. 6C), suggesting that there was incomplete reinnervation across differing regions of the bulb at 3 weeks post MeBr-lesion.

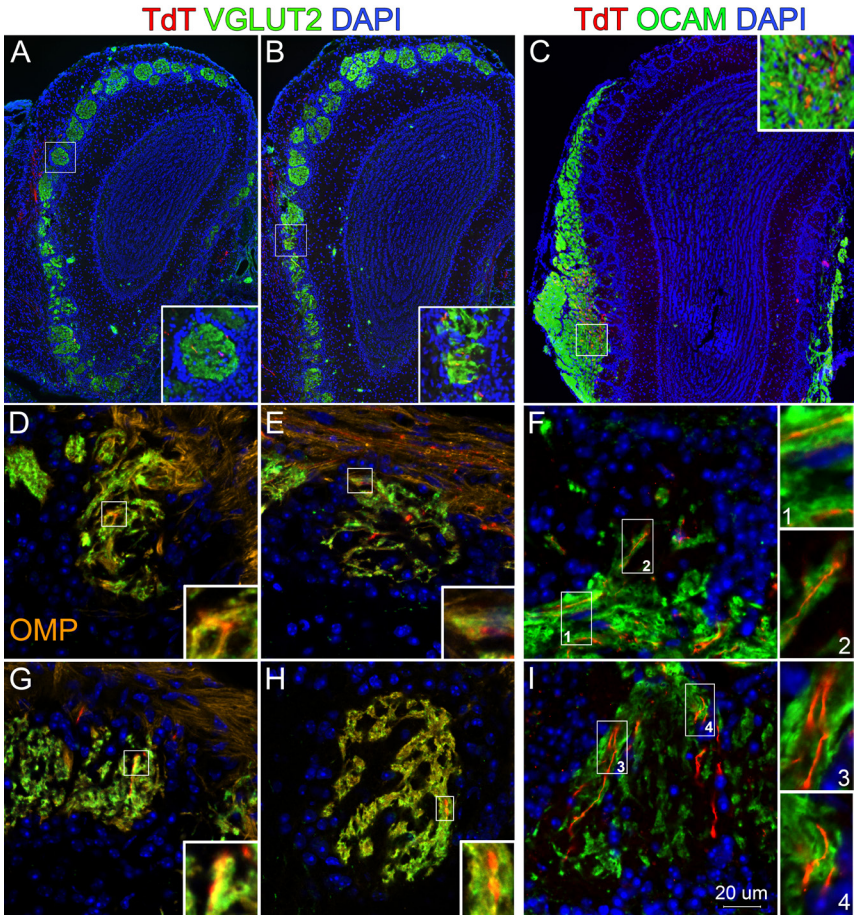

Figure 6. Graft-derived OSNs target the bulb and form glomerular synapses.
(A-B, D-E, G-H) TdT (+) graft-derived neuronal axons project to the olfactory bulb, enter glomeruli, and co-localize with the pre-synaptic marker V-GLUT2 **(C, F, I)** TdT (+) graft-derived neuronal axons project to the OCAM (+) region of the olfactory bulb. In **(C)** OCAM (+) axons have not entered into the glomeruli at this posterior level in the olfactory bulb, suggesting the complete re-innervation has not yet been achieved across the bulb.

4.2 NQO1/OCAM spatial plasticity is decreased by HDAC inhibition

After determining that 85% of transplanted stem cells adapt to the host region, I sought to pursue the mechanisms of stem cell spatial plasticity. To identify non-genetic mechanisms of cellular memory, I manipulated epigenetic modifications during the transplantation procedure. In fact, there is a growing literature on the importance of epigenetic modifications in OSN diversification (Magklara et al., 2011; Lyons et al., 2014). In choosing an epigenetic modification to manipulate, I settled on histone deacetylases (HDACs) for the three following reasons: (1) HDACs have been shown to play critical roles in stem cell pluripotency and differentiation (Foti et al., 2013; Yang et al., 2014, 2015; Qiao et al., 2015), (2) HDAC2 is present in globose basal cells (Coleman et al., manuscript in preparation), and (3) I was able to verify activity of a pan-histone deactylase inhibitor (HDACi), Oxamflatin, in culture; specifically, incubation with this molecule in a horizontal basal cell (HBC) culture system results in accumulation of H3K9 acetylation (Fig. 7). HDACs remove transcriptionally activating acetylation (Rodd et al., 2012); thus, HDAC inhibition has the effect of leaving "open" chromatin in an open state. For the transplant experiments, I incubated dorsally isolated cells with Oxamflatin prior to transplantation into the ventral OE of host animals. This treatment resulted in a significant decrease in spatial plasticity; i.e., a larger portion of graft-derived OSNs expressed the marker of the donor region (NQO1) in the

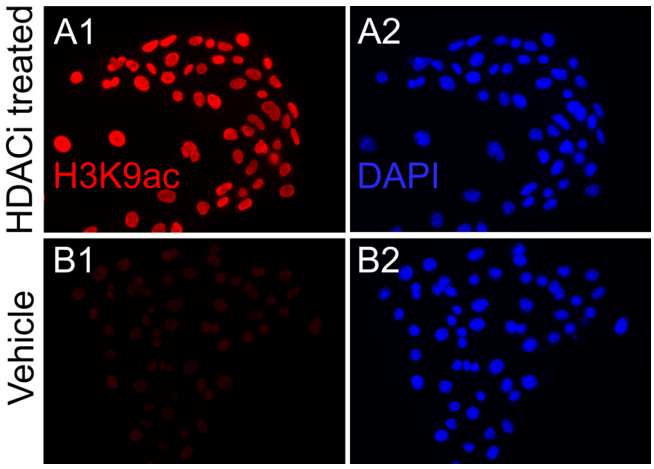

Figure 7. Treatment with the HDAC inhibitor Oxamflatin results in acetyl accumulation at H3K9. **(A)** An HBC culture treated with the HDACi Oxamflatin has robust staining for H3K9ac. **(B)** Vehicle-treated HBC cultures have lower H3K9ac staining. All images were taken with the same settings and adjusted equally during photo processing.

OCAM (+) host OE (40%) than in vehicle control experiments (10%) (Fig. 8). Thus, stem cell spatial plasticity depends at least in part on removal of acetyl groups from histone tails. Notably, this treatment did not completely reverse stem cell spatial plasticity, suggesting that other mechanisms are involved.

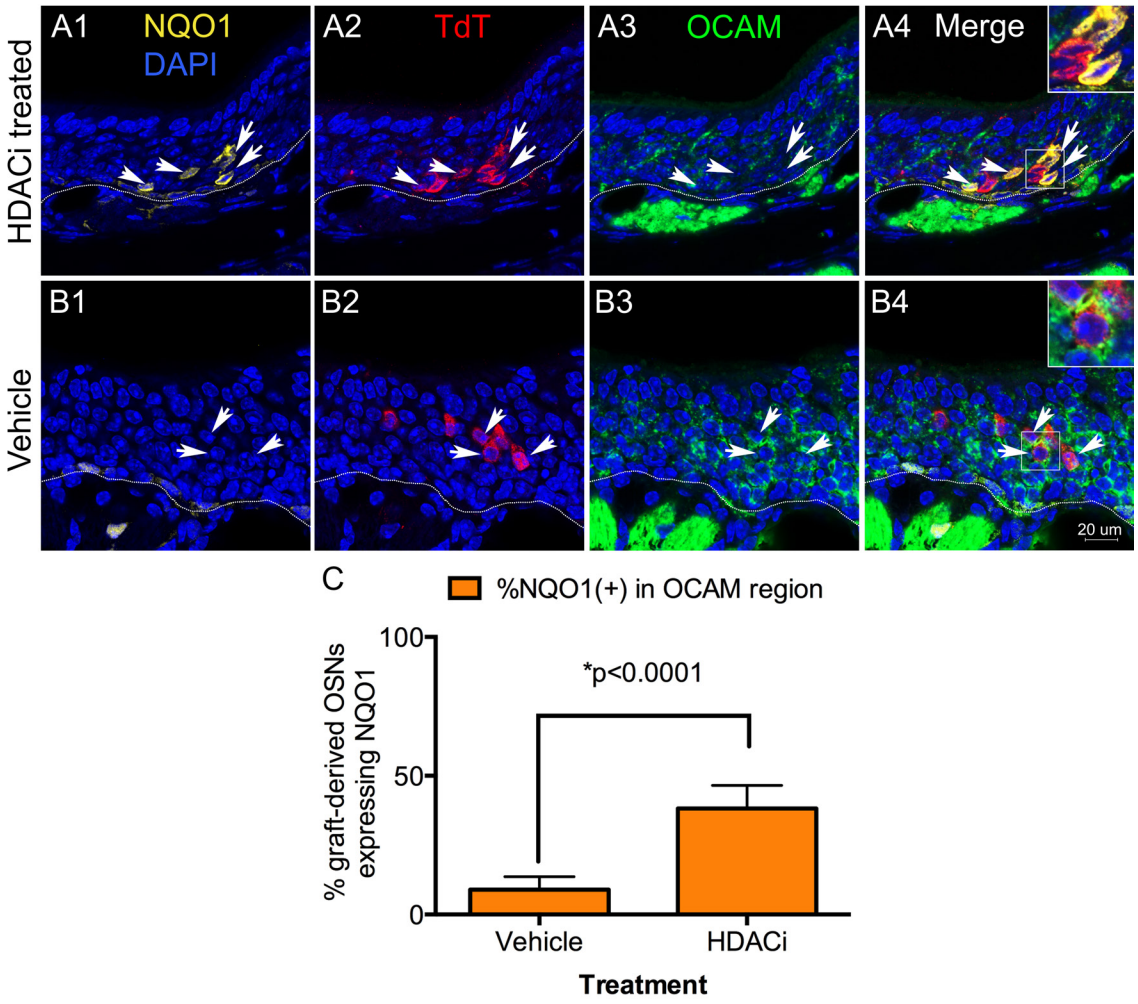

Figure 8. NQO1/OCAM stem cell spatial plasticity is decreased by HDAC inhibition. **(A)** Stem cells isolated from the dorsal OE, treated with a pan HDAC inhibitor (Oxamflatin) and transplanted into the ventral OE had a large portion of non-adaptive graft-derived OSNs expressing NQO1 in the OCAM region. **(B)** Vehicle control dorsal to ventral transplants showed adaptive OCAM (+) neurons in the OCAM region. **(C)** Quantification of the % of NQO1 (+) graft-derived neurons out of the total number of graft-derived neurons for both vehicle and HDACi-treated dorsal to ventral transplants. Vehicle: graphed is the mean of two animals (total 254 graft-derived OSNs). Dorsal to ventral: graphed is the mean of three animals (total 934 graft-derived OSNs); error bars represent SEM. Statistics: Chi-square with Yates' correction; $p<0.0001$. Dotted white line indicates the basal lamina.

Importantly, transplants of control vehicle-treated cells closely matched the adaptive rates of those found in the original dorsal to ventral transplant experiments (85% of graft-derived OSNs expressed the marker of the host region (OCAM) in the original experiments vs. 90% in the vehicle treated experiments). Lastly, incubating cells in HDACi did not impair global regeneration in the host OE as demonstrated by equivalent OMP and Tuj1 staining in the vehicle-treated and HDACi-treated transplant (Fig. 9).

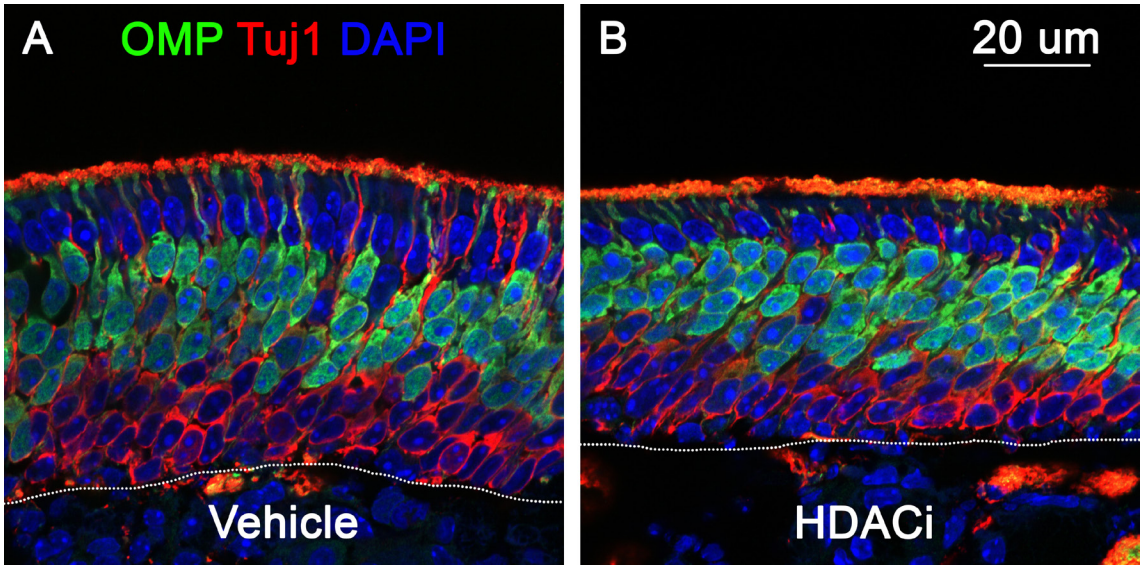

Figure 9. Incubation of donor cells in HDAC inhibitor does not disrupt neuronal maturation in the host OE.
(A) OMP and Tuj1 staining in vehicle treated transplants. **(B)** OMP and Tuj1 staining in HDACi treated transplants. Dotted white line indicates the basal lamina.

4.3 Young animal and Neurog1-eGFP transplants

To assess whether the age of the donor animal influences stem cell spatial plasticity, I isolated cells from the dorsal OE of three-week old donor pan-TdT animals and transplanted into the ventral OE of host animals (Fig. 10A,D). Under these circumstances, I observed that an average of 40% of graft-derived OSNs expressed the marker of the host region (OCAM) and 60% expressed the marker of the donor region (NQO1) (Fig. 9A,D). Thus, donor cells isolated from 3-week old animals demonstrate less spatial plasticity than those isolated from 6-7 week olds animals (Fig. 10).

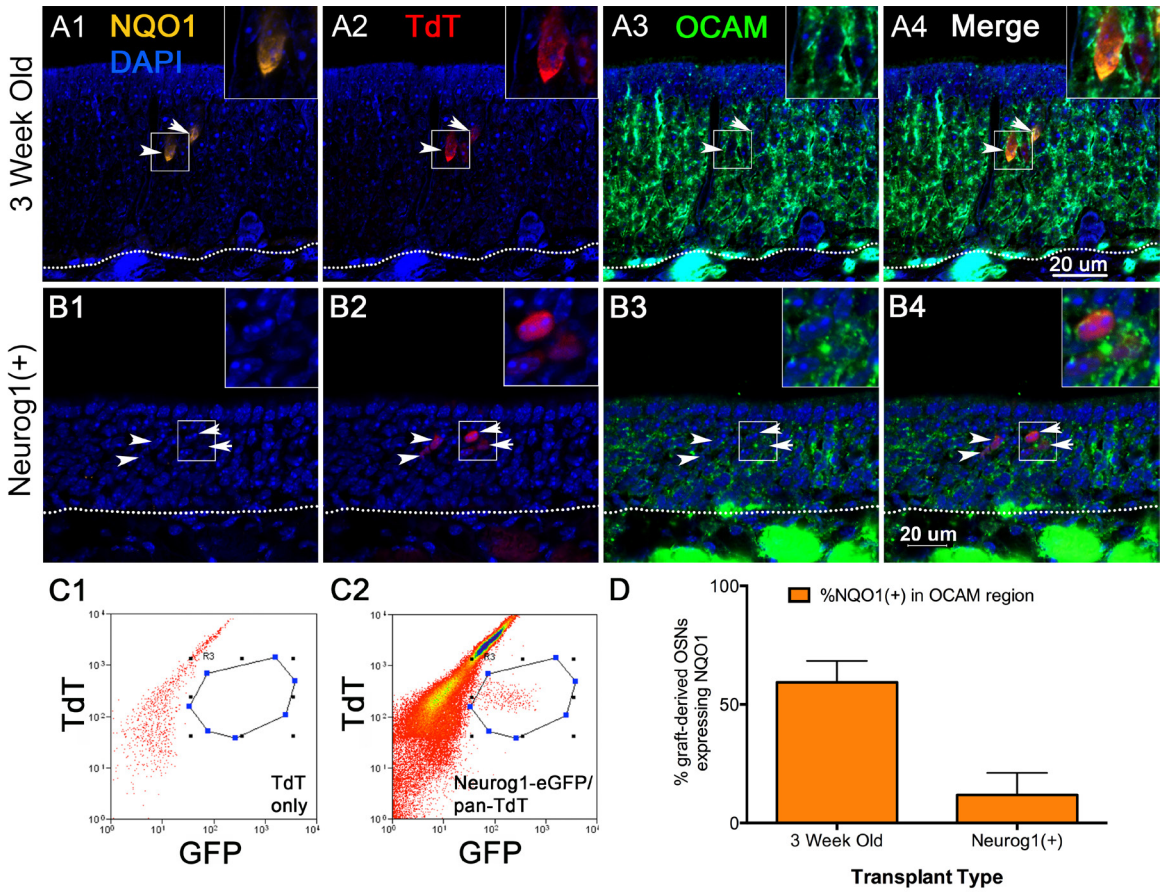

Figure 10. Transplants from 3 week old animals demonstrate decreased NQO1/OCAM stem cell spatial plasticity and transplants from Neurog1-eGFP GBCs demonstrate average stem cell spatial plasticity.
(A) Stem cells isolated from the dorsal OE of 3 week old animals and transplanted in the ventral OE show a high percentage of NQO1 (+) neuronal progeny. **(B)** Sorted Neurog1-eGFP GBCs from a whole OE preparation show a number of OCAM (+) cells in the ventral OE. **(C)** Neurog1-eGFP FACS strategy: (C1) TdT only control (C2) Neurog1-eGFP/panTdT. **(D)** Quantification of the % of NQO1 (+) graft-derived neurons out of the total number of graft-derived neurons for both 3 week old and Neurog1-eGFP transplants. 3 week old: graphed is the mean of four animals (total 568 graft-derived OSNs). Neurog1-eGFP: graphed is the mean of two animals (total 92 graft-derived OSNs); error bars represent SEM. Dotted white line indicates the basal lamina.

It may be the case that progenitors closest to terminal neuronal differentiation make up the non-plastic portion of cells expressing the donor marker (NQO1) in the host region. To assess this, I transplanted sorted Neurog1-eGFP (+) GBCs (the immediate neuronal precursors) into the ventral region of a host animal (Fig. 10B-D). Due to low numbers of isolatable Neurog1-eGFP cells, these data represent donor cells isolated from the entire OE, not specifically the dorsal, NOQ1 (+) OE. With this experimental

paradigm, I found that an average of 88% of graft-derived OSNs expressed the marker of the host region (OCAM) and 12% expressed the marker of the donor region (NQO1). While a concrete conclusion is confounded by the fact that I isolated the entire OE (by necessity), it is highly suggestive that cell stage does not account for the non-adaptive cells, as I did not see a significantly larger portion of non-plastic cells mis-expressing NQO1 in the host OE.

4.4 Spatial cues direct neuronal diversification in respect of OR gene selection

The olfactory receptors (ORs) are expressed in stripes across the epithelium (Iwema et al., 2004; Miyamichi, 2005) and most of these ORs fall into either the NQO1 or OCAM region exclusively (Fig. 11). Given that stem cells can be spatially plastic in respect to NQO1/OCAM expression (Fig. 4), I asked whether the same is true with respect to spatial OR expression. To address this question, I performed similar transplantation experiments – this time using OMP-GFP/pan-TdT donor animals, allowing for FACS isolation of graft-derived OSNs (via single cell sorting) from host animals followed by RT-PCR mediated OR identification and localization (via *in situ* hybridization) (Fig. 12, Fig. 13). As previously mentioned, all donor cells were isolated from the dorsal OE and engrafted into the ventral OE (Fig. 13A-C).

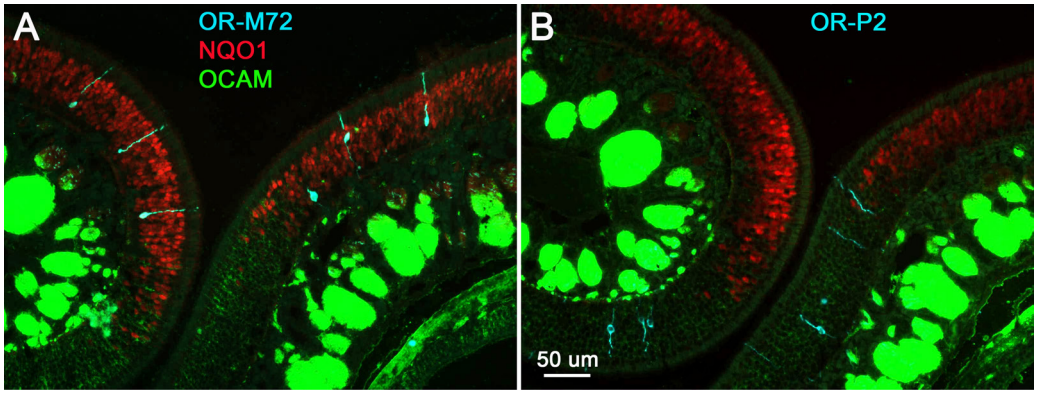

Figure 11. Olfactory receptor expression patterns respect the NQO1/OCAM division.
(A) The OR M72 is expressed in the dorsal, NQO1 (+) OE. **(B)** The OR P2 is expressed in the ventral, OCAM (+) OE.

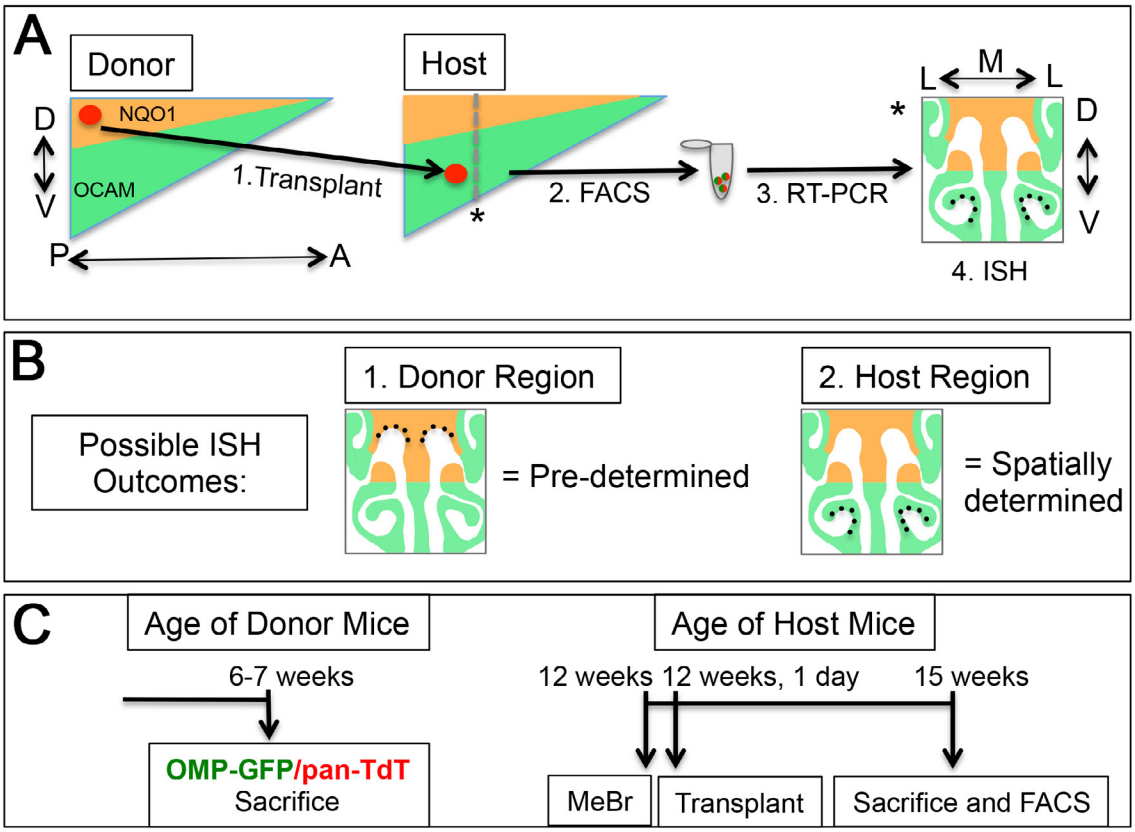

Figure 12. Experimental design to determine OR plasticity upon transplantation
(A) The dorsal OE of OMP-GFP/pan-TdT animals was dissected and transplanted into lesioned host animals. Single graft-derived neuronal progeny were FACS isolated and ORs were amplified by single-cell RT-PCR. Normal expression patterns of the identified ORs were assessed *by in situ* hybridization and literature data-mining. **(B)** Possible ISH outcomes and interpretations. **(C)** Animal timeline: Donor mice were sacrificed at 6-7 weeks; Host animals were lesioned at 12 weeks, transplanted the next day and sacrificed three weeks later.

To validate my single-cell RT-PCR technique, I first isolated single OMP-GFP and Sox2-eGFP positive cells from normal (untransplanted) animals (Fig. 14A). I found that the OMP-GFP (+) cells expressed mRNA for both *actin* and *OMP* by PCR amplification and that the Sox2-eGFP (+) cell was positive for *actin* but not *OMP* (Fig. 14A). It should be noted that there is a faint *OMP* band in the Sox2-eGFP (+) cell; this is likely due to genomic contamination as *OMP* does not contain introns and thus the primers cannot be designed to span introns as the *actin* primers do. *ORs* were amplified from the OMP-GFP (+) single cells using the degenerate *OR* primer pair P26/P27 (Malnic et al., 1999); these OR products were restriction enzyme digested. The digest products summed to the weight

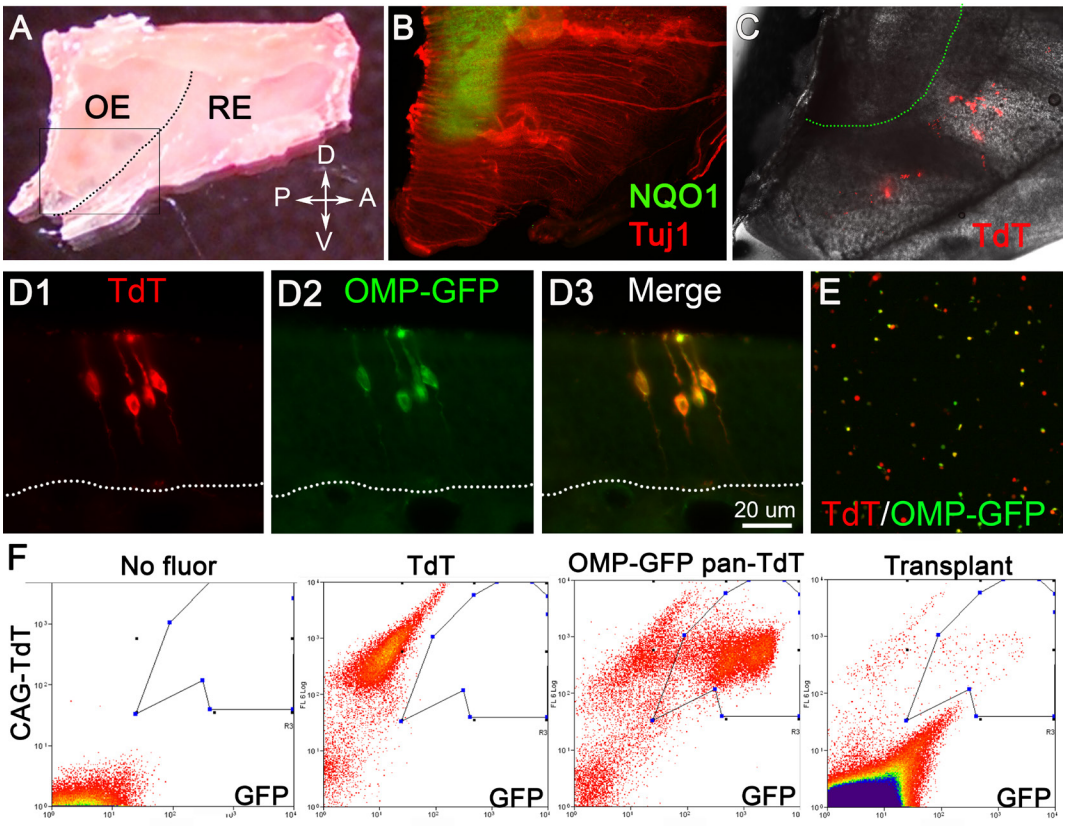

Figure 13. Engrafted neurons are isolated from the ventral OE, express TdT and GFP, and are FACS isolated via GFP/TdT expression.
(A) Whole mount septum preparation showing the OE/RE delineation. The black box corresponds to the zoomed in area in **(B)** where the NQO1/OCAM boundary is depicted via NQO1 and Tuj1 CLARITY staining. **(C)** Engrafted TdT (+) cells are located in the NQO1 (-) region in a host septum. **(D)** Neuronal progeny of engrafted cells express both TdT and GFP. **(E)** Dissociated OMP-GFP/pan-TdT cells show a mixture of TdT (+) and TdT (+)/GFP (+) cells. **(F)** FACS isolation of graft-derived TdT (+)/GFP (+) OSNs: (Left) No flour control (Middle Left) TdT only control (Middle Right) OMP-GFP/pan-TdT control (Right) Transplant dissociation. Dotted white line indicates the basal lamina.

of the original uncut band, demonstrating isolation of an OSN with a single, unique OR gene (Fig. 14B). Furthermore, upon sequencing the *OR* products, the digest patterns match those of the predicted digest based on the *OR* sequences (Fig. 14B). Notably, the regions amplified by the degenerate OR primers are transmembrane regions 4 and 5, just as P26/P27 primers are designed (Malnic et al., 1999) (Fig. 14C). Lastly, but importantly, no-RT controls contained no PCR products from either *actin* or *ORs* in either pooled or

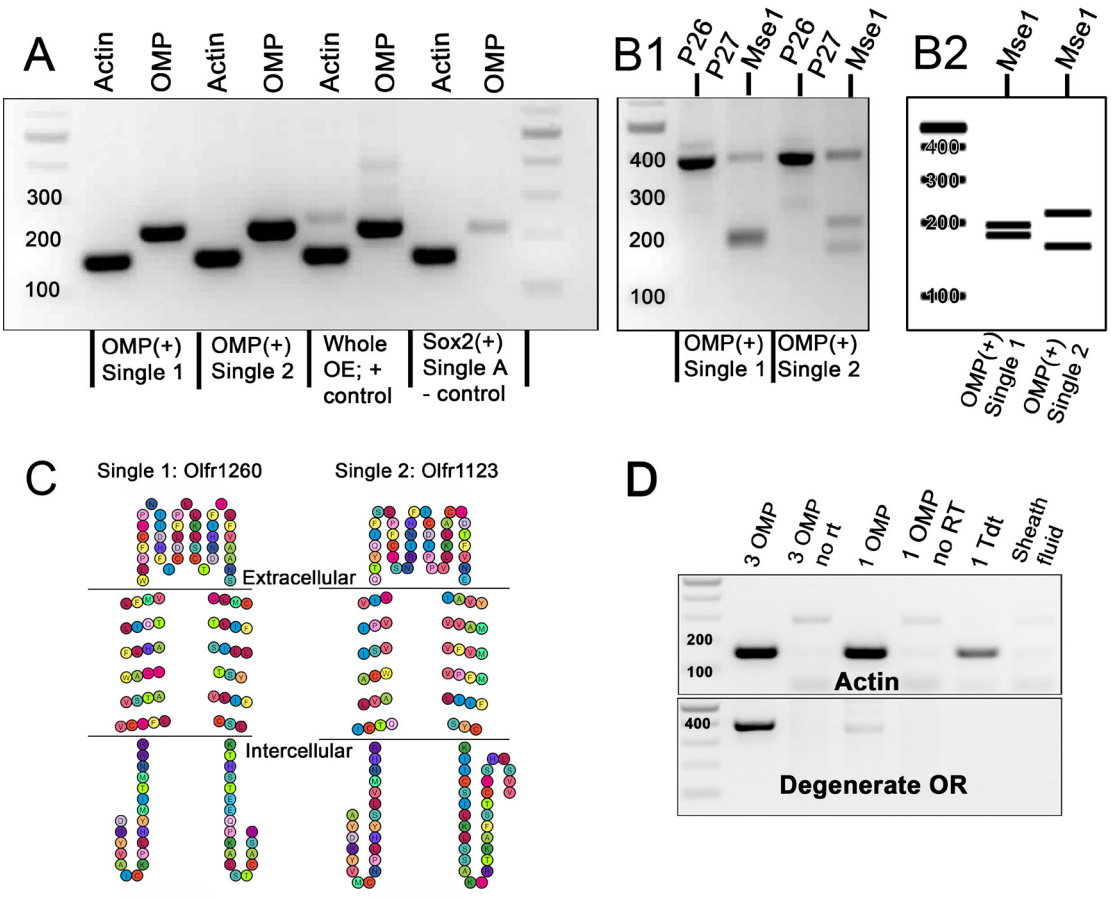

Figure 14. Single-cell RT-PCR controls.
(A) Single sorted OMP-GFP cell express both *actin* and *OMP*; a sorted Sox2-eGFP cell expresses *actin* and not *OMP*. **(B1)** Single sorted OMP-GFP cells contain *ORs* that digest to **(B2)** match the sequenced results. **(C)** Amplified OR regions span transmembrane domains 4 and 5. **(D)** No RT and sheath fluid controls show that actin and ORs are not amplified in the sheath fluid or without RT.

single OSNs (Fig. 14D). A FACS sheath fluid control also showed no PCR products from *actin* or *OR* PCR reactions (Fig 14D). Given my single cell control experiments, I have demonstrated that this protocol has the sensitivity and specificity to identify OR genes expressed in single, OMP (+) OSNs.

In my first cohort of transplants, I verified cDNA isolation of graft-derived OSNs by PCR for *OMP* (to assure isolation of OSNs), *TdTomato* (to assure graft-derivation), and *actin* (to assure cDNA quality as these primers span introns) (Fig. 15). Cells that met these criteria were used for degenerate *OR* PCR using primers P26/P27 (Malnic et

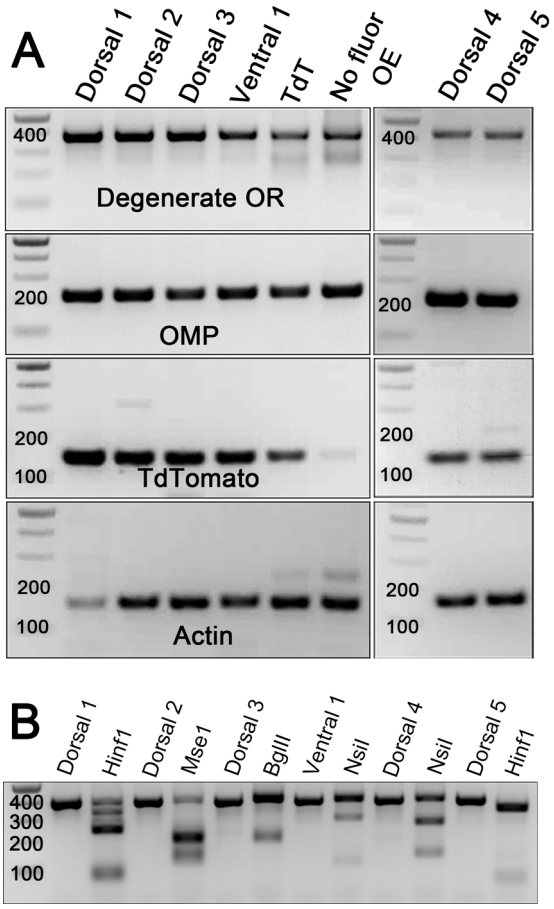

Figure 15. Individual, graft-derived neurons express mRNAs for ORs, OMP, TdT, and actin.
(A) PCR amplification was performed on cDNA created from each single cell. Dorsal 1-5 are from dorsal to ventral transplants, Ventral 1 is from a ventral to ventral transplant, TdT is whole OE from a pan-TdT animals and no flour OE is from whole OE of a control animal. **(B)** Digests of amplified OR products suggest that multiple ORs are present in the single graft-derived OSNs.

al., 1999) (Fig. 15). Surprisingly, digests of the degenerate OR products produced multiple bands which, in several cases, summed to higher than the uncut 400 bp band, suggesting that the cells express mRNA for greater than one OR gene; furthermore, digests were not 100% complete, again suggesting multiple *ORs* per cell (Fig. 15B). Based on this observation that the graft-derived OSNs likely expressed multiple *ORs*, the fact that not all graft-derived OSNs have reinnervated glomeruli (Fig. 6), and the fact that immature OSNs can express more than one OR (Hanchate et al., 2015; Tan et al., 2015), I hypothesized that the graft-derived OSNs could be cells transitioning to maturity. Accordingly, in my second cohort of graft-derived OSNs, I performed additional PCR reactions for the immature neuronal markers *Tuj1* and *GAP43*, and the GBC/Sus marker *Sox2* (as a negative control) (Fig. 16). I found that most of the graft-derived OSNs were positive for *OMP*, *Tuj1*, and *GAP43*, while not positive for the GBC/Sus marker *Sox2*, suggesting that these cells are not fully mature OSNs. Again, digest patterns of these *ORs* suggests amplification of multiple OR genes per cell (Fig. 16D). In sequencing the *OR*

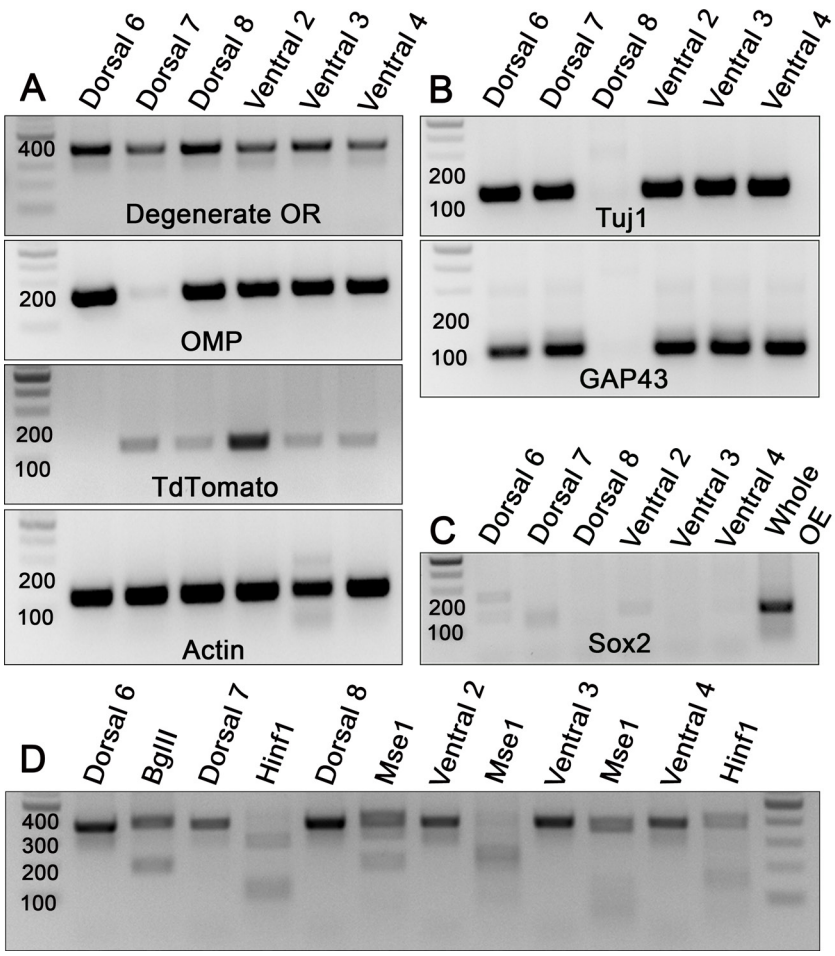

Figure 16. Most graft-derived neurons express mRNA for immature neuronal markers Tuj1 and GAP43.
(A) Single graft-derived neurons express *ORs*, *OMP*, *TdT*, and *actin*. *Note: Dorsal 6 is not positive for *TdT* and therefore was not included in any analysis. **(B)** Almost all graft-derived neurons also express mRNA for immature neuronal markers Tuj1 and GAP43, but not the GBC marker **(C)** Sox2. **(D)** Digests of amplified *OR* products suggest that multiple OR mRNAs are present in the single graft-derived OSNs.

products from each cell, I found that more than half of the cells contained greater than one *OR* (Table 1).

Out of the single cells expressing *ORs*, *OMP, TdT*, and *actin*, I found that 100% of the ventral to ventral control transplants expressed ventrally-located ORs, and of the dorsal to ventral transplants, 50% expressed ORs of the host region (ventral), 37.5% expressed ORs from both the host and donor region, and 12.5% expressed ORs of the

donor region (dorsal) (Fig. 17, Table 1). This data was collected by both my own *in situ* hybridization data (Fig. 17A-C) and by literature references (Table 1). Based on my finding that many of these cells are transitioning from immature to mature OSNs, I performed a third set of dorsal to ventral transplants, this time waiting 4 weeks post

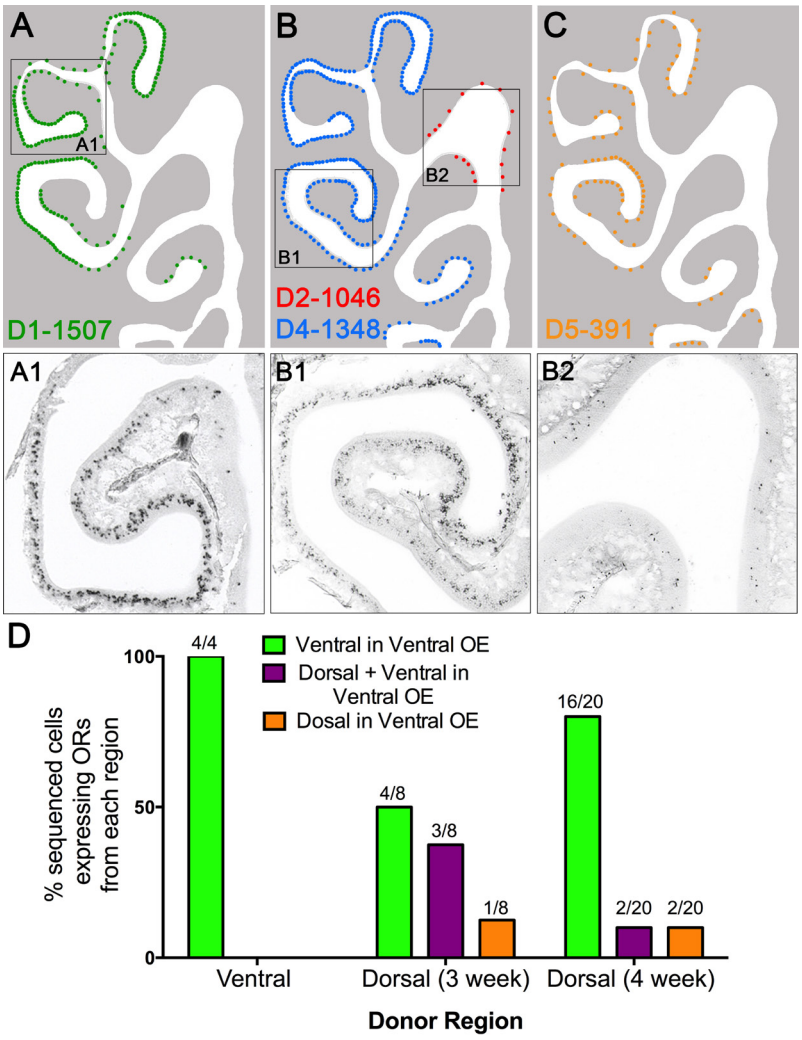

Figure 17. Spatial cues direct neuronal diversification in respect to OR gene selection.
(A-C) Location of ORs amplified from graft-derived OSNs by *in situ* hybridization. **(D)** Quantification of OR expression region from graft derived OSNs. All ventral-to-ventral transplants are expressed in the ventral OE; 50% of dorsal-to-ventral transplants express ventral ORs at 3-weeks post transplantation; 80% of dorsal-to-ventral transplants express ventral ORs at 4-weeks post transplantation from single-cell RNA-seq experiments.

transplantation to isolate graft-derived OSNs. In this experiment, I isolated single cells by FACS (as before) and subsequently used a Fluidigm C1 Autoprep IFC to capture single cells for Illumina deep sequencing. Under these circumstances, 80% of graft-derived OSNs expressed ORs of the host region, 10% expressed both host and donor ORs, and 10% expressed ORs of the donor region (Fig. 17D, Table 1).

Table 1. ORs identified in graft-derived OSNs and their location in the OE

Cell Designation (Single-cell RT-PCR)	**Olfr (dominant OR)**	**Alternative gene names**	**Region in the OE - Zone (reference) [family member]**
Dorsal 1	1507 (dominant)	MOR244-1, MOR28	Ventral – Z4 (Serizawa et al., 2000) + (my in situs)
	1026	MOR196-4	
Dorsal 2	1046 (dominant)	MOR194-1	Dorsal – Z1 (my in situs)
	61	MOR253-1	Ventral – Z3 (Miyamichi, 2005) [family]
Dorsal 3	1406	MOR267-5	Dorsal – Z1 (Kobayakawa et al., 2007) [family]
Dorsal 4	1348 (dominant)	MOR235-2	Ventral – Z4 (Miyamichi, 2005) + (my in situs)
	1231	MOR103-9	Ventral – Z3/Z4 (Miyamichi, 2005) [family]
Dorsal 5	391	MOR135-24	Ventral – Z4 (my in situs)
Dorsal 7	99 (dominant)	MOR156-1	Dorsal – Z1 (my in situs)
	235	MOR214-3	
	16	MOR267-13, MOR23	Dorsal – Z1 (Grosmaitre et al., 2006) + (my in situs)
	1420	MOR266-4	Ventral (my in situs)
Dorsal 8	582 (dominant)	MOR30-3	Dorsal – Z1 (Tsuboi et al., 2006)

	16	MOR267-13, MOR23	Dorsal – Z1 (Grosmaitre et al., 2006)
	466	MOR209-1	Ventral – Z2.8 (Miyamichi, 2005)
Dorsal 9	1241	MOR231-14	Ventral – Z3-Z4 (Miyamichi, 2005) [family]
Ventral 1	481 (dominant)	MOR204-2	
	1123	MOR264-17	
	541	MOR253-3	Ventral – Z3.5 (Miyamichi, 2005)
	862	MOR146-1	
Ventral 2	1420 (domiant)	MOR266-4	Ventral (my in situs)
	391	MOR135-24	Ventral – Z4 (my in situs)
Ventral 3	317	MOR256-47	Ventral (Zhao et al., 2013) [family]
Ventral 4	539 (dominant)	MOR253-9	Ventral – Z3.2 (Miyamichi, 2005)
	1507	MOR244-1, MOR28	Ventral – Z4 (Serizawa et al., 2000) + (my in situs)
Cell Designation (RNA-seq)	**Olfr (dominant OR; counts)**	**Alternative gene names**	**Region in the OE – Zone (reference) [family member]**
1	524 (3211)	MOR103-14	Ventral – Z3/4 (Miyamichi, 2005) [family]
2	667 (7553)	MOR34-2	Dorsal (Tsuboi et al., 2006)
3	733 (9883)	MOR241-2	Dorsal – Z1.7 (Miyamichi, 2005) [family]
4	1347 (7723)	MOR103-11	Ventral – Z3/4 (Ressler et al., 1993; Miyamichi, 2005) [family]
5	1364 (11522)	MOR256-13	Ventral – Z2/3 (Ressler et al., 1993; Zhao et al., 2013) [family]

6	1226 (7201)	MOR233-2	Ventral – Z4.4 (Miyamichi, 2005)
7	393 (dominant; 1726)	MOR125-7	Dorsal (Kobayakawa et al., 2007) [family]
	132 (206)	MOR256-49	Ventral – Z2/3 (Ressler et al., 1993; Zhao et al., 2013) [family]
8	1098 (dominant; 16523)	MOR206-1	
	1097 (113)	MOR206-2	
	140 (289)	MOR235-1	Ventral – Z4 (Miyamichi, 2005)
9	168 (2488)	MOR271-1	Ventral –Z4 (Zhao et al., 2013) [family]
10	190 (dominant; 13926)	MOR183-4	
	1372-ps1 (455)	MOR256-54P	Ventral – Z2/3 (Ressler et al., 1993; Zhao et al., 2013) [family]
	57 (1319)	MOR139-3	Ventral – Z3 (Miyamichi, 2005) [family]
	192 (202)		
11	1274-ps (896)	MOR228-4,5	Ventral Z2.2 (Miyamichi, 2005) [family]
12	220 (dominant; 894)	MOR103-17,13P	Ventral – Z3/4 (Miyamichi, 2005) [family]
	1030 (90)	MOR196-2	
	1080 (165)	MOR192-1	
	120 (90)	MOR263-3	
	691 (46)	MOR31-6	Dorsal – Z1 (Tsuboi et al., 2006)
13	140 (771)	MOR235-1	Ventral – Z4 (Miyamichi, 2005)
14	1212 (14087)	MOR233-17,20	Ventral – Z2-4 (Miyamichi, 2005) [family]

15	140 (2259)	MOR235-1	Ventral – Z4 (Miya-michi, 2005)
16	15 (27)	MOR256-17	Ventral – Z2/3 (Ressler et al., 1993; Zhao et al., 2013) [family]
17	179 (279)	MOR256-64	Ventral – Z2/3 (Ressler et al., 1993; Zhao et al., 2013) [family]
18	168 (329)	MOR271-1	Ventral – Z4 (Zhao et al., 2013) [family]
19	168 (dominant; 487)	MOR271-1	Ventral – Z4 (Zhao et al., 2013)
	911-ps1 (66)	MOR165-1/ MOR166-1	
20	1372 (dominant; 197)	MOR256-54P	Ventral – Z2/3 (Zhao et al., 2013) [family]
	984 (94)	MOR239-6	
	1346 (10)	MOR103-6	Ventral – Z3/4 (Miyamichi, 2005) [family]

Table Key: Dorsal 1-9 are graft-derived OSNs from dorsal to ventral transplants sequenced via single-cell RT-PCR; Ventral 1-4 are graft-derived OSNs from ventral to ventral transplants sequenced via single-cell RT-PCR; 1-20 are graft-derived OSNs from dorsal to ventral transplants sequenced via RNA-seq. Zones are reported as classified by Miyamichi et al., 2005. OR locations identified by association with OR family members are indicated by [family].

4.5 Expression of multiple ORs in OMP (+) OSNs

In the experiments reported in section 4.4, I found that many graft-derived OSNs contained multiple ORs (Table 1). To be precise, 66% of the 3-week post-transplant cells expressed multiple ORs and 30% of the 4-week post-transplant cells expressed multiple ORs. It is not unprecedented that mature OSNs express multiple ORs; several recent studies reported multiple OR expression in OMP (+) OSNs (Hanchate et al., 2015; Tan et al., 2015; Scholz et al., 2016). These same studies found that the frequency of multiple

OR expression is higher in immature OSNs (Hanchate et al., 2015; Tan et al., 2015). Given my finding that many of the graft-derived OSNs contain immature markers *GAP43* and *Tuj1* along with *OMP* (Fig. 16), and the fact that not all graft-derived OSNs have entered glomeruli (Fig. 6), I sought to characterize OR multiplicity in OMP (+) OSNs that have not yet reached the bulb, and are likely in a transitory stage from immature to mature OSNs. To do so, I FACS isolated OMP-GFP (+) OSNs from bulbectomized animals (such that OMP-GFP (+) cells do not synapse in the bulb), captured cells on a Fluidigm IFC and performed RNA-seq on the single isolated cells as before. Cells were counted as OMP (+) if they had above 1139 OMP transcripts per million (TPM), a cutoff determined using the R package OptimalCutpoints implementing the Youden Index Method (Youden, 1950; Schisterman et al., 2005; López-Ratón et al., 2014). Using this strategy, I found that 54% of the sequenced cells contained multiple ORs (21/39) and 46% contained a single OR (18/39) (Fig. 18). Comparing these results to those previously reported, I found that these percentages are significantly different from OMP (+) cells isolated from intact, normal OE, and are not statistically different from immature

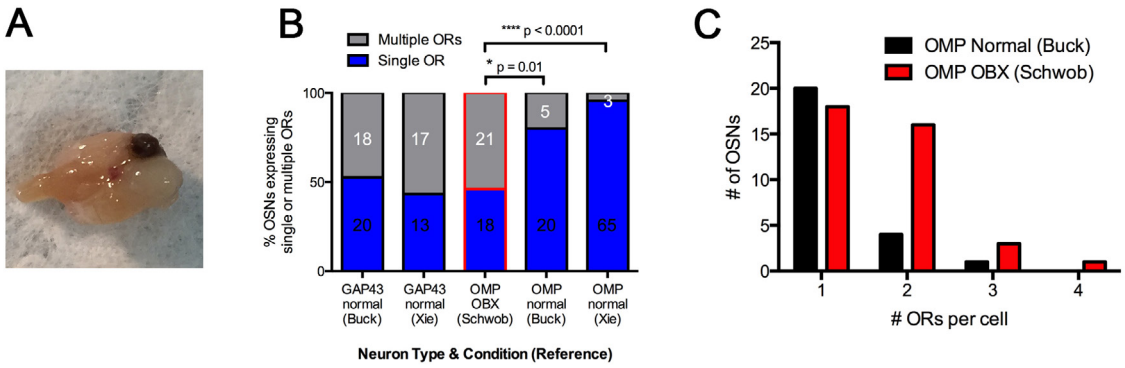

Figure 18. OMP (+) OSNs from 3-week post bulbectomized animals have a tendency to express multiple ORs.
(A) Image of unilateral bulbectomy used in this experiment. OE from the OBX side (top right) was collected and dissociated and OMP cells were collected via FACS for OMP-GFP **(B)** Quantification of the % of sequenced OSNs expressing single or multiple ORs. OBX data is compared to that in the literature (Hanchate et al., 2015; Tan et al., 2015). The ratio of cells containing single or multiple ORs is significantly different between OMP (+) cells from OBX animals as compared to OMP (+) cells from normal animals in reports by Buck and Xie (Chi-square with Yates correction; $p = 0.01$ and $p < 0.0001$ respectively). **(C)** OMP (+) cells from OBX animals contained 1-4 ORs; OMP (+) cells from normal animals contained 1-3 ORs.

OSNs from normal OE (Fig. 18). Thus, I have identified an additional stage in neuronal maturation when ~50% of OSNs express multiple ORs: the time when OMP is expressed, but OSNs have yet to enter the olfactory bulb. These data suggest that contact with the bulb may assist in singular OR expression/stabilization.

4.6 RALDH1 borders correspond to OCAM/NQO1 boundaries and shift together with improper regeneration

Previous studies have implicated retinoic acid (RA) as a spatially secreted factor that could influence pattern generation in the OE (LaMantia et al., 2000; Norlin et al., 2001; Peluso et al., 2012). In support of this hypothesis, the RA synthetic enzymes, the RALDHs are spatially expressed across the OE (Norlin et al., 2001; Peluso et al., 2012). In fact, RALDH1 is expressed in Sus cells of the OE strictly in the NQO1 (-) region of the OE (Fig. 19A). Furthermore, NQO1 borders shift along with RALDH1 borders in a harsh epithelial lesion that disrupted pattern regeneration in a unilateral MeBr-lesion (Fig. 19B). These results suggest that RA could be one of the spatial cues that play an instructional role in neuronal diversification in the OE.

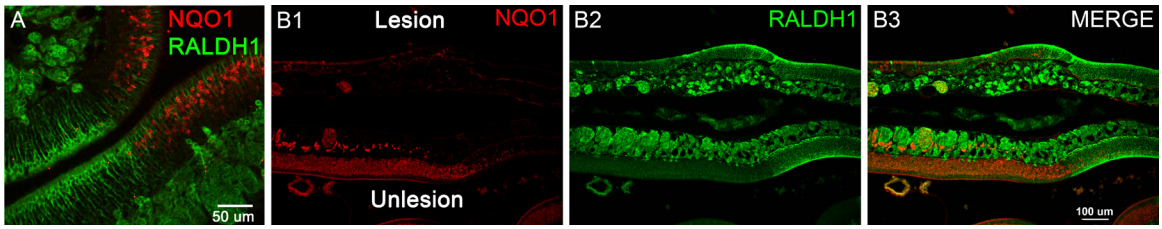

Figure 19. RALDH borders align with OCAM/NQO1 boundaries and shift together with improper regeneration.
(A) NQO1 and RALDH are inversely expressed in the OE with a sharp border corresponding to the NQO1/OCAM line. **(B)** NQO1 expression patterns shift with RALDH1 borders in a harsh unilateral lesion with improper spatial regeneration.

Summary

In this chapter of my thesis work, I determined that spatial cues direct neuronal diversification in respect to both NQO1/OCAM and ORs (Fig. 1-6; Fig. 11-17), and that this spatial plasticity relies at least in part on HDAC activity, is decreased in cells isolated from 3 week old donor animals, and may rely in part on retinoic acid signaling (Fig. 7-10, 19). Lastly, ~50% of cells that express OMP, but have not yet reached the olfactory bulb express multiple ORs (Fig. 18).

Chapter 5. Results

LSD1-dependent neuronal maturation in the olfactory epithelium

Adapted from:

Coleman JH, Lin B, Schwob JE. Dissecting LSD1-dependent neuronal maturation in the olfactory epithelium. Manuscript in preparation.

Rationale

Neurons in the olfactory epithelium (OE) each express a single dominant olfactory receptor (OR) allele from among roughly 1000 different OR genes (Buck and Axel, 1991). While (near) monogenic and monoallelic OR expression has been appreciated for over two decades, regulators of this process are still being described; most recently, epigenetic modifiers have been of high interest as silent OR genes are decorated with transcriptionally repressive histone 3, lysine 9 (H3K9) methylation whereas active OR genes are decorated with transcriptionally activating histone 3, lysine 4 (H3K4) methylation (Magklara et al., 2011). Lysine specific demethylase 1 (LSD1) demethylates at both of these lysine residues and has been shown to disrupt neuronal maturation and OR expression in the developing embryonic OE (Shi et al., 2004; Metzger et al., 2005; Garcia-Bassets et al., 2007; Lyons et al., 2013; Laurent et al., 2015). Despite the growing literature on LSD1 expression in the OE, a complete characterization of the timing of LSD1 expression in relation to neuronal maturation and the function of LSD1 in neuronal diversification in the adult OE have yet to be reported. To fill this gap, in this chapter of my thesis work, I investigated (1) The timing of LSD1 expression in relation to OSN maturation and OR expression; (2) The presence of LSD1 binding partners in LSD1 (+) cells in the mouse OE, which necessarily direct LSD1 susbstrate specificity (Lee et al, 2005; Laurent et al., 2015); and (3) The effect of inducible *Lsd1* knockout in 3 basal cell populations: HBCs, Ascl1 (+) transit-amplifying, neuronally committed GBCs ($GBC_{TA\text{-}Ns}$), and Neurog1 (+) immediate neuronal precursor GBCs (GBC_{INPs}) (Fig. 1).

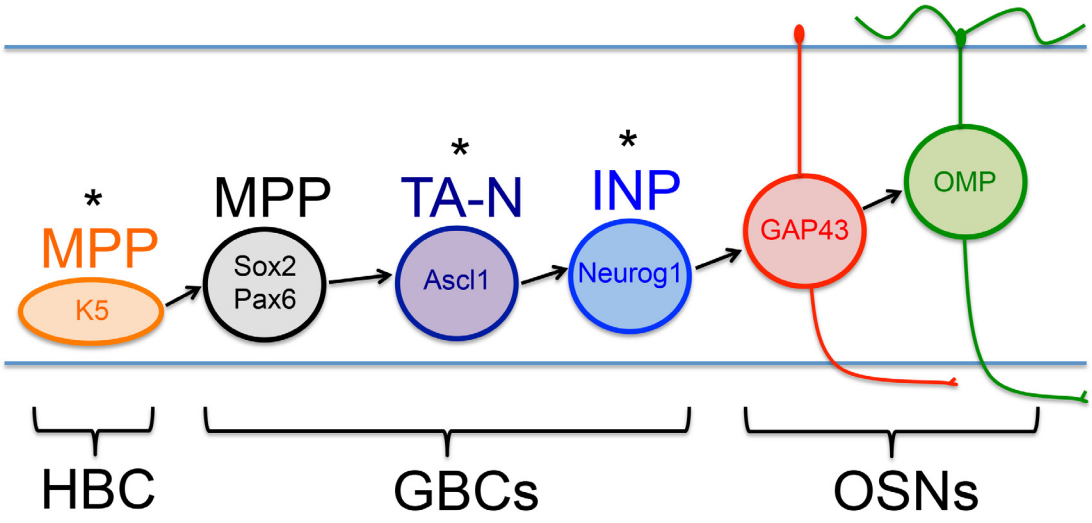

Figure 1. Stem and progenitor progression in the neuronal lineage
Horizontal basal cells (HBCs) are K5 (+) multipotent progenitors (MPPs) able to give rise to all cell types of the OE following activation. GBCs can be broken down into stages of progenitor capacity: GBC MPPs express Sox2 and Pax6; GBC transit-amplifying neuronally-committed (TA-N) cells express Ascl1; GBC immediate neuronal precursors (INP) express Neurog1. Immature OSNs express GAP43 and mature OSNs express OMP. Asterisks mark progenitor stages where I used *CreER*^{T2} drivers to conditionally delete *Lsd1*.

5.1 OR expression during OSN maturation

To contextualize the timing of OR and LSD1 expression, I first characterized the timing of OSN maturation using EdU pulse-chase experiments – looking specifically for EdU co-labeling with GAP-43, to mark immature OSNs, and with OMP, to mark mature OSNs (Fig. 2). GBCs are the predominant cycling cell within the OE, representing over 90% of the cells that incorporate thymidine analogues (such as EdU) during S phase and retain them (Salic and Mitchison, 2008). In the normal unlesioned OE, GBCs give rise exclusively to neurons (Schwartz Levey et al., 1991; Caggiano et al., 1994; Schwob et al., 1994; Huard and Schwob, 1995) and incorporated EdU label can be chased from the labeled progenitors into the neuronal population. Because cells among the GBC population may divide more than once, the time at which the leading edge of the double-labeled cells appears represents the shortest interval to that stage in differentiation.

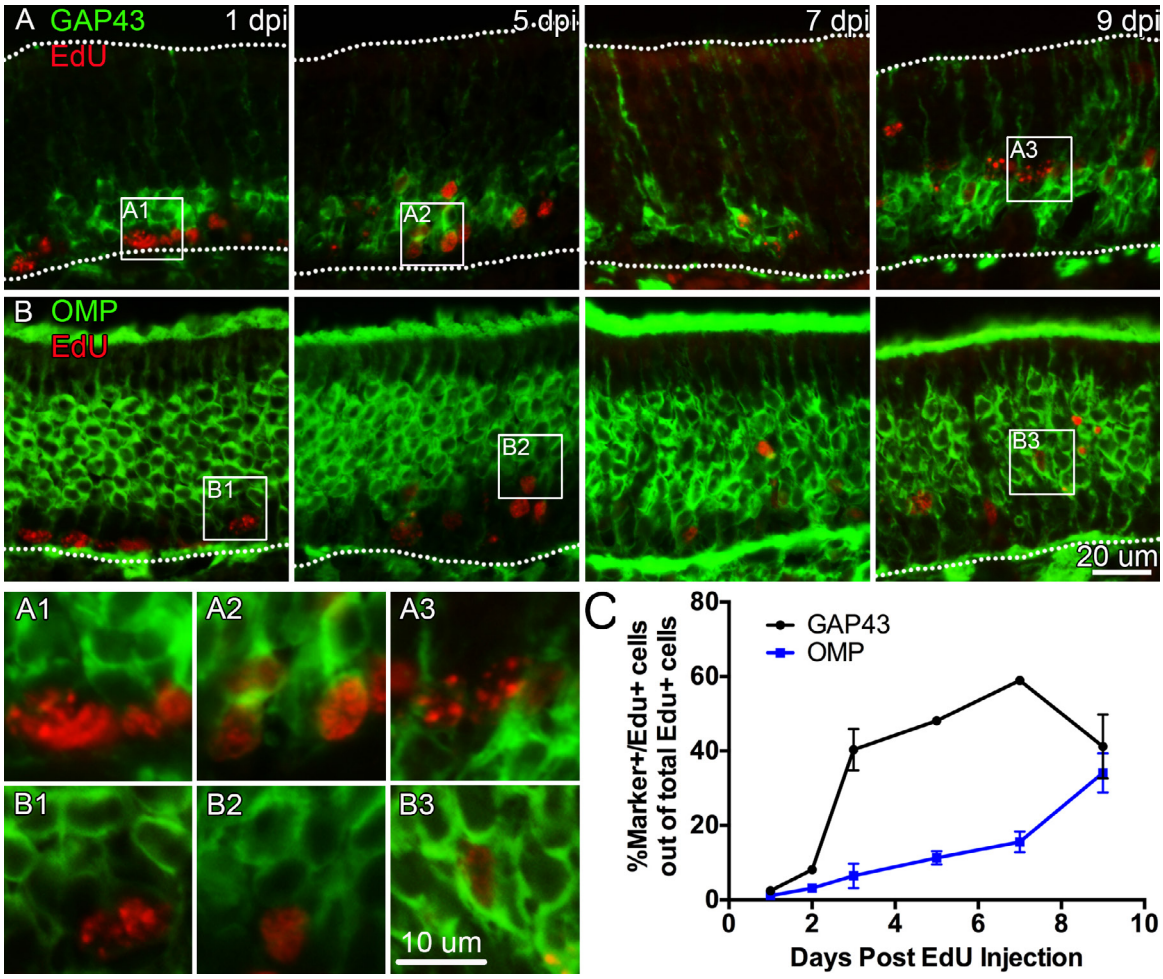

Figure 2. A transition from immature to mature OSNs begins at 7 days post basal cell division.
(A) GAP-43 and EdU costaining at 1, 5, 7 and 9 days post EdU injection (DPI). Double positive cells are rare at 1 DPI, abundant at 3, 5, and 7 DPI, and decrease by 9 DPI. **(B)** OMP and EdU costaining. Double positive cells are most abundant at 9 DPI. **(C)** Quantification of Marker (+)/ EdU (+) cells out of the total number of EdU (+) cells; data points represent the mean of three animals and error bars = SEM. Dotted white line indicates the basal lamina (bottom) and the apical surface (top).

For EdU pulse chase experiments, I gave a single dose of EdU to 8 week-old wild-type mice and sacrificed the animals at 1, 3, 5, 7 and 9 days post injection (DPI). EdU (+)/GAP-43 (+) cells were found as early as 1 DPI at low numbers when an average of 2.5% of total EdU (+) were GAP-43 (+)/EdU (+) (Fig. 2C). At 2 DPI, this percent increased to 8%, and a drastic jump occurred at 3 DPI with 40% of EdU (+) cells being

double positive for GAP-43 and EdU (Fig. 2C). GAP-43 (+)/EdU (+) cells peaked at 7 DPI to ~60% and decreased by 9 DPI back to the 40% seen at 3 DPI, likely reflecting the timeframe when GAP-43 (+) OSNs transition to OMP (+) OSNs (Fig. 2A,C). By comparison, OMP (+)/Edu (+) cells were rare for the first few days post injection, and then gradually increased to 11% at 5 DPI and 34% at 9 DPI, again demonstrating that the emergence of OMP (+) OSNs is beginning to accelerate at the end of that period (Fig. 2B,C).

Similarly, the timing of OR expression following basal cell division was determined by analyzing numbers of OR (+)/EdU (+) cells following EdU incorporation (Fig. 3). In these experiments, I assayed three different ORs: (1) the P2 receptor, a Class II OR located on Chromosome 7 and expressed in the ventral to ventrolateral swath of OE (Mombaerts et al., 1996) (Fig. 3A) (2) MOR28, a Class II OR located on Chromosome 14 and concentrated in the dorsolateral OE (Serizawa et al., 2003) (Fig. 3B) and (3) M72 a Class II OR located on Chromosome 9 and expressed in the dorsomedial OE (Feinstein and Mombaerts, 2004) (Fig. 3C). In these experiments, I compared the number of OR (+)/Edu (+) cells to both total OR (+) and EdU (+) cells respectively.

P2 (+)/Edu (+) cells were found as early as 2 DPI at an average of 0.04% of total EdU (+) cells and an average of 0.15% of total P2 (+) cells (Fig. 3D,E). P2 (+)/EdU (+) cells peaked at 5-7 DPI to 0.48% of total EdU (+) cells and to 1.74% of total P2 (+) cells (Fig. 3D,E). At 9 DPI, P2 (+)/EdU (+) cells decreased, potentially reflecting an OR switch at the time of full OSN maturation or cell death (Fig. 3D,E). The first MOR28 (+)/EdU (+) cells were found as early as 1 DPI at 0.06% of total EdU (+) cells and 0.03% of total MOR28 (+) cells. Following this rare sighting, another MOR28 (+)/EdU (+) cell was not apparent until 5 DPI at 2.44% of total EdU (+) cells and 1.23% of total MOR28 (+) cells (Fig. 3B,F). After this timepoint, the number of MOR28 (+)/EdU (+) cells increased out of the total EdU (+) cells but remained constant out of total MOR28 (+) cells (Fig 3. B,F). Thus, it appears that MOR28 (+) cells appear in a burst around 5 days post cell

division and remain constant as OSNs shift from immature to mature OSNs. Similarly, M72 (+)/EdU (+) cells were found as early as 5 DPI at 1% of total EdU (+) cells and 4% of total M72 (+) cells (Fig. 3C and data not shown). The number of M72 (+)/EdU (+) cells remained consistent from 5-9 DPI again suggesting that this OR also turns on at 5 days post cell division. Of the three ORs assessed, M72 was the least expressed, with an average of ~10 ORs counted per section (unilaterally) making my analysis quite variable, but nonetheless consistent with an onset of OR expression at 5 DPI.

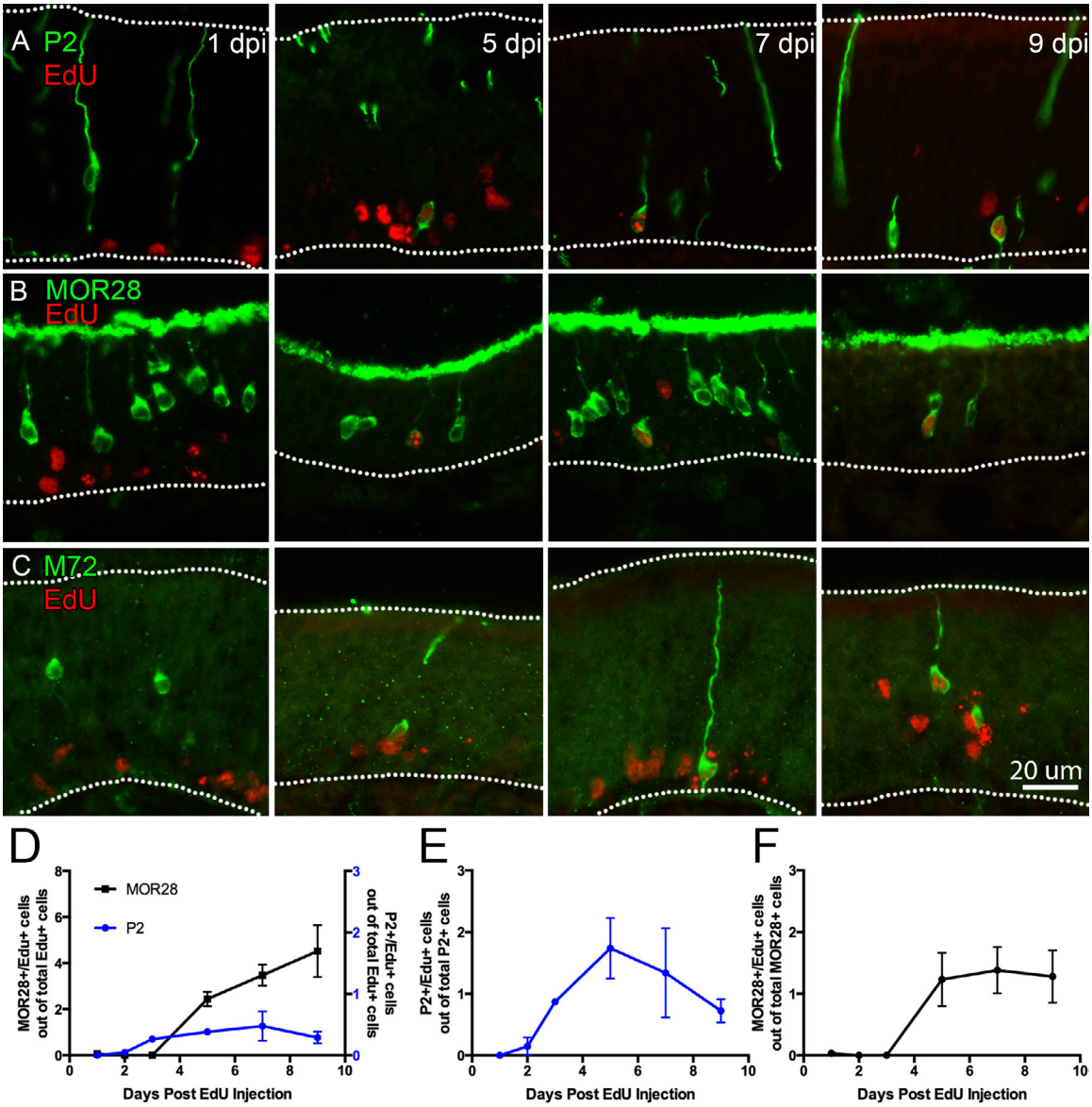

Figure 3. ORs become prominent at 5 days post basal cell division.
(A) P2 and EdU co-staining at 1, 5, 7, and 9 days post EdU injection. Double positive cells can be found at 5 days post injection (DPI). P2 was detected via beta-galactosidase staining in *P2-IRES-taulacZ* transgenic mice. **(B)** MOR28 and EdU co-staining. MOR28 was detected using an antibody made by Dr. Gilad Barnea. **(C)** M72 and EdU co-staining. M72 was detected via GFP staining in *M72-IRES-tauGFP* transgenic mice. **(D)** Quantification of OR (+)/EdU (+) cells out of total EdU (+) cells. P2 double positive cells increase prior to MOR28 double positive cell and begin to decrease starting at 7 DPI whereas MOR28 double positive cells trend toward increases (or remain constant) from 5 days post injection (DPI) to 9 DPI. **(E)** Quantification of P2 (+)/EdU (+) cells out of total P2 (+) cells. **(F)** Quantification of MOR28 (+)/EdU (+) cells out of total MOR28 (+) cells. **(D-F)** Data points represent the mean of three animals and error bars = SEM. Dotted white line indicates the basal lamina (bottom) and the apical surface (top).

5.2 LSD1 expression during OSN maturation

A hypothesized role for LSD1 in epigenetic regulation of OR gene transcription requires its expression with a timing that coincides with or precedes receptor expression. LSD1 immunostaining patterns in the OE have been published with several different anti-LSD1 antibodies (Krolewski et al., 2013; Lyons et al., 2013; Kilinc et al., 2016). The described staining patterns are overlapping, though not completely concordant. Moreover, the distribution of tissue staining with the rabbit polyclonal antibody used here for immunoprecipitation (Abcam ab#62582) has not been described. The antibody has been validated in my hands as specific for LSD1 as shown by the lack of staining on LSD1 knock-out tissue (see below). Herein, I determined when and where LSD1 is expressed during OSN maturation using EdU pulse-chase experiments, and whether LSD1 is associated with its binding partner, CoREST, by immunostaining and co-immunoprecipitation.

With respect to the timing of LSD1 expression, EdU pulse-chase experiments demonstrate that LSD1 (+)/EdU (+) cells are abundant at 1 DPI encompassing 74% of the EdU (+) cells (Fig. 4A,C). With respect to subsequent stages, LSD1 (+)/EdU (+) cells remain high until 9 DPI at the time of OSN maturation to OMP (+) neurons (Fig. 4A,C and Fig. 2C). I also looked at the timing of expression of the LSD1 corepressor, CoREST, as LSD1 binding partners play a signifacant role in LSD1 substrate specificity (Lee et al., 2005). CoREST expression as a function of time after injection of EdU mimics that of LSD1 suggesting that the two proteins are likely expressed in the same cell populations (Fig. 4B,C). Indeed, by immunostaining both proteins are co-expressed in the vast majority of labeled cells in the normal OE, which are situated immediately superficial to the CK14 (+)/LSD1 (-)/CoREST (-) HBCs (Fig. 5G). The immunostaining results are supported by the detection of both proteins in homogenized OE via Western blot (Fig. 5H). By comparison with my data on the timing of OR expression, LSD1 and CoREST are detectable prior to OR expression (as defined by either co-expression of a marker

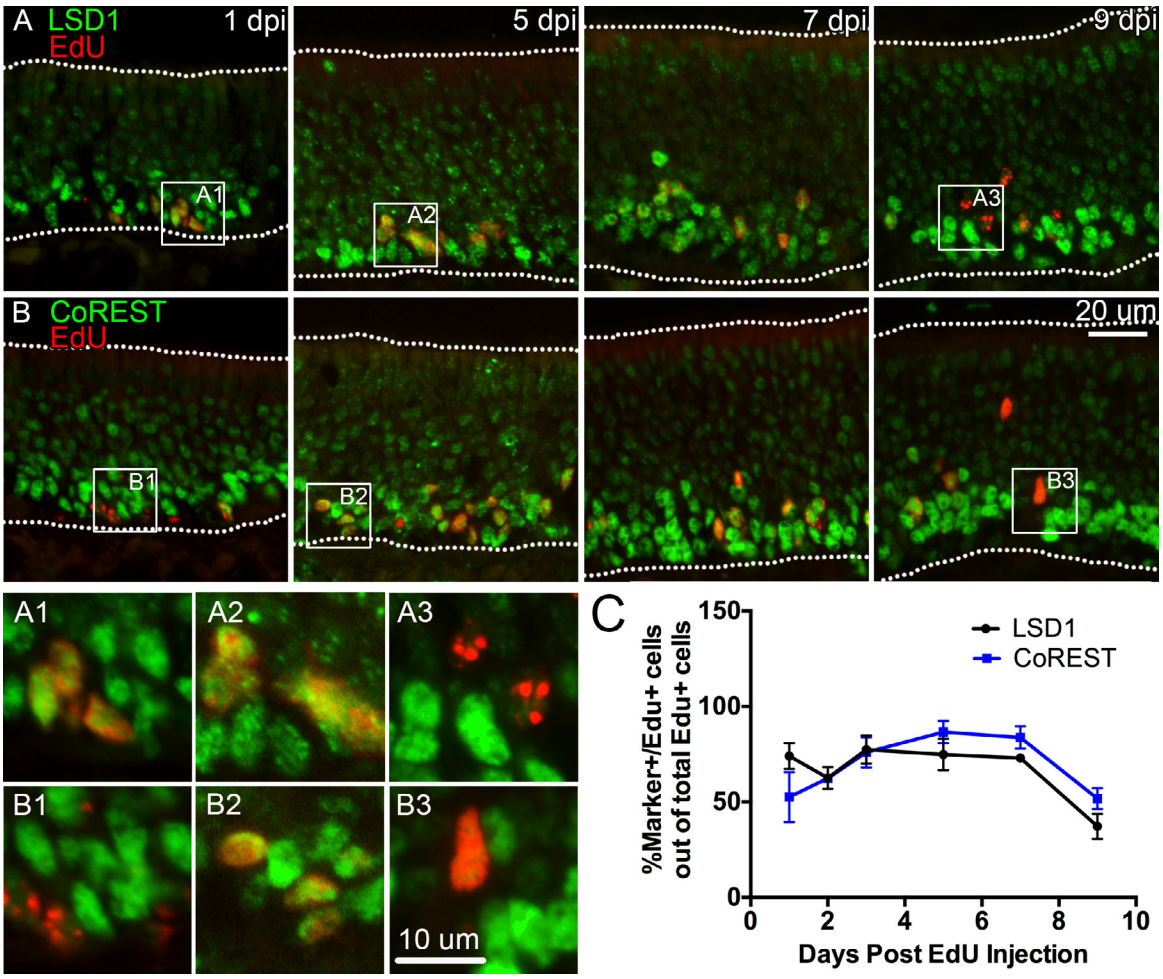

Figure 4. LSD1 and CoREST are prevalent in early dividing cells and begin to decrease starting at 7 days post basal cell division.
(A) LSD1 and EdU costaining at 1, 5, 7, and 9 days post EdU injection. Double positive cells are abundant until 9 days post injection (DPI). **(B)** CoREST and EdU costaining. Double positive cells are abundant until 9 days post injection (DPI). **(C)** Quantification of Marker (+)/Edu (+) cells out of total Edu (+) cells. Data points represent the mean of three animals and error bars = SEM. Dotted white line indicates the basal lamina (bottom) and the apical surface (top).

protein or immunostaining for the OR) and full neuronal maturity, i.e., OMP expression (cf. Figs 3,4).

Classification of the cells that co-express LSD1 and CoREST was accomplished using several markers for the different types of GBCs and for the maturation of OSNs (Fig. 5). Both LSD1 and CoREST are found in Neurog1-eGFP (+) GBC_{INP} and Tuj1 (+) immature OSNs (Fig. 5A, B, D, E). By immunohistochemistry, neither LSD1 nor CoREST is highly expressed in OMP (+) mature OSNs (Fig. 5C,F).

Finally, I demonstrated directly that LSD1 and CoREST can interact and bind *in vivo* as revealed by co-immunoprecipation of CoREST when immunoprecipitating LSD1 from the OE (Fig. 5I). To further characterize the LSD1/CoREST complex that is present in GBC_{INPs}, I immunostained for another member of this epigenetic silencing complex,

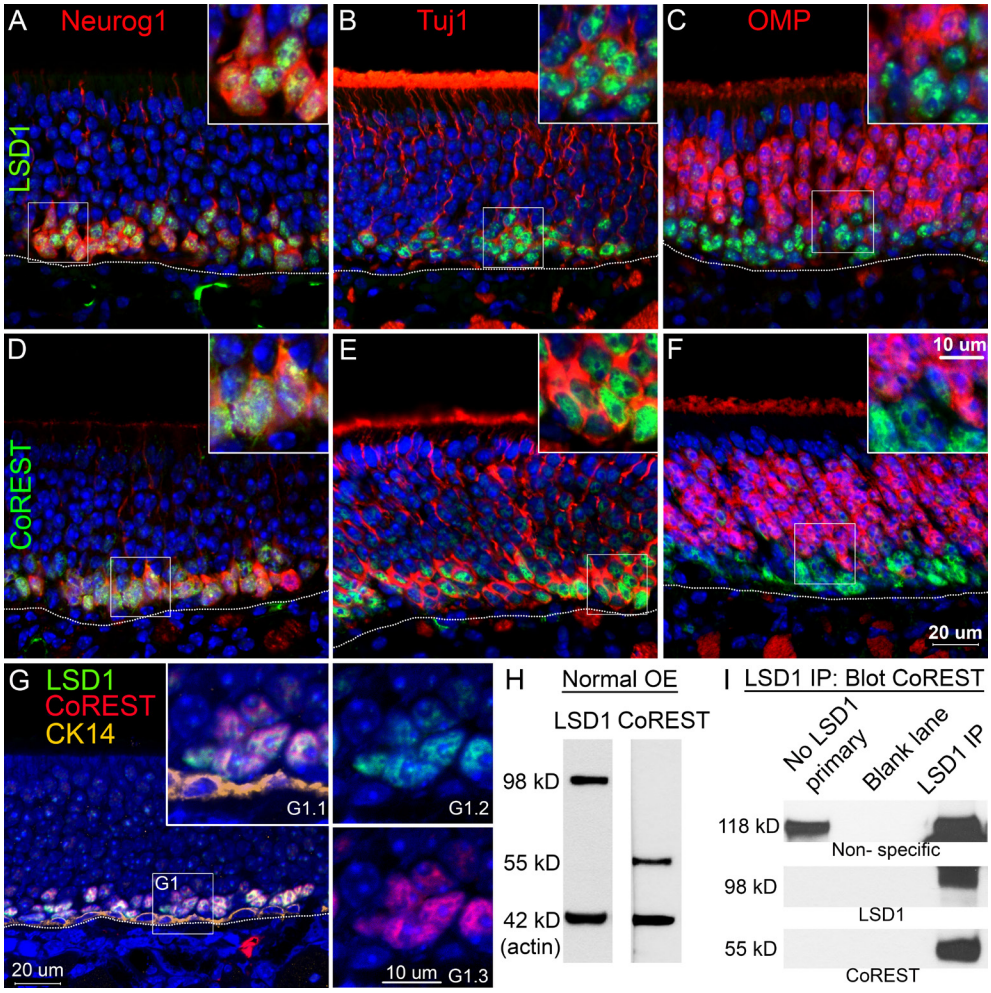

Figure 5. LSD1 and CoREST are expressed in the same population of cells and complex together in the mouse OE.
(A-C) LSD1 costains with Neurogenin 1 (stained for GFP in *Neurog1-eGFP* animals), Tuj1, and OMP. High LSD1 expression if found in Neurog1 (+) and Tuj1 (+) cells but not in OMP (+) OSNs. **(D-E)** CoREST costains with Neurog1, Tuj1 and OMP in the same tissue imaged in A-C. **(G)** LSD1 and CoREST are expressed in overlapping cells and are not found in CK14 (+) HBCs. **(H)** LSD1 and CoREST are abundantly expressed in the mouse OE with molecular weights of 98 kD and 55 kD, respectively. **(I)** LSD1 immunoprecipitate blots positive for CoREST, demonstrating that the two proteins are in complex together in the OE. Dotted white line indicates the basal lamina.

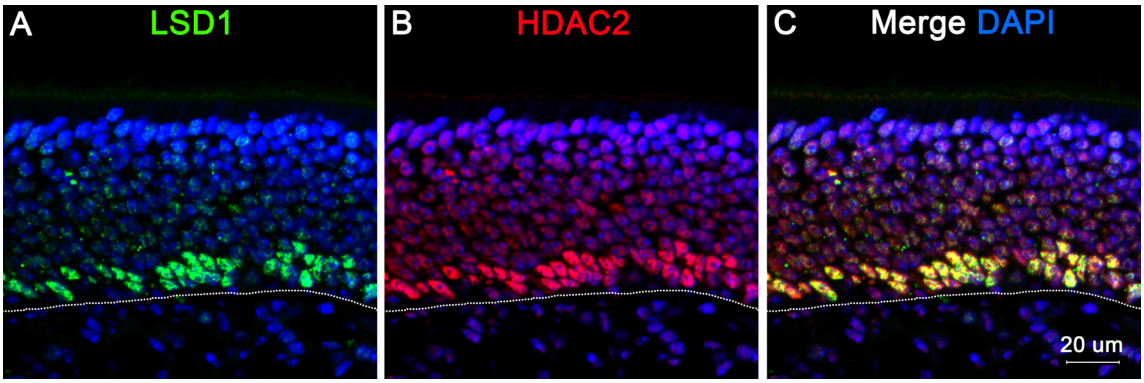

Figure 6. LSD1 and HDAC2 are co-expressed in the mouse OE.
(A-C) LSD1 (+) and HDAC (+) cells overlap in expression in the basal layers of the adult OE. Dotted white line indicates the basal lamina.

HDAC2 and found that HDAC2 expression is almost completely overlapping with that of LSD1 (Fig. 6) (Lee et al., 2005).

Previous descriptions suggested that LSD1 expression patterns change following OE lesion (Krolewski et al., 2013); therefore, I assessed LSD1 and CoREST patterns in two injury models: olfactory bulbectomy (OBX) and methylbromide (MeBr)-lesion (Fig. 7). As expected, LSD1 (+) and CoREST (+) cells increased post OBX (Fig. 7A-D), in line with the increase in Neurog1-eGFP (+) GBC_{INPs} and immature OSNs following bulbectomy (Iwema and Schwob, 2003; Krolewski et al., 2013). LSD1 and CoREST appear in CK14 (+) HBCs following MeBr lesion (Fig. 7E-H), a finding previously reported by our lab using a different LSD1 antibody (Krolewski et al., 2013). Thus, activating HBCs represent the earliest cell type expressing LSD1 and CoREST in the adult mouse OE.

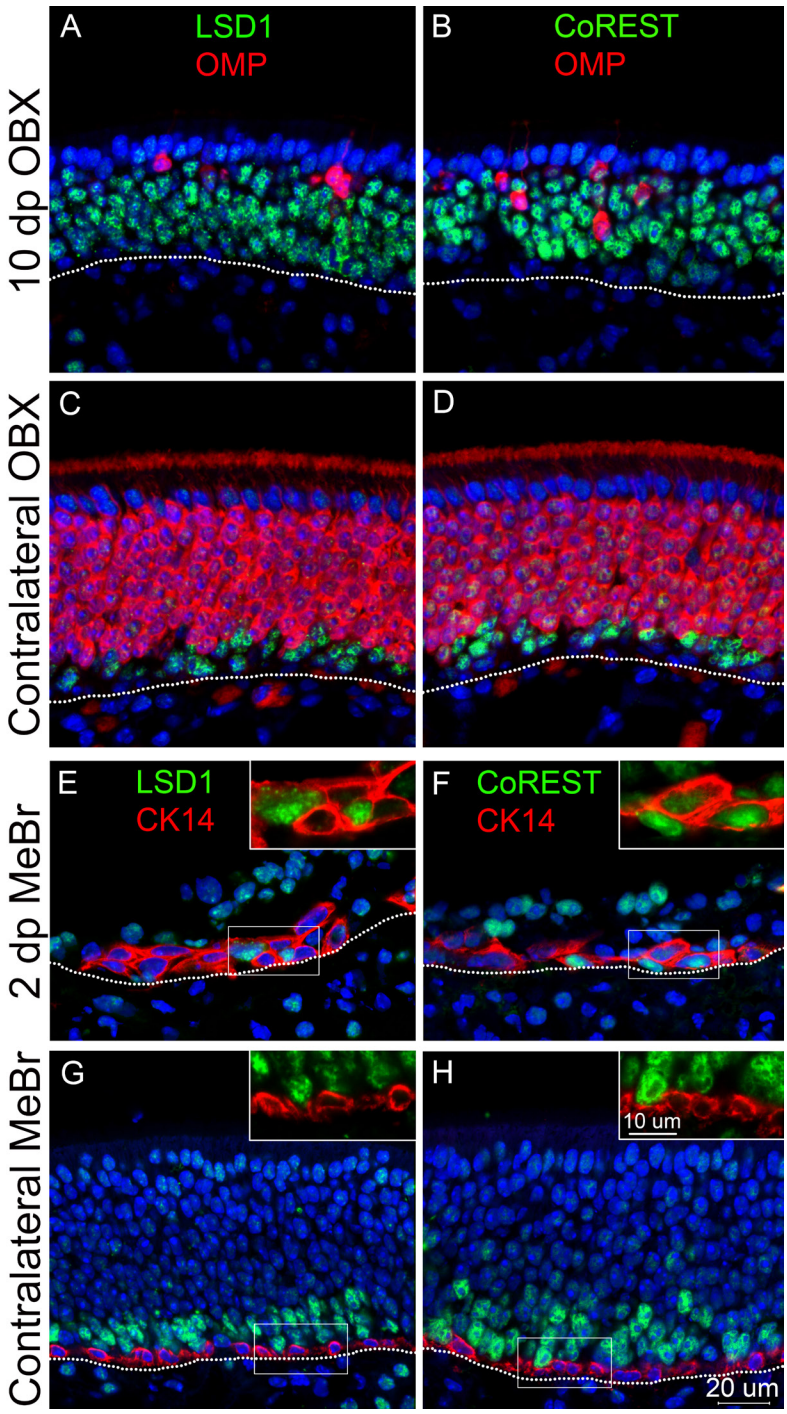

Figure 7. LSD1 and CoREST populations expand following bulbectomy and appear in activating HBCs at 2 days post MeBr lesion. **(A,B)** LSD1 and CoREST populations expand on the ablated side at 10 days post OBX as compared to the **(C,D)** contralateral control sides respectively. **(E,F)** LSD1 and CoREST appear in CK14 (+) HBCs at 2 days post unilateral MeBr lesion whereas on the **(G,H)** contralateral, unlesionsed side, LSD1 and CoREST are not found in CK14 (+) HBCs. Dotted white line indicates the basal lamina.

5.3 LSD1 knockout in activating K5 (+) HBC_{MPPs} and Ascl1 (+) $GBC_{TA\text{-}Ns}$ aborts OSN maturation while knockout in Neurog1 (+) GBC_{INPs} does not.

Previous studies of LSD1 function in the OE used a *Foxg1-Cre* driver to knock out *Lsd1* as early as E10.5 in the olfactory placode (Duggan et al., 2008; Lyons et al., 2013). Because elimination of *Lsd1* precedes all but the very earliest stage in GBC and neuronal differentiation, one cannot draw any conclusion regarding the specific cell types in which the gene is functioning and how Foxg1 expression relates to the timing of OR expression and OR choice. Here, I take advantage of $CreER^{T2}$ drivers in order to excise *Lsd1* at defined, distinct, stages in the emergence of OSNs from the stem and progenitor populations. Specifically, I used a *K5-*$CreER^{T2}$ driver to excise *Lsd1* in the population of reserve stem cells, i.e., the HBCs, prior to the activation by injury. Additionally I used an *Ascl1-*$CreER^{T2}$ driver to accomplish recombination at the $GBC_{TA\text{-}N}$ stage and a *Neurog1-*$CreER^{T2}$ to do the same at the GBC_{INP} stage.

For the first set of experiments, mice with the following genotype *K5-*$CreER^{T2}$*; R26Rfl(stop)TdTomato (TdT);* $Lsd1^{fl/fl,}$ were given tamoxifen (TAM) at 6 weeks of age to excise Exon 6 of *Lsd1* and induce heritable expression of the TdT reporter (Fig. 8A) (Wang et al., 2007). Two weeks later, the K5 (+) HBCs were activated by MeBr lesion followed by tissue harvest 3 weeks post-injury, allowing adequate time for large numbers of traced HBCs to mature into OMP (+) OSNs (Fig. 8B,C) (Schwob et al., 1995). For animals that are either wild-type ($Lsd1^{+/+}$) or heterozygous ($Lsd1^{fl/+}$) at the *Lsd1* locus, an average of ~60% of the total number of TdT (+) neurons (OMP (+) and Tuj1 (+) cells inclusive) were OMP (+) at 3 weeks post lesion (Fig. 8C-F, I). In strong contrast, in the homozygous conditional knockout animals ($Lsd1^{fl/fl}$), only ~6% of total TdT (+) neurons were OMP (+) (Fig. 8G-I). That a small percentage TdT (+) cells reach full maturation and OMP expression in the $Lsd1^{fl/fl}$ mice most likely reflects a relative inefficiency for recombination of both alleles at the *Lsd1* locus, by comparison with excision of the stop motif at the *ROSA26* locus, such that the small minority of the TdT (+) cells that achieve

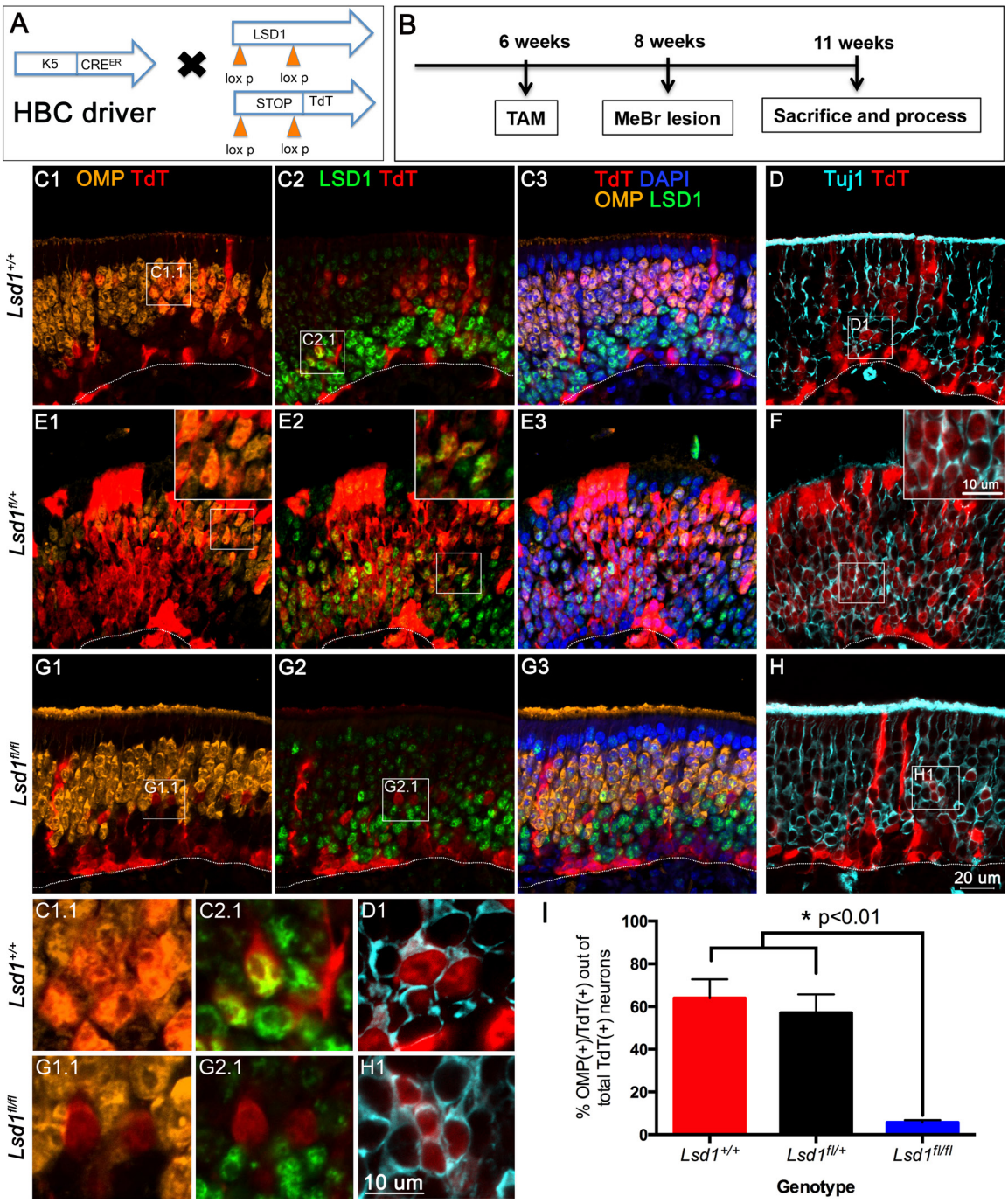

Figure 8. Neuronal maturation is halted in activated HBCs lacking LSD1.
(A,B) Transgenic mice and experimental design. **(C-F)** Activated HBCs from *Lsd1*$^{+/+}$ and *Lsd1*$^{fl/+}$ mice mature into OMP (+) OSNs by 3 weeks post MeBr lesion. **(G-H)** Activated HBCs from *Lsd1*$^{fl/fl}$ mice are unable to mature into OMP (+) OSNs and instead halt in maturation as Tuj (+) immature OSNs. **(I)** Quantification of the percent of activated HBCs that are OMP (+) cells out of the total number of lineage traced neurons (both OMP (+) and Tuj (+) OSNs). Bar graphs represent the mean counts of 3 animals per phenotype and error bars = SEM. Dotted white line indicates the basal lamina.

OMP expression in the homozygous mice are not null for *Lsd1*. Indeed, some of the TdT (+) cells in the homozygote are labeled by immunostaining for LSD1, demonstrating variability in Cre recombination at the two loci. Incomplete recombination has been demonstrated immunohistochemically for several other gene targets (unpublished observations), underscoring the necessity of verifying knockout of the gene of interest whenever possible to avoid confounding variables. Importantly, staining for LSD1 in the homozygous knockout mice demonstrated also that the efficiency of recombination varied across the plane of the epithelium; in areas with a greater overall degree of recombination, indicated by a higher percentage of TdT (+) HBCs, fewer TdT (+) cells retained LSD1 immunoreactivity (data not shown). In order to minimize the consequences of incomplete recombination, I screened first for loss of LSD1 expression via immunostaining; in regions where the knockout appeared to be complete, TdT (+)/OMP (+) and TdT (+)/Tuj1 (+) neurons were counted in the matching area on the adjacent sections (screening TdT/LSD1/OMP/Tuj1 together was not possible due to antibody incompatibility). Despite these precautions, it remains possible that I counted a portion of TdT (+) cells that retained one or more copies of the non-recombined floxed-*Lsd1* allele; these cells likely account for the TdT (+) cells with the ability to mature into OMP (+) OSNs.

My results demonstrate that LSD1 is required for the progression from activated HBC_{MPPs} to fully mature, OMP (+) OSNs. These findings phenocopy the results obtained with Foxg1-driven excision of *Lsd1* in early development (Lyons et al., 2013).

To rule out any contribution that MeBr lesion might make to the failure to mature, I took advantage of the very low, but noticeable activation of HBCs following ablation of the olfactory bulb. Thus, I bulbectomized *K5-CreER^{T2}; R26Rfl(stop)TdTomato (TdT); Lsd1$^{fl/fl}$* mice (Fig. 9). Once again, in the homozygous *Lsd1$^{fl/fl}$* animals, neurons failed to mature to express OMP (+) while adjacent cells were able to express OMP (Fig. 9C-F).

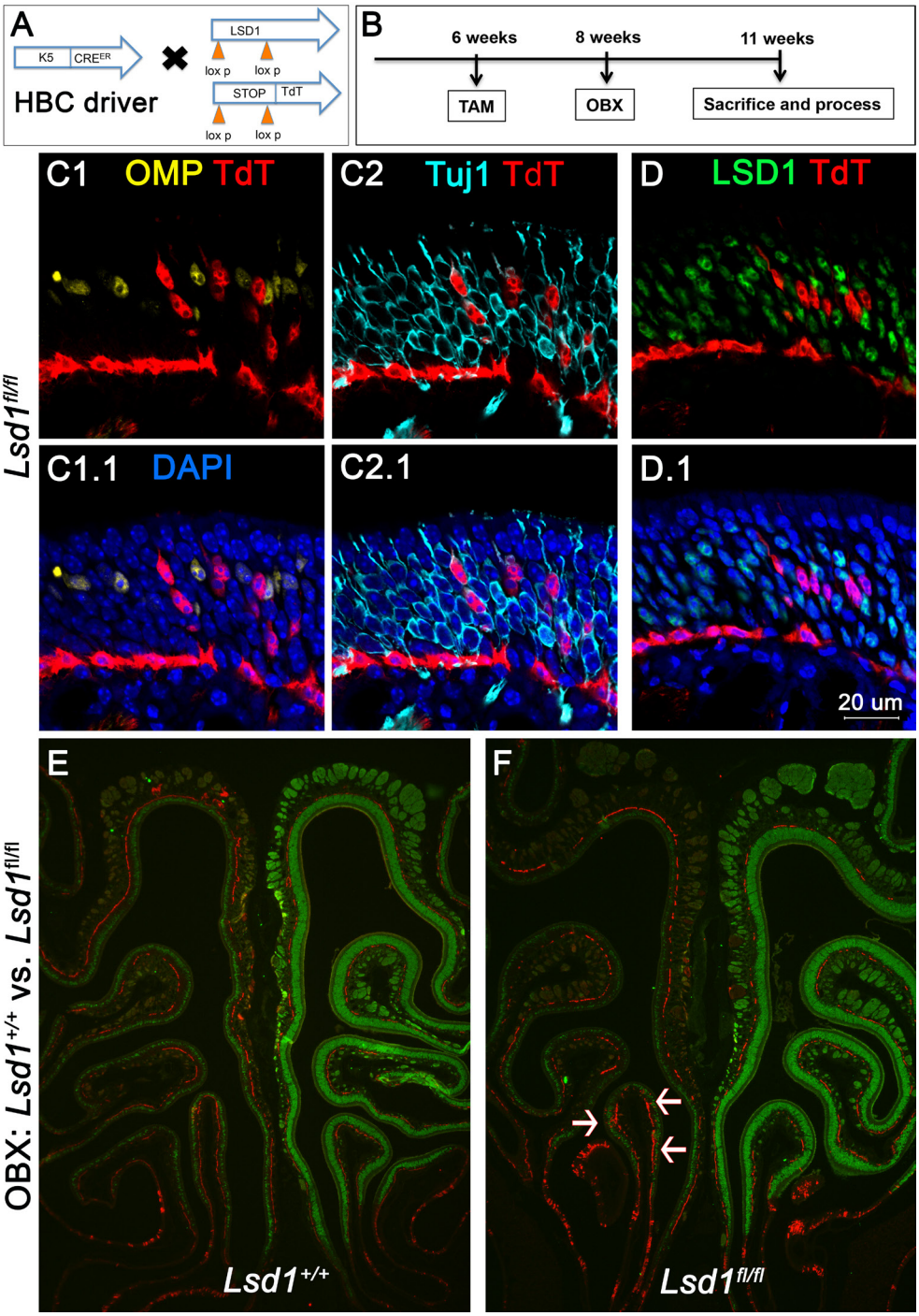

Figure 9. Rare HBCs activated by OBX and lacking LSD1 do not mature into OMP (+) OSNs.

(A,B) Transgenic mice and experimental design. **(C-D)** Rare HBCs activated by OBX and lacking LSD1 do not mature into OMP (+) OSNs. **(E)** Control TdT reporter tissue (*Lsd1*$^{+/+}$) showing no activation upon bulbectomy. **(F)** LSD1 conditional knockout tissue shows rare HBC activation upon bulbectomy in regions highlight by the 3 white arrows. Dotted white line indicates the basal lamina.

For the second set of experiments investigating cell-stage specific deletion of *Lsd1*, mice with the following genotype *Ascl1-CreER^{T2}; R26Rfl(stop)TdTomato (TdT); Lsd1$^{fl/fl,}$* were given TAM at 6 weeks of age to excise Exon 6 of *Lsd1* and induce heritable expression of the TdT reporter, in order to interrogate LSD1 function at the Ascl1 (+) GBC_{TA-N} stage (Figs. 10,11). In these experiments, I assessed neuronal maturation in the unlesioned OE (Fig. 10) and following direct epithelial injury by injection of methimazole (Bergman et al., 2002) (Fig. 11); methimazole was used because the strain background of these transgenic mice is resistant to the olfactotoxic effects of MeBr. As with the K5-driver, I observed incomplete recombination at the *Lsd1* locus in the *Ascl-CreER^{T2}* mice despite robust recombination at the *ROSA* locus (Fig. 10G2, Fig. 11G2). Nonetheless, there were large swaths of TdT (+)/LSD1 (-) cells, particularly in methimazole-lesioned animals (Fig. 10G2, Fig. 11G2). While the variable efficiency of Cre-mediated recombination made cell counting more complicated (as described above), the intermingling of TdT (+)/LSD1 (+) and TdT (+)/LSD1 (-) cells in the same section presented a within-animal control demonstrating that cells that lack LSD1 expression fail to mature and do not express OMP, whereas cells that retain LSD1 immunoreactivity do mature (Figure 10G). Again, for cell counts, I screened for TdT (+)/LSD1 (-) regions and counted adjacent sections for TdT, OMP, and Tuj1 and found a significant decrease in TdT (+)/OMP (+) cells out of total OSNs (OMP (+) and Tuj (+) cells) in the *Lsd1* homozygous knock out animals under both unlesioned and lesioned conditions (Fig. 10I, Fig. 11I). Specifically, for animals that were either wild-type (*Lsd1$^{+/+}$*) or heterozygous (*Lsd1$^{fl/+}$*) at the *Lsd1* locus, an average of ~85% (under non-lesioned conditions) and ~70% (under lesioned conditions) of the total number of TdT (+) neurons (OMP (+) and Tuj1 (+) cells inclusive) were OMP (+) at 2 weeks post TAM/lesion (Fig. 10I, Fig. 11I). In contrast, in the homozygous conditional knockout animals (*Lsd1$^{fl/fl}$*), only ~25% of total TdT (+) neurons were OMP (+) under both unlesioned and lesioned conditions (Fig. 10I, Fig. 11I).

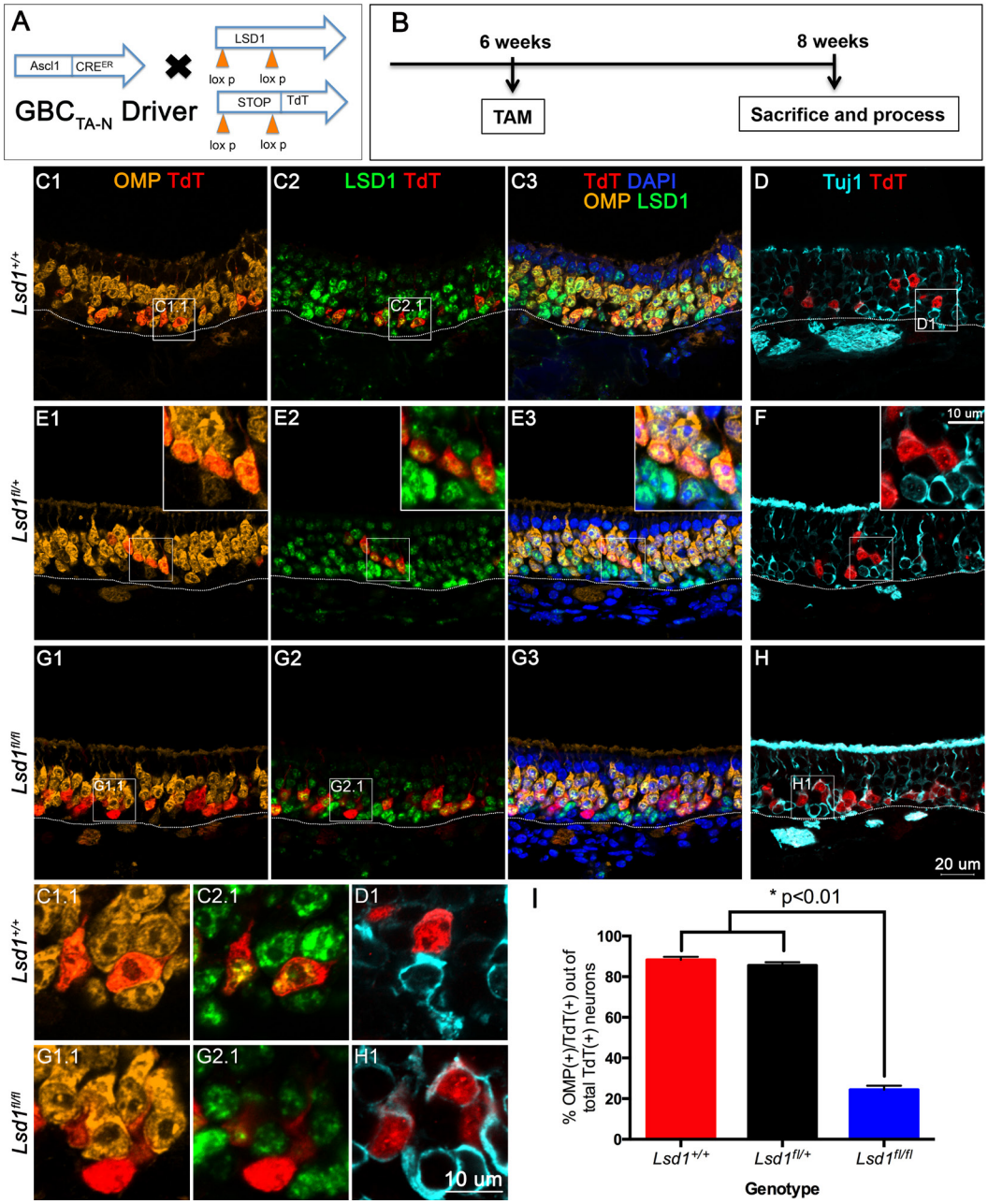

Figure 10. Neuronal maturation is halted in maturing transit-amplifying Ascl1 (+) GBCs that lack LSD1.

(A,B) Transgenic mice and experimental design. **(C-F)** Ascl1-GBCs from *Lsd1*$^{+/+}$ and *Lsd1*$^{fl/+}$ mice mature into OMP (+) OSNs by 2 weeks post Tamoxifen administration. **(G-H)** Ascl1-GBCs from *Lsd1*$^{fl/fl}$ mice are unable to mature into OMP (+) OSNs and instead halt in maturation as Tuj (+) immature OSNs. **(I)** Quantification of the percent of Ascl1-GBC progeny that are OMP (+) cells out of the total number of lineage traced neurons (both OMP (+) and Tuj (+) OSNs). Bar graphs represent the mean counts of 3 animals per phenotype and error bars = SEM. Dotted white line indicates the basal lamina.

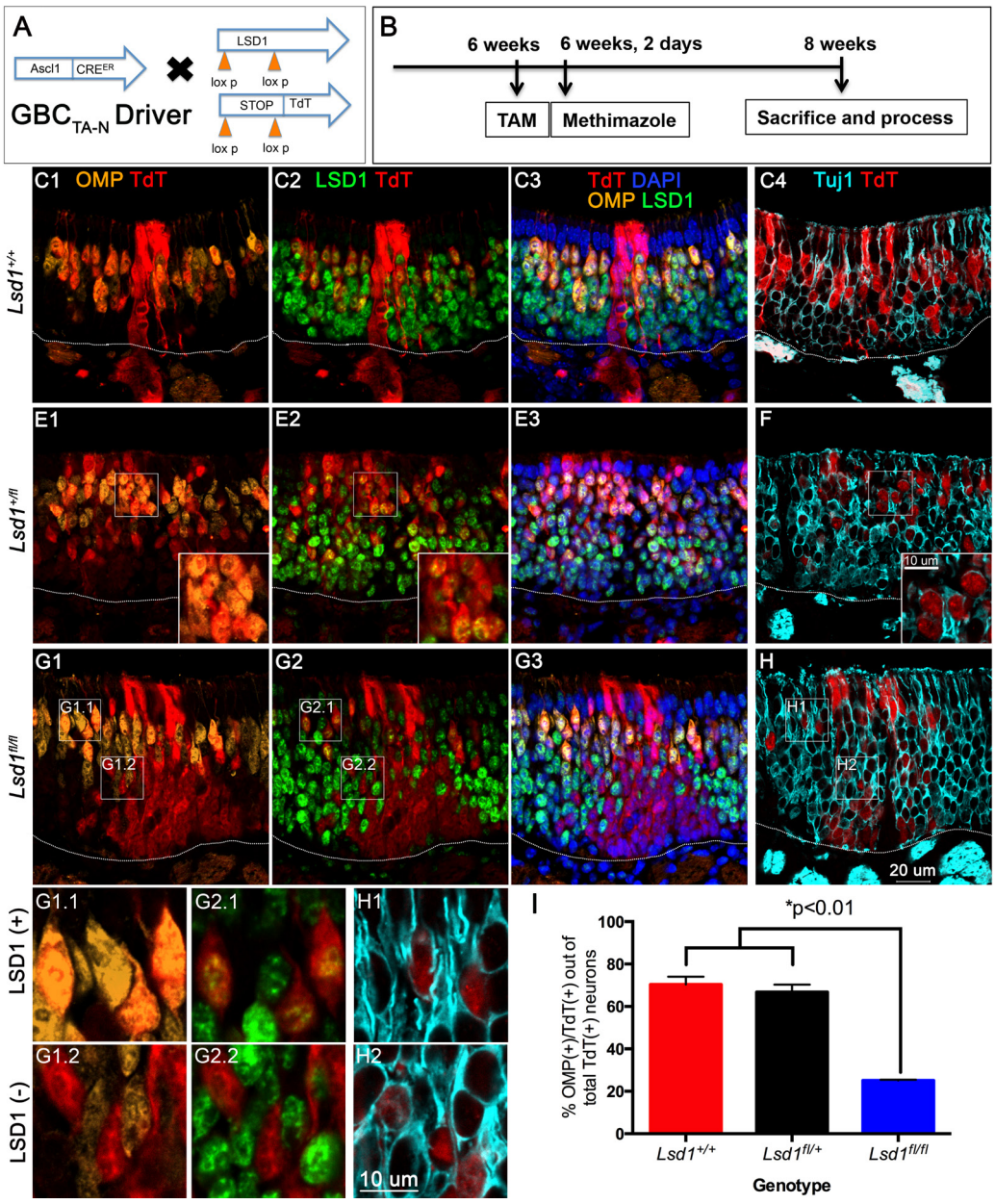

Figure 11. Neuronal maturation is halted in maturing transit-amplifying Ascl1 (+) GBCs that lack LSD1 following olfactory lesion.

(A,B) Transgenic mice and experimental design. **(C-F)** A portion of Ascl1-GBCs from *Lsd1*$^{+/+}$ and *Lsd1*$^{fl/+}$ mice mature into OMP (+) OSNs by 2 weeks post methimazole lesion. **(G-H)** Ascl1-GBCs from *Lsd1*$^{fl/fl}$ mice are unable to mature into OMP (+) OSNs and instead halt in maturation as Tuj (+) immature OSNs. **(I)** Quantification of the percent of Ascl1-GBC progeny that are OMP (+) cells out of the total number of lineage traced neurons (both OMP (+) and Tuj (+) OSNs). Bar graphs represent the mean counts of 3 animals per phenotype and error bars = SEM. Dotted white line indicates the basal lamina.

For the third set of experiments, mice with the genotype *Neurog1-CreER^{T2}; R26Rfl(stop)TdTomato (TdT); Lsd1$^{fl/fl,}$* were given tamoxifen (TAM) at 6 weeks of age to excise Exon 6 of *Lsd1* and induce heritable expression of the TdT reporter in order to interrogate LSD1 function at the Neurog1 (+) GBC_{INP} stage (Fig. 12). Conditional knockout of *Lsd1* from Neurog1 (+) GBC_{INPs} under both basal and lesioned conditions did not interfere with the maturation of the OSNs that were progeny of the targeted GBCs. Unlike conditional deletion of *Lsd1* at either the K5 (+) HBC_{MPP} or Ascl1 (+) GBC_{TA-N} stage in the progression, Neurog1 (+) GBC_{INPs} lacking LSD1 were capable of maturing into OMP (+) OSNs during the same timeframe in both *Lsd1$^{+/+}$* and *Lsd1$^{fl/+}$* control animals (Fig 12C-J). Once again, I observed evidence of differential Cre recombination at *Lsd1* and the *TdT* reporter loci, for which I compensated as described above. Thus, I was able to demonstrate numerous TdT (+) cells that co-expressed OMP, despite their complete lack of detectable LSD1 expression (Fig. 12G, H). Thus, LSD1 is not required for neuronal maturation during the progression from Neurog1 (+) GBC_{INPs} to mature OSNs (Results summarized in Fig. 13).

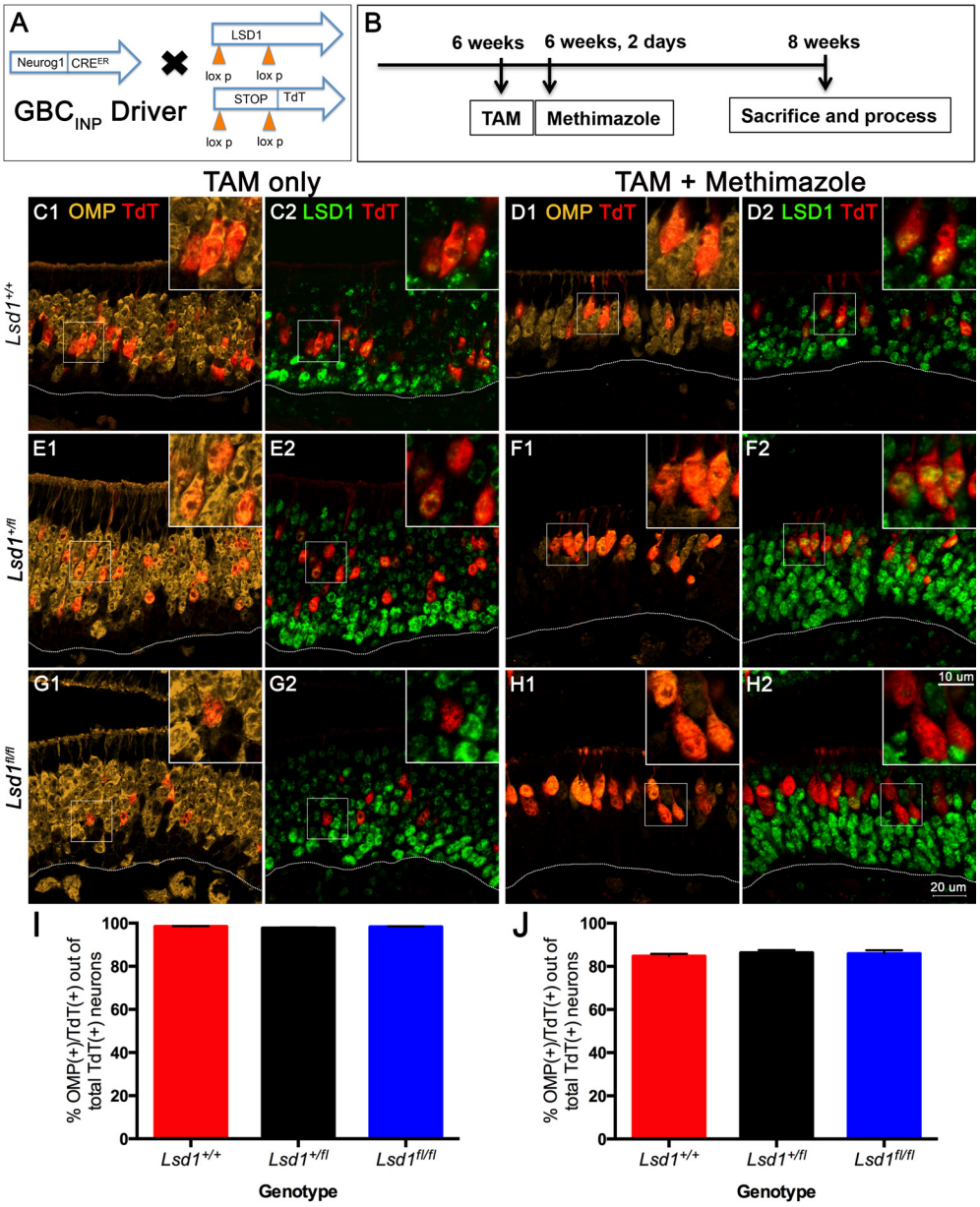

Figure 12. Neurog1-GBC$_{INPs}$ lacking LSD1 are capable of maturing into OMP (+) OSNs under both basal and lesioned conditions.
(A,B) Transgenic mice and experimental design. **(C,E,G)** Neurog1-GBCs from from *Lsd1*$^{+/+}$, *Lsd1*$^{fl/+}$, and *Lsd1*$^{fl/fl}$ mice mature into OMP (+) OSNs by 2 weeks post tamoxifen administration. **(D,F,H)** *Lsd1*$^{+/+}$, *Lsd1*$^{fl/+}$, and *Lsd1*$^{fl/fl}$ mice mature into OMP (+) OSNs by 2 weeks post methimazole lesion. **(I,J)** Quantification of the percent of Neurog1-GBC progeny that are OMP (+) cells out of the total number of lineage traced neurons (both OMP (+) and Tuj (+) OSNs) under both tamoxifen only and lesioned conditions. Bar graphs represent the mean counts of 3 animals per phenotype and error bars = SEM. Dotted white line indicates the basal lamina.

Summary

The present study determined that LSD1 (1) is expressed in early dividing cells before OR expression and neuronal maturation and decreases at the time of OR stabilization (Fig. 2-4); (2) colocalizes with CoREST and HDAC2 in these early dividing cells (Fig. 5-7); and (3) is required for neuronal maturation during a distinct time window between activating reserve, multipotent stem cells (horizontal basal cells) and Neurogenin1 (+) (Neurog1) immediate neuronal precursors (Fig. 8-13). Thus, this study clarifies the role of LSD1 in olfactory neuronal maturation (Fig. 13).

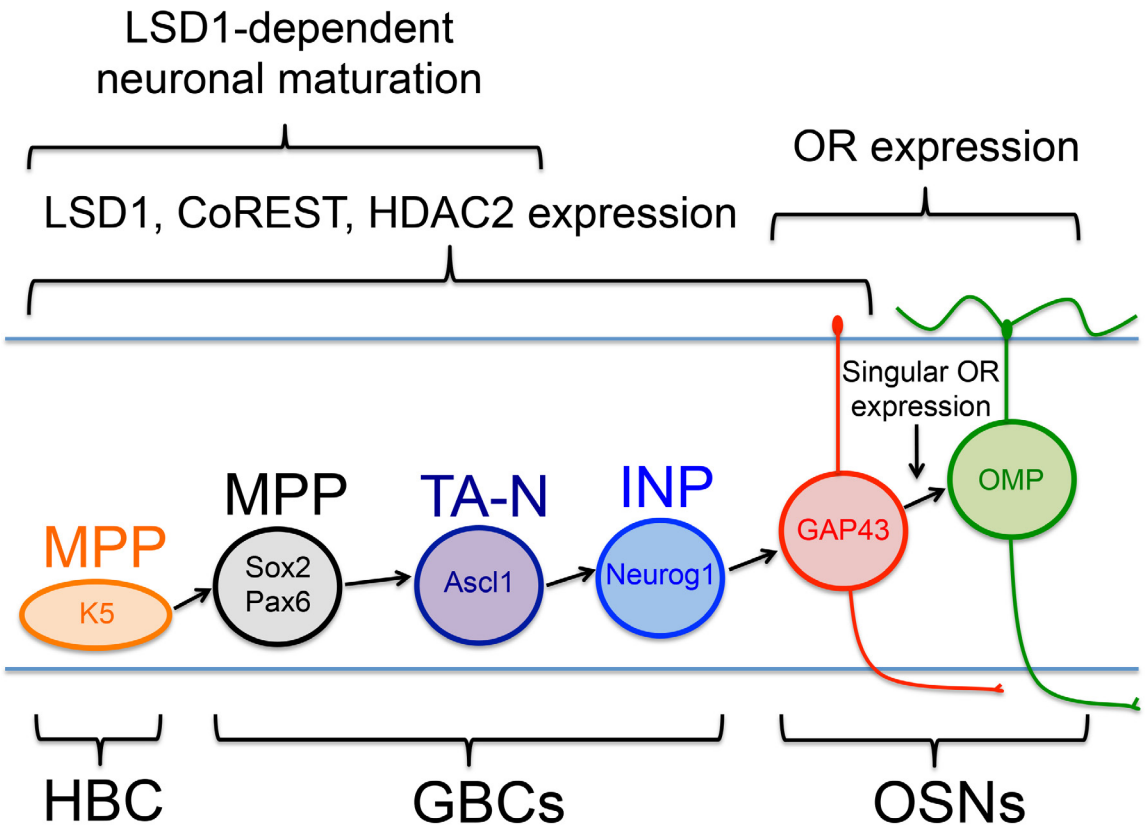

Figure 13. LSD1 in neuronal maturation: Results Summary
LSD1 is expressed in early dividing cells before OR expression and neuronal maturation and decreases at the time of OR stabilization. LSD1 colocalizes with CoREST and HDAC2 and is required for neuronal maturation during a distinct time window between activating reserve stem cells (HBCs) and Neurog1 (+) GBC immediate neuronal precursors (INPs).

Chapter 6.

Discussion and Future Directions

6.1 Dedifferentiation in the OE

In the Chapter 3 of my thesis work, I sought to optimize and validate olfactory transplants as a reliable model to assay biologically relevant stem cell potencies. Through these control experiments, in close collaboration with a fellow graduate student in the lab, Brian Lin, we discovered a previously un-described plasticity in the immediate neuronal precursor (INP) population, the Neurog1 (+) GBC_{INP}. Specifically, we found that injury to the OE via bulb ablation allows previously neuronally committed progenitors to dedifferentiate and give rise to all OE cells types under the transplantation experimental paradigm. Furthermore, this *in vivo* reprogramming correlated with an up-regulation of the transcription factor *Sox2*, a Yamanaka factor that plays a pivotal role in progenitor potency in many adult epithelial populations including the testes, stomach, and lens (Arnold et al., 2011), as well as during embryonic development (Ellis et al., 2004; Hutton and Pevny, 2011).

Following up on our transplantation experiments, Brian Lin has now demonstrated that Neurog1-eGFP (+) GBC_{INPs} can dedifferentiate following epithelial injury *in situ* via genetic lineage tracing. Furthermore, the progenitor capacity of the Neurog1 (+) GBC_{INPs} is titratable by the extent of injury: bulb ablation initiates minimal but detectable dedifferentiation as assayed by non-neuronal lineage traced cells, whereas methimazole lesion initiates larger scale dedifferentiation and production of abundant non-neuronal progeny (data not shown). Based on our observation of *Sox2* appearing in Neurog1 (+) cells following bulb ablation, Brian knocked out *Sox2* from Neurog1 (+) cells via genetic excision. Under these circumstances, the Neurog1 (+) cells were no longer capable of injury-induced dedifferentiation, definitively demonstrating that *Sox2* is required for injury-induced Neurog1 (+) GBC_{INP} plasticity. Importantly, OE lacking *Sox2* in the Neurog1 (+) cells did not regenerate to full capacity as compared to control animals, suggesting that dedifferentiation plays an important role in the regenerative process, contributing significantly to cell replacement.

Dedifferentiation has now been described in several *in vivo* settings including the liver, airway, and intestine (Michalopoulos et al., 2005; Tata et al., 2013; Yanger et al., 2013; Zhao et al., 2014; Tetteh et al., 2016). In each case, the differentiative capacity of "terminally differentiated" cells was altered following injury to the tissue and/or removal of the defined stem cell population. Similarly, in our model, we find that neuronally committed cells are capable of dedifferentiation upon severe epithelial injury. Importantly, our description is the first example of dedifferentiation in a neuronal lineage; furthermore, our work describes a mechanism involving *Sox2* up-regulation. The question thus arises, why do several systems have the capacity for cells to dedifferentiate? We posit a simple answer: to assist in tissue regeneration. In fact, we observed that tissue impaired in dedifferentiation did not regenerate to the same extent as control tissue. This suggests that dedifferentiation plays a significant role in tissue repair, assisting the *bona fide* stem cells to replace cells lost during injury.

Given the growing literature on induced pluripotent stem cells (iPSCs), whereby differentiated cells can be induced into stem cells *ex vivo*, it is not surprising that machinery for dedifferentiation exists *in vivo*. But, can this unlocked *in vivo* plasticity be utilized similarly to iPSCs for regenerative medicine? Some propose that *in vivo* dedifferentiation should actually replace (or, more so—overstep) iPSCs for use in regenerative medicine (Lazaro and Kostarelos, 2014; Lázaro et al., 2014). If mature cells can be induced to dedifferentiate *in situ* and assist in tissue repair, many of the concerns involved with iPSCs diminish – most notably tumorigenesis, as this type of regeneration assists in tissue repair without altering the integrity of the tissue. Advancements of this type of clinically-initiated *in situ* dedifferentiation will depend on our understanding of the mechanisms and factors driving this process.

Future Directions

We are currently working to elucidate more effectors of Neurog1 (+) GBC_{INP} injury-induced dedifferentiation. Of immediate relevance are the three other Yamanaka factors (aside from *Sox2*): *Oct3/4*, *c-Myc*, and *Klf4*. In fact, we found that both *c-Myc* and *Klf4* increase in expression in Neurog1 (+) GBC_{INPs} following bulb ablation by single-cell RNA-seq. Aside from the Yamanaka factors, we also hypothesize that epigenetic factors play a significant role in differentiation in the OE. We are specifically interested in following up on a role for Polycomb repressive complex components in the dedifferentiative process.

Outside of currently pursued future directions, it will be interesting to determine if further differentiated cells can be pushed to dedifferentiate – such as the Sus cells or OSNs. Lineage tracing experiments with *OMP-CreER^{T2}* and *CK18-CreER^{T2}* genetic mice could be utilized to address this question. If these cells are incapable of dedifferentiating *in situ*, they may still be able to be pushed in culture via addition of Yamanaka factors or epigenetic inhibitors.

Another intriguing avenue to follow up on are the upstream factors that play a role in "unlocking" the differentiative capacity of previously committed cells. What signals, induced by injury, are responsible for recruiting differentiated cells to assist in tissue repair? What roles do inflammation, apoptosis, and necrosis play in this pathway? Answers to these questions will provide the most important clues for harnessing these cells for regenerative medicine.

Outside of the OE, dedifferentiation is likely to work via similar mechanisms, especially given that all the reported incidences are injury-induced. Thus, insights from the OE will inform the dedifferentiative processes in other systems. On that note, it will be of high interest to determine if dedifferentiation in the gut and airway epithelium depend on Sox2 expression – or expression of other Yamanaka factors. Intriguingly, liver regeneration has been shown to partially rely on transdifferentiation, a slightly different

process involving the direct conversion of one cell type to another—in this case relying on Notch signaling, while it appears that Notch signaling does not play such a role in unlocking dedifferentiation (Yanger et al., 2013). Gaining a global understanding of these processes across multiple tissue types will determine whether there are tissue specific factors in this process, or whether the same mechanisms apply across systems. On a related note, can injury-induced plasticity push cells from the OE to a potency that allows them to differentiate appropriately in an ectopic location, such as the airway epithelium – or even the brain or spinal cord?

General Conclusions

Overall, this study elucidated a previously uncharacterized capacity for immediate neuronal precursors to dedifferentiate and assist in tissue repair. Future studies aim to clarify the mechanisms upstream and downstream of this process and to inform unforeseen plasticity in other systems.

6.2 Spatial cues direct neuronal diversification in the OE

In Chapter 4 of my thesis work, I demonstrated that spatial cues instruct neuronal diversification in respect to both NQO1/OCAM and OR expression. Transplantation experiments revealed that stem cells isolated from one region of the OE and engrafted into another are capable of maturing into neurons characteristic of the host region – proving that these stem cells can be spatially plastic and are influenced by local spatial cues. Furthermore, this spatial plasticity depends, at least in part, on HDAC activity, as incubation with an HDAC inhibitor decreased the number of graft-derived neurons adapting to the host OE region. Surprisingly, spatial plasticity is also decreased when cells are isolated from young (3 week old) animals. Finally, as a follow-up to an observation of OR multiplicity in graft-derived OSNs, I determined that "mature" OMP (+) OSNs that have not yet innervated the olfactory bulb are capable of expressing multiple ORs.

The hypothesis that spatial cues drive neuronal diversification in the OE has been proposed many times (Norlin et al., 2001; McClintock, 2010; Peluso et al., 2012), largely based on the fact that ORs and other neuronal markers are expressed in patterns across the OE (Schwob and Gottlieb, 1986; Ressler et al., 1993; Vassar et al., 1993; Gussing and Bohm, 2004). Furthermore, OR patterns can be identically regenerated after epithelial lesion and recovery, suggesting that spatial cues involved in original pattern formation persist into adulthood (Iwema et al., 2004). Alternatively, it could be the case that residual stem cells left over after lesion are already "hardwired" to develop into region-specific OSNs. As one review states:

> The continuous turnover of [OSNs], which appears to happen without altering OR zonality, argues either that [a] gradient is permanent or that a transient gradient laid down instructions that are permanent. If the latter is correct, then basal progenitor cells may be inherently biased to produce sensory neurons that will select from a zonal subset of OR genes. Experiments that test this idea, such as basal cell transplantation studies, have not yet been reported. (McClintock, 2010)

Here, I report that the former is correct – that a gradient is permanent. However, I did not find that 100% of the transplanted stem cells were influenced by spatial cues; with respect to both NQO1/OCAM and OR expression, ~80% of the graft-derived OSNs adapted to the host region while the remaining ~20% did not. Why were some stem cells influenced by spatial cues while others were not? One explanation is that the progenitor-stage is a critical determinant of whether spatial cues can instruct neuronal diversification—as in, early progenitors may be more malleable to spatial cues while later progenitors, such as the immediate neuronal precursors (INPs) may be less plastic. Importantly, in the majority of my transplantation experiments, I transplanted a mélange of proliferative cells ranging from multipotent progenitors (MPPs) to INPs. To directly address this hypothesis, I isolated Neurog1-eGFP (+) GBC_{INPs} for transplantation experiments. Under these circumstances, unfortunately, I was not able to isolate enough GBC_{INP} from only the dorsal OE, and so I isolated INPs from the entire OE of the donor animals. Here, I found that 11% of graft-derived OSNs did not adapt to the host region (the ventral, OCAM (+) region). While is it difficult to make an absolute conclusion based on this data, it is suggestive that the GBC_{INPs} do not account for the non-adaptive cells. It has been estimated that the Dorsal:Ventral (NQO1:OCAM) epithelial sheet ratio is ~1:3 (Schwob and Gottlieb, 1986); thus if all the INPs were not adapting to the host OE, I would expect to see ~33% of the graft-derived OSNs expressing the dorsal marker (NQO1) in the host OE (the ventral, OCAM(+) OE). However, this 1:3 ratio may be too simplistic, as it does not take into account the varying thickness of the OE; therefore, experiments isolating the dorsal OE and sorting numbers of Neurog1 (+) GBC_{INPs} suitable for transplantation will be necessary to make definitive conclusions.

To tackle the hypothesis that progenitor stage is critical for spatial plasticity from a different angle, I transplanted dorsal OE from 3-week old animals into the ventral OE of host animals (outside of this experiment, all of my donor animals were 6-7 weeks old). Younger animals have a larger ratio of multipotent progenitors (MPPs) to mature OSNs

as compared to more mature mice (Manglapus et al., 2004); therefore I hypothesized that OE from young animals would be more spatially plastic than that from older animals. Surprisingly, I found that 60% of the graft-derived OSNs expressed the marker of the donor region and only 40% adapted to the host region. Why are stem cells isolated from 3-week old mice less influenced by spatial cues than stem cells isolated from 6-7 week old mice? While my original hypothesis was that increased MPPs would result in increased plasticity, it may be the case that the MPP markers, such as Pax6 decrease stem cell spatial plasticity. If this is the case, spatial plasticity should also be decreased following OBX and MeBr injury as these transcription factors are increased following injury (Manglapus et al., 2004). Indeed, in pilot dorsal to ventral transplant from 7 days post OBX animals, I found that 50% of the graft-derived OSNs expressed the marker of the donor region (NQO1) (data not shown).

As another means to determine important factors in stem cell spatial plasticity, I incubated dorsally isolated donor cells in a pan-histone deacetylase inhibitor (HDACi). In these experiments, I found that incubation with the HDACi decreased stem cell spatial plasticity. Because only proliferative cells engraft into the regenerating OE (Chen et al., 2004; Schnittke et al., 2015), these data demonstrate that inhibiting HDAC activity in actively proliferating cells impairs their ability to respond to spatial cues that instruct appropriate neuronal diversification. As HDACs remove transcriptionally activating acetyl groups from histone tails (Rodd et al., 2012), inhibiting HDACs allows for accumulation of activating acetylation. Thus, poising alleles for activation (at least in respect to histone acetylation) in basal cells of the OE disrupts normal responses to instructional spatial cues. It may be that spatial cues are interpreted through a silencing mechanism that is no longer functional with HDAC inhibition, or it may be that the original regional choice (from the donor OE) is simply “locked” in an activated state that is no longer flexible due to HDAC inhibition. While the second explanation is the most practical and straightforward, further experiments investigating HDAC-regulated spatial

plasticity will be necessary to determine the exact mechanism of this effect. Interestingly, in other systems, HDAC inhibition has been shown to play a role in neuronal differentiation, either by promoting or inhibiting differentiation depending on the setting (Yang et al., 2014, 2015; Qiao et al., 2015). Notably, I did not see any obvious effects on neuronal differentiation in the HDACi-treated transplantation experiments.

If spatial cues drive neuronal diversification in the OE, what are these spatial cues? One likely candidate is retinoic acid (RA), as it is involved in pattern generation in many developing and regenerating settings including gastrulation, limb bud formation, motor neuron differentiation, and epithelial differentiation in the intestine and trachea (Tickle et al., 1982; Niederreither et al., 2002; Appel and Eisen, 2003; Rhinn and Dollé, 2012). Furthermore, the RA synthetic enzymes (the RALDHs) are regionally expressed across the OE, with RALDH (-)/RALDH (+) borders directly aligning with the NQO1/OCAM border (Norlin et al., 2001; Peluso et al., 2012). In this thesis, I showed that RALDH1 borders shift with NQO1 borders in a harsh unilateral lesion where the OE does not regenerate appropriate regional patterns. This data further provides correlative evidence that secreted RA influences pattern generation in the OE. Experiments manipulating RA levels in specific regions of the OE will be necessary to draw a causative line between RA secretion and pattern generation and/or disruption. Unfortunately, this type of experiment has many technical challenges and has yet to be definitively tackled.

Aside from RA, other secreted factors that could be involved in pattern generation in the OE (and have been proposed by others) include fibroblast growth factors (FGFs), sonic hedgehog (SHH), epidermal growth factors (EGFs), bone morphogenic proteins (BMPs), and semaphorins. To date, the only reported instances of regionally expressed proteins involved in these pathways are the semaphorin receptor, Neuropilin-2, expressed in the ventrolateral OE, and the BMP-type 1 receptor, Alk6, expressed in the dorsomedial OE (Norlin et al., 2001). Further studies investigating regionally secreted factors within

the developing and adult OE will be necessary to tease out which spatial cues direct neuronal diversification.

In the second half of my transplantation experiments, I found that many OMP (+) graft-derived OSNs expressed multiple ORs. Recent studies have reported that mature, OMP (+) cells can express multiple ORs, albeit at lower levels to a single dominant OR allele (Hanchate et al., 2015; Tan et al., 2015; Scholz et al., 2016). Furthermore, GAP-43 (+) immature OSNs commonly express multiple ORs, with up to 12 ORs found in a single immature OSN (Hanchate et al., 2015). Interestingly, many of the graft-derived OSNs expressed *GAP43* in addition to *OMP* and not all graft-derived OSNs reinnnervate glomeruli in the olfactory bulb. Based on these observations, I tested for OR multiplicity in OMP (+) cells that have not synapsed at the bulb, by sorting for OMP-GFP (+) cells following OBX. Remarkably, I found that 54% of OMP (+) cells expressed multiple ORs as compared to the 20% and 4.5% found in OMP (+) cells under normal, non-OBX conditions in two separate studies (Hanchate et al., 2015; Tan et al., 2015). The approximate 50% rate of OR multiplicity matches the frequency reported in immature OSNs (Hanchate et al., 2015; Tan et al., 2015), suggesting the contact with the bulb may play an unappreciated role in singular OR stabilization and/or maintenance. Furthermore, in regard to my transplant data, these results indicate that the OMP (+) cells expressing multiple ORs are likely still transitioning to full maturity and have not yet innervated the olfactory bulb.

Although the work in Chapter 4 focuses on spatial cues directing neuronal diversification, it is certainly the case that multiple factors play a role in OR gene selection. In fact, many ORs are expressed in almost identical regions/stripes of the OE, calling for further, intra-stripe regulation of OR gene selection. In this regard, several studies have demonstrated that stochastic epigenetic modifications play a crucial role in OR gene selection (Magklara et al., 2011; Lyons et al., 2013, 2014). It will be of high interest to determine whether spatial cues influence these epigenetic modifications.

Future Directions

There are many future directions to pursue in light of this work, many of which have been previously mentioned in the discussion above. First and foremost is to continue to manipulate the dorsal to ventral transplants in pursuit of pushing all the graft-derived neurons to adapt to the host environment. This will be necessary if olfactory transplants are to serve as a therapeutic for anosmic patients, as transplanted cells will need to recapitulate olfactory function without distorting sensory information.

Transplanting sorted multipotent progenitors (MPPs) may decrease the number of non-adaptive, graft-derived OSNs; *Sox2-eGFP/pan-TdT* mice could be used for this purpose. While it will be important to know if MPPs demonstrate increased spatial plasticity, it may be more informative to continue to manipulate dissociated OE during the transplantation procedure (similar to the HDAC inhibitor treatment) as a way to understand the mechanisms underlying spatial plasticity. In this vein, one could treat with more epigenetic inhibitors, or signaling pathway inhibitors. The process of incubating donor cells prior to transplantation can also be used to screen potential secreted factors that may drive neuronal diversification. For instance, incubating dorsal donor cells in RA could increase adaptability in the ventral OE (where RALDH1 expressed). I have piloted this experiment and did not find effect of RA incubation; however, a thorough analysis of RA concentrations and timings will be necessary to determine if this treatment can increase spatial plasticity in the ventral OE.

In addition to manipulating the transplantation experiments, it will be essential to identify more signaling factors in the OE that contribute to OSN patterning. This can simply begin by screening candidates for regional expression via *in situ* hybridization or immunohistochemistry. Candidates proposed already by the field, but without any verification include FGF, EGF, and SHH.

Lastly, the fact that OMP (+) OSNs in OBX animals express multiple ORs opens a field of questions regarding OR multiplicity in regenerative settings. It will be

informative to assess OR multiplicity in OMP (+) cells at multiple timepoints following MeBr lesion to continue to pinpoint the timeframe of singular OR stabilization in maturing OSNs.

Expanding my focus outside of the OE, this research has implications for transplantation therapeutics in other systems. It is always necessary that transplanted cells adapt appropriately and develop into not only the cell type of the engrafted region (e.g. neuron), but also the specific cell sub-type (e.g. dopinergic neuron, in the case of cell replacement therapy for Pakinson's Disease). Mechanisms and manipulations in the OE will inform mechanisms that could influence stem cell plasticity in other systems.

General Conclusions

This study determined that spatial cues direct neuronal diversification in the OE and that this spatial plasticity depends at least in part on HDAC activity. In a separate but related set of experiments, it was determined that OMP (+) OSNs that have not yet contacted the olfactory bulb express multiple ORs. Future studies aim to clarify the mechanisms and spatial cues involved in neuronal diversification and to further characterize the timing of OR singularity in maturing OSNs.

6.3 LSD1-dependent neuronal maturation

The results presented in Chapter 5 begin with a characterization of the timing of critical events in the maturation of OSNs in the adult OE relative to the incorporation of EdU by proliferating progenitor cells. These critical events include the onset of neuronal differentiation as marked by the expression of GAP-43, neuronal maturation as marked by OMP, and the emergence of immunodetectable or marker-associated OR expression. For each stage, there tends to be a gradual increase and then a relatively abrupt inflection in the labeling index as a function of time. For example, although a few differentiating neurons are seen 1 day after the EdU pulse, their numbers sharply increase between 2 and 3 days after injection. Likewise, mature OSNs are evident, though sparse, by 3 days before the major accumulation between 7 and 9 days of pulse-chase. As expected from previous work from our lab and others (Iwema and Schwob, 2003; Rodriguez-Gil et al., 2015), OR (+) neurons become evident between those two time points, offset by about 2 days relative to the curve mapping GAP-43 (+) neurons as a function of time. These data present a higher resolution time course of neuronal maturation than available from previous studies of the adult OE (Iwema and Schwob, 2003), and their concordance with data obtained in the context of early development (Rodriguez-Gil et al., 2015) suggests that neuronal differentiation progresses similarly in both settings. Also important is the opportunity to compare the timing of these events to the expression of LSD1, given the suggestion that it acts as a key regulator of OR expression and singularity (Lyons et al., 2013).

Within the context of neuronal maturation and OR expression, both LSD1 and one of its binding partners, CoREST, are highly expressed in dividing GBCs, reach peak expression 5 days post EdU pulse and then begin to decline by 7 days – around the time immature, GAP-43 (+) OSNs transition to mature, OMP (+) OSNs. Thus, both proteins anticipate terminal mitosis and singular OR gene expression and decrease when OR numbers stabilize (Hanchate et al., 2015; Tan et al., 2015). Thus, on temporal grounds,

LSD1 could play a role prior to, at the time of, or shortly following OR gene expression. However, LSD1 is not likely to play a role achieving or maintaining OR singularity, since its expression declines precipitously when neurons express OMP, which precedes the expression of a single OR (Shykind et al., 2004; Hanchate et al., 2015; Tan et al., 2015).

That LSD1 and CoREST anticipate OR expression by several days is consistent with a hypothesized role in suppressing OR transcription prior to OR gene choice. Additionally, the physical association of LSD1 and CoREST demonstrated by co-immunoprecipitation and, putatively, of HDAC2, is most consistent with a suppressive effect given the established role for this particular complex in other settings (Lee et al., 2005; Shi et al., 2005). Furthermore, the appearance of LSD1 and CoREST in HBCs that are undergoing activation in response to epithelial injury is suggestive that some type of suppression is underway as early as the HBC-to-GBC transition. Consistent with that notion is the absence of H3K9me3 at OR loci in HBCs, which contrasts with their deposition in GBC_{INPs} and immature OSNs (Magklara et al., 2011). Unfortunately, the methylation status of OR-associated H3K4s has not been defined in HBCs.

LSD1 is not exclusively associated with gene repression. Indeed, LSD1/CoREST complexes which replace HDAC2 with C-terminal binding protein (CtBP) have been found to activate transcription at select genes (Ray et al., 2014). Thus, a second role for LSD1 in activating the OR locus eventually selected for singular expression has also been posited (Lyons et al., 2013; Tan et al., 2013). Furthermore, LSD1 compartmentalizes in early post-mitotic cells (immature OSNs) and co-localizes with 1-3 OR loci during this timeframe, suggesting that LSD1 may in fact modify specific OR alleles around the time of OR gene choice (Kilinc et al., 2016). Given the duality of LSD1 function at both H3K4 and H3K9, it is very possible that LSD1 plays a role in both repression and activation of OR genes at different timepoints during OSN maturation. A similar idea was recognized by Lomvardas' group in their observation that LSD1 overexpression in mature OSNs decreased OR expression (Lyons et al., 2013); however, the concept of LSD1 OR

repression prior to OR gene choice has received little attention.

In light of the complexities of LSD1 and CoREST expression in the OE and in other tissues, I knocked out *Lsd1* in three different adult progenitor cell populations: HBCs, the reserve stem cells (Leung et al., 2007; Packard et al., 2011; Fletcher et al., 2011; Schnittke et al., 2015), Ascl1 (+) $GBC_{TA\text{-}Ns}$ (Cau et al., 1997), and Neurog1 (+) GBC_{INPs} (Cau et al., 2002; Manglapus et al., 2004). I found that *Lsd1* deletion in HBCs and Ascl1 (+) $GBC_{TA\text{-}Ns}$ prevented OSN maturation at the immature neuronal stage, which complements my observation that LSD1 and CoREST expression remained high through the period of neuronal immaturity. Thus LSD1 is playing an important role in gene regulation during neurogenesis in the adult OE, as in the embryo (Lyons et al., 2013).

Lsd1 deletion in Neurog1 (+) GBC_{INPs}, on the other hand, did not disrupt OSN maturation, as cells with *Lsd1* deletion at this stage make the transition into OMP (+) OSNs. It is surprising that conditional *Lsd1* knock out in the immediate neuronal precursors does not share the maturation phenotype given the abundant expression of LSD1 in this cell type (Krolewski et al., 2013; Lyons et al., 2013; Kilinc et al., 2016). However, as previously discussed, LSD1 may be playing different roles in gene regulation at different stages, with later roles not as critical for neuronal maturation. Taken together, my data demonstrate a critical time window for LSD1-dependent neuronal maturation that begins as HBCs activate to GBCs and ends short of the Neurog1 (+) GBC_{INP} stage.

It seems unlikely that the disruption in neuronal maturation caused by *Lsd1* KO at an early stage in the progenitor cell hierarchy is due exclusively to abnormalities of OR gene expression, based on the fact that ORs are not expressed (and are likely not selected) before the Neurog1 (+) GBC_{INP} stage when the maturational phenotypes arises (Iwema and Schwob, 2003; Shykind et al., 2004). Given that the inception of the phenotype anticipates OR expression, these data are more consistent with a lack of proper repression rather than a failure to select an OR. For example, if LSD1 is inhibiting OR expression

in neuronal precursors by removing methyl groups at H3K4me1/2, the halt in maturation may be due to the overexpression of multiple OR genes. This multiplicity, in turn, might have consequences for the transition to OMP expression and/or for axon targeting to and at the olfactory bulb. Further investigation into OR multiplicity under the background of LSD1 knockout will be needed to clarify the nature of the defect.

The effect of *Lsd1* knockout on neuronal maturation may be completely independent of an OR phenotype. In fact, LSD1 has been shown to be required for terminal differentiation (from precursor cells) in several cell types including pituitary cells, adipocytes, photoreceptor cells, gastrointestinal endocrine cells, hematopoietic cells, and neurons (Saleque et al., 2007; Wang et al., 2007; Musri et al., 2010; Sun et al., 2010; Ray et al., 2014; Laurent et al., 2015; Popova et al., 2015). Thus, future studies are necessary to further clarify the link between LSD1 removal and inability of OSNs to mature.

Future Directions

This study focused on the timing of LSD1 expression during neuronal maturation and the effect of *Lsd1* KO at specific stages in neuronal maturation. Follow-up studies will necessarily investigate the mechanisms of LSD1-dependent neuronal maturation and the effect of *Lsd1* KO on OR singularity/multiplicity. Of immediate interest are the specific OR phenotypes in each stage-specific *Lsd1* ablation experiment. Do immature OSNs generated from HBCs and $GBC_{TA\text{-}Ns}$ lacking LSD1 turn on OR expression? Do these immature OSNs express multiple ORs? Conversely do the OMP (+) mature OSNs generated from Neurog1 (+) GBC_{INPs} lacking LSD1 express ORs; and if they do, are the ORs singular in expression?

Outside of potential OR phenotypes, it will be necessary to characterize the mechanism of LSD1-dependent neuronal maturation. If the phenotype is not OR dependent, what LSD1-regulated genes are essential for neuronal maturation? Chromatin

immunoprecipitation experiments, cross comparing LSD1-associated genes at differing progenitors stages will provide insight into essential genes in this process.

In light of the fact that *Lsd1* deletion aborts neuronal maturation at the immature OSN stage, it will also be important to determine how long these immature OSNs persist. Are they trophic-independent, surviving far longer than normal, or do they simply die off at a later point having made the switch to trophic-dependence? I would hypothesize that these immature OSNs would eventually die off if they never stabilize at the olfactory bulb; it will be of high importance to investigate bulb innervation in each of the LSD1 conditional KO animals.

With regard to LSD1 binding partners, this study focused on co-repressor complex components; investigation into LSD1 co-activator complex components will be necessary to make further insights into LSD1 function in specific cell types of the OE. In this regard, it will also be important to identify if the LSD1 isoform LSD1-8a, thought to be largely involved in gene activation (Laurent et al., 2015), is present in cells of the OE.

General Conclusions

These studies determined that LSD1 and its CoREST complex components are abundantly expressed before OR expression and OSN maturation, and that LSD1 is required for terminal differentiation during a distinct developmental timeframe from activating reserve stem cells to immediate neuronal precursors. Future studies will reveal whether this maturational phenotype in the adult OE is dependent on OR gene regulation.

THESIS CONCLUSION

This thesis work investigated the processes of neuronal maturation and diversification in the olfactory epithelium (OE). Through transplantation and genetic excision experiments, I demonstrated that spatial cues can direct neuronal diversification and that LSD1 is necessary for terminal neuronal differentiation during a distinct developmental time-window. Overall, I conclude that both the nature of proliferative cells –whether or not they contain LSD1—and their nurturing environment play critical roles in the progression of stem cells to diversified neurons in the OE. Thus, it is not necessarily "Nature vs. Nurture", but more likely "Nature & Nurture" that direct the complex process of neuronal diversification in the olfactory epithelium.

REFERENCES

Abaffy T, Matsunami H, Luetje CW. 2006. Functional analysis of a mammalian odorant receptor subfamily. J Neurochem 97:1506–1518.

Abdus-Saboor I, Al Nufal MJ, Agha M V, Ruinart de Brimont M, Fleischmann A, Shykind BM. 2016. An Expression Refinement Process Ensures Singular Odorant Receptor Gene Choice. Curr Biol:1–8.

Adamo A, Sesé B, Boue S, Castaño J, Paramonov I, Barrero MJ, Izpisua Belmonte JC. 2011. LSD1 regulates the balance between self-renewal and differentiation in human embryonic stem cells. Nat Cell Biol 13:652–659.

Adrian ED. 1950. Sensory discrimination with some recent evidence from the olfactory organ. Br Med Bull 6:330–3.

Akins MR, Benson DL, Greer CA. 2007. Cadherin expression in the developing mouse olfactory system. J Comp Neurol 501:483–97.

Alenius M, Bohm S. 2003. Differential function of RNCAM isoforms in precise target selection of olfactory sensory neurons. Development 130:917–27.

Alioto TS, Ngai J. 2005. The odorant receptor repertoire of teleost fish. BMC Genomics 6:173.

Amente S, Lania L, Majello B. 2013. The histone LSD1 demethylase in stemness and cancer transcription programs. Biochim Biophys Acta - Gene Regul Mech 1829:981–986.

Andrés ME, Burger C, Peral-Rubio MJ, Battaglioli E, Anderson ME, Grimes J, Dallman J, Ballas N, Mandel G. 1999. CoREST: a functional corepressor required for regulation of neural-specific gene expression. Proc Natl Acad Sci U S A 96:9873–9878.

Appel B, Eisen JS. 2003. Retinoids run rampant: multiple roles during spinal cord and motor neuron development. Neuron 40:461–4.

Araneda RC, Kini AD, Firestein S. 2000. The molecular receptive range of an odorant receptor. Nat Neurosci 3:1248–55.

Arnold K, Sarkar A, Yram MA, Polo JM, Bronson R, Sengupta S, Seandel M, Geijsen N, Hochedlinger K. 2011. Sox2(+) adult stem and progenitor cells are important for tissue regeneration and survival of mice. Cell Stem Cell 9:317–29.

Asan E, Drenckhahn D. 2005. Immunocytochemical characterization of two types of microvillar cells in rodent olfactory epithelium. Histochem Cell Biol 123:157–168.

Bakalyar H a, Reed RR. 1990. Identification of a specialized adenylyl cyclase that may mediate odorant detection. Science 250:1403–6.

Ballas N, Battaglioli E, Atouf F, Andres ME, Chenoweth J, Anderson ME, Burger C, Moniwa M, Davie JR, Bowers WJ, Federoff HJ, Rose DW, Rosenfeld MG, Brehm P, Mandel G. 2001. Regulation of neuronal traits by a novel transcriptional complex. Neuron 31:353–65.

Banger KK, Foster JR, Lock EA, Reed CJ. 1994. Immunohistochemical localisation of six glutathione S-transferases within the nasal cavity of the rat. Arch Toxicol 69:91–8.

Belluscio L, Gold GH, Nemes A, Axel R. 1998. Mice deficient in G(olf) are anosmic.

Neuron 20:69–81.
Bergman U, Östergren A, Gustafson AL, Brittebo E. 2002. Differential effects of olfactory toxicants on olfactory regeneration. Arch Toxicol 76:104–112.
Berkowicz D a, Trombley PQ, Shepherd GM. 1994. Evidence for glutamate as the olfactory receptor cell neurotransmitter. J Neurophysiol 71:2557–61.
Bernstein BE, Mikkelsen TS, Xie X, Kamal M, Huebert DJ, Cuff J, Fry B, Meissner A, Wernig M, Plath K, Jaenisch R, Wagschal A, Feil R, Schreiber SL, Lander ES. 2006. A Bivalent Chromatin Structure Marks Key Developmental Genes in Embryonic Stem Cells. Cell 125:315–326.
Bhasin N, Maynard TM, Gallagher PA, LaMantia AS. 2003. Mesenchymal/epithelial regulation of retinoic acid signaling in the olfactory placode. Dev Biol 261:82–98.
Bhattacharyya S, Bronner-Fraser M. 2008. Competence, specification and commitment to an olfactory placode fate. Development 135:4165–4177.
Boekhoff I, Breer H. 1990. Differential stimulation of second messenger pathways by distinct classes of odorants. Neurochem Int 17:553–557.
Borders a S, Hersh M a, Getchell ML, van Rooijen N, Cohen D a, Stromberg a J, Getchell T V. 2007. Macrophage-mediated neuroprotection and neurogenesis in the olfactory epithelium. Physiol Genomics 31:531–43.
Bozza T, Feinstein P, Zheng C, Mombaerts P. 2002. Odorant receptor expression defines functional units in the mouse olfactory system. J Neurosci 22:3033–43.
Brechbühl J, Klaey M, Broillet M-C. 2008. Grueneberg ganglion cells mediate alarm pheromone detection in mice. Science 321:1092–1095.
Breer H, Boekhoff I, Tareilus E. 1990. Rapid Kinetics of Second Messenger Formation in Olfactory Transduction. Nature 345:66–68.
Brittebo EB. 1995. Metabolism-dependent toxicity of methimazole in the olfactory nasal mucosa. Pharmacol Toxicol 76:76–9.
Brittebo EB. 1997. Metabolism-dependent activation and toxicity of chemicals in nasal glands. Mutat Res - Fundam Mol Mech Mutagen 380:61–75.
Bronshteín AA, Minor A V. 1977. [Regeneration of olfactory flagella and restoration of the electroolfactogram following application of triton X-100 to the olfactory mucosa of frogs]. Tsitologiia 19:33–9.
Brunet LJ, Gold GH, Ngai J. 1996. General anosmia caused by a targeted disruption of the mouse olfactory cyclic nucleotide-gated cation channel. Neuron 17:681–693.
Buck L, Axel R. 1991. A novel multigene family may encode odorant receptors: a molecular basis for odor recognition. Cell 65:175–87.
Bulfone A, Wang F, Hevner R, Anderson S, Cutforth T, Chen S, Meneses J, Pederson R, Axel R, Rubenstein JLR. 1998. An olfactory sensory map develops in the absense of normal projection neurons or GABAergic interneurons. Neuron 21:1273–1282.
Burd GD. 1993. Morphological study of the effects of intranasal zinc sulfate irrigation on the mouse olfactory epithelium and olfactory bulb. Microsc Res Tech 24:195–213.
Caggiano M, Kauer JS, Hunter DD. 1994. Globose basal cells are neuronal progenitors in the olfactory epithelium: a lineage analysis using a replication-incompetent retrovirus. Neuron 13:339–52.
Calof a L, Chikaraishi DM. 1989. Analysis of neurogenesis in a mammalian neuroepithelium: proliferation and differentiation of an olfactory neuron precursor in

vitro. Neuron 3:115–27.
Carr VM, Farbman AI. 1993. The dynamics of cell death in the olfactory epithelium. Exp Neurol 124:308–314.
Carter LA, MacDonald JL, Roskams AJ. 2004. Olfactory horizontal basal cells demonstrate a conserved multipotent progenitor phenotype. J Neurosci 24:5670–83.
Cau E, Casarosa S, Guillemot F. 2002. Mash1 and Ngn1 control distinct steps of determination and differentiation in the olfactory sensory neuron lineage. Development 129:1871–1880.
Cau E, Gradwohl G, Casarosa S, Kageyama R, Guillemot F. 2000. Hes genes regulate sequential stages of neurogenesis in the olfactory epithelium. Development 2332:2323–2332.
Cau E, Gradwohl G, Fode C, Guillemot F. 1997. Mash1 activates a cascade of bHLH regulators in olfactory neuron progenitors. Development 124:1611–21.
Ceballos-Chavez M, Rivero S, Garcia-Gutierrez P, Rodriguez-Paredes M, Garcia-Dominguez M, Bhattacharya S, Reyes JC. 2012. Control of neuronal differentiation by sumoylation of BRAF35, a subunit of the LSD1-CoREST histone demethylase complex. Proc Natl Acad Sci 109:8085–8090.
Chehrehasa F, St John JA, Key B. 2006. Implantation of a scaffold following bulbectomy induces laminar organization of regenerating olfactory axons. Brain Res 1119:58–64.
Chen X, Fang H, Schwob JE. 2004. Multipotency of purified, transplanted globose basal cells in olfactory epithelium. J Comp Neurol 469:457–74.
Chess A, Simon I, Cedar H, Axel R. 1994. Allelic inactivation regulates olfactory receptor gene expression. Cell 78:823–34.
Cho JH, Lepine M, Andrews W, Parnavelas J, Cloutier JF. 2007. Requirement for Slit-1 and Robo-2 in zonal segregation of olfactory sensory neuron axons in the main olfactory bulb. J Neurosci 27:9094–9104.
Christensen MD, Holbrook EH, Costanzo RM, Schwob JE. 2001. Rhinotopy is disrupted during the re-innervation of the olfactory bulb that follows transection of the olfactory nerve. Chem Senses 26:359–69.
Clowney EJ, Legros MA, Mosley CP, Clowney FG, Markenskoff-Papadimitriou EC, Myllys M, Barnea G, Larabell CA, Lomvardas S. 2012. Nuclear aggregation of olfactory receptor genes governs their monogenic expression. Cell 151:724–737.
Clowney EJ, Magklara A, Colquitt BM, Pathak N, Lane RP, Lomvardas S. 2011. High-throughput mapping of the promoters of the mouse olfactory receptor genes reveals a new type of mammalian promoter and provides insight into olfactory receptor gene regulation. Genome Res 21:1249–59.
Costanzo RM. 1985. Neural Regeneration and Functional Reconnection Following Olfactory Nerve Transection in Hamster Surgical procedures. Brain Res 361:258–266.
Cuschieri A, Bannister LH. 1974. Some histochemical observations on the mucosubstances of the nasal glands of the mouse. Histochem J 6:543–58.
Cuschieri A, Bannister LH. 1975a. The development of the olfactory mucosa in the mouse: electron microscopy. J Anat 119:471–98.
Cuschieri A, Bannister LH. 1975b. The development of the olfactory mucosa in the

mouse: light microscopy. J Anat 119:277–286.
Dahl R, Hadley WM, Hahn FF, Benson JM, McClellan RO. 1982. Cytochrome P-450-dependent monooxygenases in olfactory epithelium of dogs: possible role in tumorigenicity. Science 216:57–9.
Deckner ML, Risling M, Frisén J. 1997. Apoptotic death of olfactory sensory neurons in the adult rat. Exp Neurol 143:132–40.
DeMaria S, Ngai J. 2010. The cell biology of smell. J Cell Biol 191:443–452.
Donner AL, Episkopou V, Maas RL. 2007. Sox2 and Pou2f1 interact to control lens and olfactory placode development. Dev Biol 303:784–799.
Døving KB, Trotier D. 1998. Structure and function of the vomeronasal organ. J Exp Biol 201:2913–25.
Duggan CD, DeMaria S, Baudhuin A, Stafford D, Ngai J. 2008. Foxg1 is required for development of the vertebrate olfactory system. J Neurosci 28:5229–5239.
Dulac C, Axel R. 1995. A novel family of genes encoding putative pheromone receptors in mammals. Cell 83:195–206.
Dupé V, Matt N, Garnier J-M, Chambon P, Mark M, Ghyselinck NB. 2003. A newborn lethal defect due to inactivation of retinaldehyde dehydrogenase type 3 is prevented by maternal retinoic acid treatment. Proc Natl Acad Sci 100:14036–14041.
Eggan K, Baldwin K, Tackett M, Osborne J, Gogos J, Chess A, Axel R, Jaenisch R. 2004. Mice cloned from olfactory sensory neurons. Nature 428:44–9.
Ellis P, Fagan BM, Magness ST, Hutton S, Taranova O, Hayashi S, McMahon A, Rao M, Pevny L. 2004. SOX2, a persistent marker for multipotential neural stem cells derived from embryonic stem cells, the embryo or the adult. Dev Neurosci 26:148–65.
Eustis SL, Haber SB, Drew RT, Yang RS. 1988. Toxicology and pathology of methyl bromide in F344 rats and B6C3F1 mice following repeated inhalation exposure. Fundam Appl Toxicol 11:594–610.
Farbman AI, Marcolis FL. 1980. Olfactory Marker Protein during Ontogeny : Localization lmmunohistochemical. Dev Biol 215:205–215.
Feinberg TE, Mallatt J. 2013. The evolutionary and genetic origins of consciousness in the cambrian period over 500 million years ago. Front Psychol 4:1–27.
Feinstein P, Bozza T, Rodriguez I, Vassalli A, Mombaerts P. 2004. Axon guidance of mouse olfactory sensory neurons by odorant receptors and the beta2 adrenergic receptor. Cell 117:833–46.
Feinstein P, Mombaerts P. 2004. A contextual model for axonal sorting into glomeruli in the mouse olfactory system. Cell 117:817–831.
Ferreira T, Wilson SR, Choi YG, Risso D, Dudoit S, Speed TP, Ngai J. 2014. Silencing of odorant receptor genes by G protein βγ signaling ensures the expression of one odorant receptor per olfactory sensory neuron. Neuron 81:847–59.
Firestein S, Darrow B, Shepherd GM. 1991. Activation of the sensory current in salamander olfactory receptor neurons depends on a G protein-mediated cAMP second messenger system. Neuron 6:825–835.
Firestein S. 2001. How the olfactory system makes sense of scents. Nature 413:211–8.
Foster CT, Dovey OM, Lezina L, Luo JL, Gant TW, Barlev N, Bradley A, Cowley SM. 2010. Lysine-specific demethylase 1 regulates the embryonic transcriptome and

CoREST stability. Mol Cell Biol 30:4851–63.
Foti SB, Chou A, Moll AD, Roskams AJ. 2013. HDAC inhibitors dysregulate neural stem cell activity in the postnatal mouse brain. Int J Dev Neurosci 31:434–447.
Fukuda N, Yomogida K, Okabe M, Touhara K. 2004. Functional characterization of a mouse testicular olfactory receptor and its role in chemosensing and in regulation of sperm motility. J Cell Sci 117:5835–45.
Fuss SH, Omura M, Mombaerts P. 2005. The Grueneberg ganglion of the mouse projects axons to glomeruli in the olfactory bulb. Eur J Neurosci 22:2649–2654.
Fuss SH, Omura M, Mombaerts P. 2007. Local and cis effects of the H element on expression of odorant receptor genes in mouse. Cell 130:373–84.
Gale M, Yan Q. 2015. High-throughput screening to identify inhibitors of lysine demethylases. Epigenomics 7:57–65.
Garcia-Bassets I, Kwon Y-S, Telese F, Prefontaine GG, Hutt KR, Cheng CS, Ju B-G, Ohgi K a, Wang J, Escoubet-Lozach L, Rose DW, Glass CK, Fu X-D, Rosenfeld MG. 2007. Histone methylation-dependent mechanisms impose ligand dependency for gene activation by nuclear receptors. Cell 128:505–18.
Gesteland RC, Yancey RA, Farbman AI. 1982. Development of olfactory receptor neuron selectivity in the rat fetus. Neuroscience 7:3127–36.
Getchell ML, Getchell T V. 1991. Immunohistochemical Localization of Components of the Immune Barrier in the Olfactory Mucosae of Salamanders and Rats. Anat Rec 231:358–374.
Getchell ML, Getchell T V. 1992. Fine structural aspects of secretion and extrinsic innervation in the olfactory mucosa. Microsc Res Tech 23:111–127.
Gilbert MA, Lin B, Peterson J, Jang W, Schwob JE. 2015. Gene Expression Patterns Neuregulin1 and ErbB expression in the uninjured and regenerating olfactory mucosa. Gene Expr Patterns 19:1–12.
Glusman G, Yanai I, Rubin I, Lancet D. 2001. The complete human olfactory subgenome. Genome Res 11:685–702.
Gong S, Zheng C, Doughty ML, Losos K, Didkovsky N, Schambra UB, Nowak NJ, Joyner A, Leblanc G, Hatten ME, Heintz N. 2003. A gene expression atlas of the central nervous system based on bacterial artificial chromosomes. Nature 425:917–25.
Gordon MK, Mumm JS, Davis RA, Holcomb JD, Calof AL. 1995. Dynamics of MASH1 Expression in Vitro and in Vivo suggest a Non-Stem Cell Site of MASH1 Action in the Olfactory Receptor Neuron Lineage. Mol Cell Neurosci 6:363–379.
Graziadei PP, Metcalf JF. 1971. Autoradiographic and ultrastructural observations on the frog's olfactory mucosa. Zeitschrift für Zellforsch und mikroskopische Anat (Vienna, Austria 1948) 116:305–18.
Graziadei PP, Monti Graziadei GA. 1979. Neurogenesis and neuron regeneration in the olfactory system of mammals. J Neurocytol 8:1–18.
Graziadei PP., Monti Graziadei GA. 1978. Continuous Nerve Cell Renewal in the Olfactory System. In: Jacobson M, editor. Handbook of Sensory Physiology. Springer. p 55–82.
Graziadei PPC. 1973. Cell dynamics in the olfactory mucosa. Tissue Cell 5:113–131.
Grosmaitre X, Vassalli A, Mombaerts P, Shepherd GM, Ma M. 2006. Odorant responses

of olfactory sensory neurons expressing the odorant receptor MOR23: a patch clamp analysis in gene-targeted mice. Proc Natl Acad Sci U S A 103:1970–1975.
Grüneberg H. 1973. A ganglion probably belonging to the N. terminalis system in the nasal mucosa of the mouse. Zeitschrift für Anat und Entwicklungsgeschichte 140:39–52.
Guillemot F, Lo LC, Johnson JE, Auerbach A, Anderson DJ, Joyner AL. 1993. Mammalian achaete-scute homolog 1 is required for the early development of olfactory and autonomic neurons. Cell 75:463–76.
Guo Z, Packard A, Krolewski RC, Harris MT, Manglapus GL, Schwob JE. 2010. Expression of pax6 and sox2 in adult olfactory epithelium. J Comp Neurol 518:4395–418.
Gussing F, Bohm S. 2004. NQO1 activity in the main and the accessory olfactory systems correlates with the zonal topography of projection maps. Eur J Neurosci 19:2511–2518.
Haberly LB, Price JL. 1977. The axonal projection patterns of the mitral and tufted cells of the olfactory bulb in the rat. Brain Res 129:152–7.
Hakimi M-A, Bochar D a, Chenoweth J, Lane WS, Mandel G, Shiekhattar R. 2002. A core-BRAF35 complex containing histone deacetylase mediates repression of neuronal-specific genes. Proc Natl Acad Sci U S A 99:7420–5.
Halpern M, Martínez-Marcos A. 2003. Structure and function of the vomeronasal system: an update. Prog Neurobiol 70:245–318.
Hamlin J a, Fang H, Schwob JE. 2004. Differential expression of the mammalian homologue of fasciclin II during olfactory development in vivo and in vitro. J Comp Neurol 474:438–52.
Hanchate NK, Kondoh K, Lu Z, Kuang D, Ye X, Qiu X, Pachter L, Trapnell C, Buck LB. 2015. Single-cell transcriptomics reveals receptor transformations during olfactory neurogenesis. Science 350:1251–5.
Hansen A, Finger TE. 2008. Is TrpM5 a reliable marker for chemosensory cells? Multiple types of microvillous cells in the main olfactory epithelium of mice. BMC Neurosci 9:115.
Harkema JR, Carey S a, Wagner JG. 2006. The nose revisited: a brief review of the comparative structure, function, and toxicologic pathology of the nasal epithelium. Toxicol Pathol 34:252–69.
Hayami S, Kelly JD, Cho HS, Yoshimatsu M, Unoki M, Tsunoda T, Field HI, Neal DE, Yamaue H, Ponder BAJ, Nakamura Y, Hamamoto R. 2011. Overexpression of LSD1 contributes to human carcinogenesis through chromatin regulation in various cancers. Int J Cancer 128:574–586.
Hegg CC, Jia C, Chick WS, Restrepo D, Hansen A. 2010. Microvillous cells expressing IP3 receptor type 3 in the olfactory epithelium of mice. 32:1632–1645.
Hinds JW, Hinds PL, McNelly N a. 1984. An autoradiographic study of the mouse olfactory epithelium: evidence for long-lived receptors. Anat Rec 210:375–83.
Hinds JW. 1968. Autoradiographic study of histogenesis in the mouse olfactory bulb. II. Cell proliferation and migration. J Comp Neurol 134:305–322.
Hirota J, Mombaerts P. 2004. The LIM-homeodomain protein Lhx2 is required for complete development of mouse olfactory sensory neurons. Proc Natl Acad Sci U S

A 101:8751–8755.
Hirota J, Omura M, Mombaerts P. 2007. Differential impact of Lhx2 deficiency on expression of class I and class II odorant receptor genes in mouse. Mol Cell Neurosci 34:679–688.
Holbrook EH, Iwema CL, Peluso CE, Schwob JE. 2014. The regeneration of P2 olfactory sensory neurons is selectively impaired following methyl bromide lesion. Chem Senses 39:601–16.
Holbrook EH, Leopold D a, Schwob JE. 2005. Abnormalities of axon growth in human olfactory mucosa. Laryngoscope 115:2144–54.
Holbrook EH, Szumowski KE, Schwob JE. 1995. An immunochemical, ultrastructural, and developmental characterization of the horizontal basal cells of rat olfactory epithelium. J Comp Neurol 363:129–46.
Holbrook EH, Wu E, Curry WT, Lin DT, Schwob JE. 2011. Immunohistochemical characterization of human olfactory tissue. Laryngoscope 121:1687–701.
Hoover KC. 2010. Smell with inspiration: The evolutionary significance of olfaction. Am J Phys Anthropol 143:63–74.
Hoppe R, Breer H, Strotmann J. 2006. Promoter motifs of olfactory receptor genes expressed in distinct topographic patterns. Genomics 87:711–723.
Hoppe R, Frank H, Breer H, Strotmann J. 2003. The clustered olfactory receptor gene family 262: genomic organization, promotor elements, and interacting transcription factors. Genome Res 13:2674–85.
Hozumi N, Tonegawa S, Alerts E. 1976. Evidence for somatic rearrangement of immunoglobulin genes coding for variable and constant regions. Proc Natl Acad Sci U S A 73:3628–32.
Huard JM, Schwob JE. 1995. Cell cycle of globose basal cells in rat olfactory epithelium. Dev Dyn 203:17–26.
Huard JMT, Youngentob SL, Goldstein BJ, Luskin MB, Schwob JE. 1998. Adult olfactory epithelium contains multipotent progenitors that give rise to neurons and non-neural cells. J Comp Neurol 400:469–86.
Hurtt ME, Morgan T, Working PK. 1987. Histopathology of Acute Toxic Responses in Selected Tissues from Rats Exposed by Inhalation to Methyl Bromide. Fund Appl Tox 9:352–365.
Hurtt ME, Thomas DA, Working PK, Monticello TM, Morgan KT. 1988. Degeneration and regeneration of the olfactory epithelium following inhalation exposure to methyl bromide: pathology, cell kinetics, and olfactory function. Toxicol Appl Pharmacol 94:311–28.
Hutton SR, Pevny LH. 2011. SOX2 expression levels distinguish between neural progenitor populations of the developing dorsal telencephalon. Dev Biol 352:40–47.
Imai T, Suzuki M, Sakano H. 2006. Odorant receptor-derived cAMP signals direct axonal targeting. Science 314:657–61.
Indra AK, Warot X, Brocard J, Bornert JM, Xiao JH, Chambon P, Metzger D. 1999. Temporally-controlled site-specific mutagenesis in the basal layer of the epidermis: Comparison of the recombinase activity of the tamoxifen-inducible Cre-ER(T) and Cre-ER(T2) recombinases. Nucleic Acids Res 27:4324–4327.
Ishii T, Serizawa S, Kohda A, Nakatani H, Shiroishi T, Okumura K, Iwakura Y, Nagawa

F, Tsuboi A, Sakano H. 2001. Monoallelic expresion of the odourant receptor gene and axonal projection of olfactory sensory neurones. Genes to Cells 6:71–78.
Iwema CL, Fang H, Kurtz DB, Youngentob SL, Schwob JE. 2004. Odorant receptor expression patterns are restored in lesion-recovered rat olfactory epithelium. J Neurosci 24:356–69.
Iwema CL, Schwob JE. 2003. Odorant receptor expression as a function of neuronal maturity in the adult rodent olfactory system. J Comp Neurol 459:209–222.
Jang W, Chen X, Flis D, Harris M, Schwob JE. 2014. Label-retaining, quiescent globose basal cells are found in the olfactory epithelium. J Comp Neurol 522:731–749.
Jang W, Youngentob SL, Schwob JE. 2003. Globose basal cells are required for reconstitution of olfactory epithelium after methyl bromide lesion. J Comp Neurol 460:123–40.
St. John JA, Clarris HJ, McKeown S, Royal S, Key B. 2003. Sorting and convergence of primary olfactory axons are independent of the olfactory bulb. J Comp Neurol 464:131–140.
Jones DT, Reed RR. 1988. Golf ; An Olfactory Neuron Specffic-G Protein. Science 244:790–795.
Kajiya K, Inaki K, Tanaka M, Haga T, Kataoka H, Touhara K. 2001. Molecular bases of odor discrimination: Reconstitution of olfactory receptors that recognize overlapping sets of odorants. J Neurosci 21:6018–6025.
Kang N, Koo J. 2012. Olfactory receptors in non-chemosensory tissues. BMB Rep 45:612–622.
Kilinc S, Savarino A, Coleman JH, Schwob JE, Lane RP. 2016. Lysine-specific demethylase-1 (LSD1) is compartmentalized at nuclear chromocenters in early post-mitotic cells of the olfactory sensory neuronal lineage. Mol Cell Neurosci 74:58–70.
Klenoff JR, Greer CA. 1998. Postnatal development of olfactory receptor cell axonal arbors. J Comp Neurol 390:256–67.
Kobayakawa K, Kobayakawa R, Matsumoto H, Oka Y, Imai T, Ikawa M, Okabe M, Ikeda T, Itohara S, Kikusui T, Mori K, Sakano H. 2007. Innate versus learned odour processing in the mouse olfactory bulb. Nature 450:503–8.
Kobilka B. 1992. Adrenergic receptors as model for G Protein-Coupled Receptors. Annu Rev Neurosci 15:87–114.
Koundakjian EJ, Appler JL, Goodrich L V. 2007. Auditory neurons make stereotyped wiring decisions before maturation of their targets. J Neurosci 27:14078–88.
Kouzarides T. 2000. Acetylation: a regulatory modification to rival phosphorylation? EMBO J 19:1176–9.
Kouzarides T. 2007. Chromatin Modifications and Their Function. Cell 128:693–705.
Krautwurst D, Yau K, Reed RR. 1998. Identification of ligands for olfactory receptors. Cell 95:917–926.
Krolewski RC, Packard A, Schwob JE. 2013. Global expression profiling of globose basal cells and neurogenic progression within the olfactory epithelium. J Comp Neurol 521:833–859.
LaMantia AS, Bhasin N, Rhodes K, Heemskerk J. 2000. Mesenchymal / Epithelial Induction Mediates Olfactory Pathway Formation. Neuron 28:411–425.
LaMantia AS, Colbert MC, Linney E. 1993. Retinoic acid induction and regional

differentiation prefigure olfactory pathway formation in the mammalian forebrain. Neuron 10:1035–48.
Lancet D, Ben-Arie N. 1993. Olfactory receptors. Curr Biol 3:668–674.
Lander ES, Linton LM, Birren B, Nusbaum C, Zody MC, Baldwin J, Devon K, Dewar K, Doyle M, FitzHugh W, Funke R, Gage D, Harris K, Heaford A, Howland J, Kann L, Lehoczky J, LeVine R, McEwan P, McKernan K, Meldrim J, Mesirov JP, Miranda C, Morris W, Naylor J, Raymond C, Rosetti M, Santos R, Sheridan A, Sougnez C, Stange-Thomann N, Stojanovic N, Subramanian A, Wyman D, Rogers J, Sulston J, Ainscough R, Beck S, Bentley D, Burton J, Clee C, Carter N, Coulson A, Deadman R, Deloukas P, Dunham A, Dunham I, Durbin R, French L, Grafham D, Gregory S, Hubbard T, Humphray S, Hunt A, Jones M, Lloyd C, McMurray A, Matthews L, Mercer S, Milne S, Mullikin JC, Mungall A, Plumb R, Ross M, Shownkeen R, Sims S, Waterston RH, Wilson RK, Hillier LW, McPherson JD, Marra MA, Mardis ER, Fulton LA, Chinwalla AT, Pepin KH, Gish WR, Chissoe SL, Wendl MC, Delehaunty KD, Miner TL, Delehaunty A, Kramer JB, Cook LL, Fulton RS, Johnson DL, Minx PJ, Clifton SW, Hawkins T, Branscomb E, Predki P, Richardson P, Wenning S, Slezak T, Doggett N, Cheng JF, Olsen A, Lucas S, Elkin C, et al. 2001. Initial sequencing and analysis of the human genome. Nature 409:860–921.
Laurent B, Ruitu L, Murn J, Hempel K, Ferrao R, Xiang Y, Liu S, Garcia BA, Wu H, Wu F, Steen H, Shi Y. 2015. A Specific LSD1/KDM1A Isoform Regulates Neuronal Differentiation through H3K9 Demethylation. Mol Cell 57:957–970.
Lázaro I, Bussy C, Yilmazer A, Jackson MS, Humphreys NE, Kostarelos K. 2014. Generation of induced pluripotent stem cells from virus-free in vivo reprogramming of BALB/c mouse liver cells. Biomaterials 35:8312–20.
Lazaro I, Kostarelos K. 2014. In vivo cell reprogramming to pluripotency: exploring a novel tool for cell replenishment and tissue regeneration. Biochem Soc Trans 42:711–716.
Lee DY, Teyssier C, Strahl BD, Stallcup MR. 2005a. Role of protein methylation in regulation of transcription. Endocr Rev 26:147–70.
Lee MG, Wynder C, Cooch N, Shiekhattar R. 2005b. An essential role for CoREST in nucleosomal histone 3 lysine 4 demethylation. Nature 437:432–5.
Leung CT, Coulombe P a, Reed RR. 2007. Contribution of olfactory neural stem cells to tissue maintenance and regeneration. Nat Neurosci 10:720–6.
Lewcock JW, Reed RR. 2004. A feedback mechanism regulates monoallelic odorant receptor expression. Proc Natl Acad Sci U S A 101:1069–74.
Li J, Ishii T, Feinstein P, Mombaerts P. 2004. Odorant receptor gene choice is reset by nuclear transfer from mouse olfactory sensory neurons. Nature 428:393–399.
Li L, Clevers H. 2010. Coexistence of quiescent and active adult stem cells in mammals. Science 327:542–5.
Li Y, Field PM, Raisman G. 1998. Regeneration of adult rat corticospinal axons induced by transplanted olfactory ensheathing cells. J Neurosci 18:10514–10524.
Liberles SD, Buck LB. 2006. A second class of chemosensory receptors in the olfactory epithelium. Nature 442:645–650.
Liberles SD, Horowitz LF, Kuang D, Contos JJ, Wilson KL, Siltberg-Liberles J, Liberles D a, Buck LB. 2009. Formyl peptide receptors are candidate chemosensory

receptors in the vomeronasal organ. Proc Natl Acad Sci U S A 106:9842–9847.
Logan DW, Brunet LJ, Webb WR, Cutforth T, Ngai J, Stowers L. 2012. Learned recognition of maternal signature odors mediates the first suckling episode in mice. Curr Biol 22:1998–2007.
Lomvardas S, Barnea G, Pisapia DJ, Mendelsohn M, Kirkland J, Axel R. 2006. Interchromosomal interactions and olfactory receptor choice. Cell 126:403–13.
López-Ratón M, Rodríguez-Álvarez MX, Suárez CC, Sampedro FG. 2014. OptimalCutpoints : An R Package for Selecting Optimal Cutpoints in Diagnostic Tests. J Stat Softw 61.
Lv T, Yuan D, Miao X, Lv Y, Zhan P, Shen X, Song Y. 2012. Over-expression of LSD1 promotes proliferation, migration and invasion in non-small cell lung cancer. PLoS One 7:1–8.
Lyons DB, Allen WE, Goh T, Tsai L, Barnea G, Lomvardas S. 2013. An epigenetic trap stabilizes singular olfactory receptor expression. Cell 154:325–36.
Lyons DB, Magklara A, Goh T, Sampath SC, Schaefer A, Schotta G, Lomvardas S. 2014. Heterochromatin-mediated gene silencing facilitates the diversification of olfactory neurons. Cell Rep 9:884–892.
Ma L, Wu Y, Qiu Q, Scheerer H, Moran A, Yu CR. 2014. A developmental switch of axon targeting in the continuously regenerating mouse olfactory system. Science 344:194–7.
Ma M, Grosmaitre X, Iwema CL, Baker H, Greer CA, Shepherd GM. 2003. Olfactory signal transduction in the mouse septal organ. J Neurosci 23:317–24.
Mackay-Sim A, Kittel PW. 1991. On the Life Span of Olfactory Receptor Neurons. Eur J Neurosci 3:209–215.
Mackay-Sim A, St John JA. 2011. Olfactory ensheathing cells from the nose: Clinical application in human spinal cord injuries. Exp Neurol 229:174–180.
Magklara A, Yen A, Colquitt BM, Clowney EJ, Allen W, Markenscoff-Papadimitriou E, Evans ZA, Kheradpour P, Mountoufaris G, Carey C, Barnea G, Kellis M, Lomvardas S. 2011. An epigenetic signature for monoallelic olfactory receptor expression. Cell 145:555–70.
Mahanthappa NK, Schwarting GA. 1993. Peptide growth factor control of olfactory neurogenesis and neuron survival in vitro: roles of EGF and TGF-beta s. Neuron 10:293–305.
Malnic B, Godfrey PA, Buck LB. 2004. The human olfactory receptor gene family. Proc Natl Acad Sci USA 101:2584–2589.
Malnic B, Hirono J, Sato T, Buck LB. 1999. Combinatorial receptor codes for odors. Cell 96:713–23.
Man O, Gilad Y, Lancet D. 2004. Prediction of the odorant binding site of olfactory receptor proteins by human – mouse comparisons. Protein Sci 13:240–254.
Manglapus GL, Youngentob SL, Schwob JE. 2004. Expression patterns of basic helix-loop-helix transcription factors define subsets of olfactory progenitor cells. J Comp Neurol 479:216–33.
Matsunami H, Mainland JD, Dey S. 2009. Trafficking of mammalian chemosensory receptors by receptor-transporting proteins. Ann N Y Acad Sci 1170:153–156.
Matulionis DH. 1975. Ultrastructural study of mouse olfactory epithelium following

destruction by ZnSO4 and its subsequent regeneration. Am J Anat 142:67–89.
McClintock TS, Adipietro K, Titlow WB, Breheny P, Walz A, Mombaerts P, Matsunami H. 2014. In Vivo Identification of Eugenol-Responsive and Muscone-Responsive Mouse Odorant Receptors. J Neurosci 34:15669–15678.
McClintock TS. 2010. Achieving singularity in mammalian odorant receptor gene choice. Chem Senses 35:447–457.
McIntyre JC, Bose SC, Stromberg AJ, McClintock TS. 2008. Emx2 stimulates odorant receptor gene expression. Chem Senses 33:825–837.
Metzger E, Wissmann M, Yin N, Müller JM, Schneider R, Peters AHFM, Günther T, Buettner R, Schüle R. 2005. LSD1 demethylates repressive histone marks to promote androgen-receptor-dependent transcription. Nature 437:436–9.
Michalopoulos GK, Barua L, Bowen WC. 2005. Transdifferentiation of rat hepatocytes into biliary cells after bile duct ligation and toxic biliary injury. Hepatology 41:535–544.
Michaloski JS, Galante PAF, Malnic B. 2006. Identification of potential regulatory motifs in odorant receptor genes by analysis of promoter sequences. Genome Res 16:1091–1098.
Miller ML, Andringa a., Evans JE, Hastings L. 1995. Microvillar cells of the olfactory epithelium: morphology and regeneration following exposure to toxic compounds. Brain Res 669:1–9.
Miyamichi K. 2005. Continuous and Overlapping Expression Domains of Odorant Receptor Genes in the Olfactory Epithelium Determine the Dorsal/Ventral Positioning of Glomeruli in the Olfactory Bulb. J Neurosci 25:3586–3592.
Mombaerts P, Wang F, Dulac C, Chao SK, Nemes A, Mendelsohn M, Edmondson J, Axel R. 1996. Visualizing an olfactory sensory map. Cell 87:675–86.
Mombaerts P. 1999. Seven-transmembrane proteins as odorant and chemosensory receptors. Science 286:707–711.
Mombaerts P. 2004. Genes and ligands for odorant, vomeronasal and taste receptors. Nat Rev Neurosci 5:263–278.
Mombaerts P. 2006. Axonal wiring in the mouse olfactory system. Annu Rev Cell Dev Biol 22:713–37.
Mori K, Nagao H, Yoshihara Y. 1999. The olfactory bulb: coding and processing of odor molecule information. Science 286:711–5.
Morrison EE, Costanzo RM. 1990. Morphology of the human olfactory epithelium. J Comp Neurol 297:1–13.
Moulton DG, Celebi G, Fink RP. 1970. Olfaction in Mammals - Two Aspects: Proliferation of Cells in The Olfactory Epithelium and Sensitivity to Odours. Ciba Found Symp Tast Smell Vertebr:227–250.
Moulton DG. 1974. Dynamics of Cell Populations in the Olfactory Epithelium. Ann N Y Acad Sci 237:52–61.
Mumm JS, Shou J, Calof AL. 1996. Colony-forming progenitors from mouse olfactory epithelium: evidence for feedback regulation of neuron production. Proc Natl Acad Sci U S A 93:11167–72.
Murray K. 1964. THE OCCURRENCE OF EPSILON-N-METHYL LYSINE IN HISTONES. Biochemistry 3:10–5.

Murrell W, Féron F, Wetzig A, Cameron N, Splatt K, Bellette B, Bianco J, Perry C, Lee G, Mackay-Sim A, Feron F, Wetzig A, Cameron N, Splatt K, Bellette B, Bianco J, Perry C, Lee G, Mackay-Sim A, Féron F, Wetzig A, Cameron N, Splatt K, Bellette B, Bianco J, Perry C, Lee G, Mackay-Sim A. 2005. Multipotent stem cells from adult olfactory mucosa. Dev Dyn 233:496–515.

Musri MM, Carmona MC, Hanzu F a, Kaliman P, Gomis R, Párrizas M. 2010. Histone demethylase LSD1 regulates adipogenesis. J Biol Chem 285:30034–41.

Nair SS, Nair BC, Cortez V, Chakravarty D, Metzger E, Schüle R, Brann DW, Tekmal RR, Vadlamudi RK. 2010. PELP1 is a reader of histone H3 methylation that facilitates oestrogen receptor-alpha target gene activation by regulating lysine demethylase 1 specificity. EMBO Rep 11:438–44.

Nakashima A, Takeuchi H, Imai T, Saito H, Kiyonari H, Abe T, Chen M, Weinstein LS, Yu CR, Storm DR, Nishizumi H, Sakano H. 2013. Agonist-independent GPCR activity regulates anterior-posterior targeting of olfactory sensory neurons. Cell 154:1314–25.

Nakayama J -i., Rice JC, Strahl BD, Allis CD, Grewal SI. 2001. Role of histone H3 lysine 9 methylation in epigenetic control of heterochromatin assembly. Science 292:110–3.

Nef P, Hermans-Borgmeyer I, Artières-Pin H, Beasley L, Dionne VE, Heinemann SF. 1992. Spatial pattern of receptor expression in the olfactory epithelium. Proc Natl Acad Sci U S A 89:8948–8952.

Niederreither K, Fraulob V, Garnier J-M, Chambon P, Dollé P. 2002. Differential expression of retinoic acid-synthesizing (RALDH) enzymes during fetal development and organ differentiation in the mouse. Mech Dev 110:165–71.

Nishizumi H, Kumasaka K, Inoue N, Nakashima A, Sakano H. 2007. Deletion of the core-H region in mice abolishes the expression of three proximal odorant receptor genes in cis. Proc Natl Acad Sci U S A 104:20067–20072.

Norlin EM, Alenius M, Gussing F, Hägglund M, Vedin V, Bohm S. 2001. Evidence for gradients of gene expression correlating with zonal topography of the olfactory sensory map. Mol Cell Neurosci 18:283–95.

Norlin EM, Berghard A. 2001. Spatially restricted expression of regulators of G-protein signaling in primary olfactory neurons. Mol Cell Neurosci 17:872–882.

Pace U, Hanski E, Salomon Y, Lancet D. Odorant-sensitive adenylate cyclase may mediate olfactory reception. Nature 316:255–8.

Packard A, Giel-Moloney M, Leiter A, Schwob JE. 2011a. Progenitor cell capacity of NeuroD1-expressing globose basal cells in the mouse olfactory epithelium. J Comp Neurol 519:3580–96.

Packard A, Schnittke N, Romano R-A, Sinha S, Schwob JE. 2011b. DeltaNp63 regulates stem cell dynamics in the mammalian olfactory epithelium. J Neurosci 31:8748–59.

Paoloni-Giacobino a, Chen H, Antonarakis SE. 1997. Cloning of a novel human neural cell adhesion molecule gene (NCAM2) that maps to chromosome region 21q21 and is potentially involved in Down syndrome. Genomics 43:43–51.

Parmentier M, Libert F, Schurmans S, Schiffmann S, Lefort a, Eggerickx D, Ledent C, Mollereau C, Gérard C, Perret J. 1992. Expression of members of the putative olfactory receptor gene family in mammalian germ cells. Nature 355:453–455.

Peluso CE, Jang W, Dräger UC, Schwob JE, Drager UC, Schwob JE. 2012. Differential expression of components of the retinoic acid signaling pathway in the adult mouse olfactory epithelium. J Comp Neurol 520:3707–3726.
Phillips S, Prat A, Sedic M, Proia T, Wronski A, Mazumdar S, Skibinski A, Shirley SH, Perou CM, Gill G, Gupta PB, Kuperwasser C. 2014. Cell-state transitions regulated by SLUG are critical for tissue regeneration and tumor initiation. Stem Cell Reports 2:633–647.
Pichon AM, Coppin G, Cayeux I, Porcherot C, Sander D, Delplanque S. 2015. Sensitivity of Physiological Emotional Measures to Odors Depends on the Product and the Pleasantness Ranges Used. Front Psychol 6:1–12.
Pinto JM, Wroblewski KE, Kern DW, Schumm LP, McClintock MK. 2014. Olfactory dysfunction predicts 5-year mortality in older adults. PLoS One 9:1–9.
Popova EY, Pinzon-Guzman C, Salzberg AC, Zhang SS, Barnstable CJ. 2015. LSD1-Mediated Demethylation of H3K4me2 Is Required for the Transition from Late Progenitor to Differentiated Mouse Rod Photoreceptor. Mol Neurobiol 1.
Qasba P, Reed RR. 1998. Tissue and zonal-specific expression of an olfactory receptor transgene. J Neurosci 18:227–236.
Qiao Y, Wang R, Yang X, Tang K, Jing N. 2015. Dual roles of histone H3 lysine 9 acetylation in human embryonic stem cell pluripotency and neural differentiation. J Biol Chem 290:2508–2520.
Ramón-Cueto A, Nieto-Sampedro M. 1994. Regeneration into the spinal cord of transected dorsal root axons is promoted by ensheathing glia transplants. Exp Neurol 127:232–244.
Rawal S, Hoffman HJ, Bainbridge KE, Huedo-medina TB, Duffy VB. 2016. Prevalence and Risk Factors of Self-Reported Smell and Taste Alterations: Results from the 2011-2012 U.S. National Health and Nutritions Survey (NHANES). 41:69–76.
Ray SK, Li HJ, Metzger E, Schule R, Leiter a B. 2014. CtBP and Associated LSD1 are Required for Transcriptional Activation by NeuroD1 in Gastrointestinal Endocrine Cells. Mol Cell Biol 34:2308–2317.
Repicky SE, Luetje CW. 2009. Molecular receptive range variation among mouse odorant receptors for aliphatic carboxylic acids. J Neurochem 109:193–202.
Ressler KJ, Sullivan SL, Buck LB. 1993. A zonal organization of odorant receptor gene expression in the olfactory epithelium. Cell 73:597–609.
Ressler KJ, Sullivan SL, Buck LB. 1994. Information coding in the olfactory system: evidence for a stereotyped and highly organized epitope map in the olfactory bulb. Cell 79:1245–55.
Rhinn M, Dollé P. 2012. Retinoic acid signalling during development. Development 139:843–58.
Rice JC, Allis CD. 2001. Histone methylation versus histone acetylation: New insights into epigenetic regulation. Curr Opin Cell Biol 13:263–273.
Rodd AL, Ververis K, Karagiannis TC. 2012. Current and Emerging Therapeutics for Cutaneous T-Cell Lymphoma: Histone Deacetylase Inhibitors. Lymphoma 2012:1–10.
Rodriguez-Gil DJ, Bartel DL, Jaspers AW, Mobley AS, Imamura F, Greer C a. 2015. Odorant receptors regulate the final glomerular coalescence of olfactory sensory

neuron axons. Proc Natl Acad Sci:201417955.
Rodriguez-Gil DJ, Treloar HB, Zhang X, Miller AM, Two A, Iwema C, Firestein SJ, Greer CA. 2010. Chromosomal location-dependent nonstochastic onset of odor receptor expression. J Neurosci 30:10067–10075.
Roskams a J, Cai X, Ronnett G V. 1998. Expression of neuron-specific beta-III tubulin during olfactory neurogenesis in the embryonic and adult rat. Neuroscience 83:191–200.
Rothman A, Feinstein P, Hirota J, Mombaerts P. 2005. The promoter of the mouse odorant receptor gene M71. Mol Cell Neurosci 28:535–46.
Rui K, Zhang Z, Tian J, Lin X, Wang X, Ma J, Tang X, Xu H, Lu L, Wang S. 2015. Olfactory ecto-mesenchymal stem cells possess immunoregulatory function and suppress autoimmune arthritis. Cell Mol Immunol:1–8.
Sáez JE, Gómez AV, Barrios ÁP, Parada GE, Galdames L, González M, Andrés ME. 2015. Decreased expression of CoREST1 and CoREST2 together with LSD1 and HDAC1/2 during neuronal differentiation. PLoS One 10:1–16.
Saito H, Chi Q, Zhuang H, Matsunami H, Mainland JD. 2009. Odor coding by a Mammalian receptor repertoire. Sci Signal 2:ra9.
Saleque S, Kim J, Rooke HM, Orkin SH. 2007. Epigenetic Regulation of Hematopoietic Differentiation by Gfi-1 and Gfi-1b Is Mediated by the Cofactors CoREST and LSD1. Mol Cell 27:562–572.
Salic A, Mitchison TJ. 2008. A chemical method for fast and sensitive detection of DNA synthesis in vivo. Proc Natl Acad Sci 105:2415–2420.
Saraiva L, Ibarra-Soria X, Khan M, Omura M, Scialdone A, Mombaerts P, Marioni J, Logan D. 2015. Hierarchical deconstruction of mouse olfactory sensory neurons: from whole mucosa to single-cell RNA-seq. Sci Rep:1–17.
Schisterman EF, Perkins NJ, Liu A, Bondell H. 2005. Optimal cut-point and its corresponding Youden Index to discriminate individuals using pooled blood samples. Epidemiology 16:73–81.
Schnittke N, Herrick DB, Lin B, Peterson J, Coleman JH, Packard AI, Jang W, Schwob JE. 2015. Transcription factor p63 controls the reserve status but not the stemness of horizontal basal cells in the olfactory epithelium. Proc Natl Acad Sci U S A 112:E5068–77.
Scholz P, Kalbe B, Jansen F, Altmueller J, Becker C, Mohrhardt J, Schreiner B, Gisselmann G, Hatt H, Osterloh S. 2016. Transcriptome Analysis of Murine Olfactory Sensory Neurons during Development Using Single Cell RNA-Seq. Chem Senses 00:1–11.
Schwartz Levey M, Chikaraishi DM, Kauer JS. 1991. Characterization of potential precursor populations in the mouse olfactory epithelium using immunocytochemistry and autoradiography. J Neurosci 11:3556–64.
Schwarzenbacher K, Fleischer J, Breer H, Conzelmann S. 2004. Expression of olfactory receptors in the cribriform mesenchyme during prenatal development. Gene Expr Patterns 4:543–552.
Schwob JE, Gottlieb DI. 1986. The primary olfactory projection has two chemically distinct zones. J Neurosci 6:3393–404.
Schwob JE, Gottlieb DI. 1988. Purification and characterization of an antigen that is

spatially segregated in the primary olfactory projection. J Neurosci 8:3470–80.
Schwob JE, Huard JM, Luskin MB, Youngentob SL. 1994. Retroviral lineage studies of the rat olfactory epithelium. Chem Senses 19:671–82.
Schwob JE, Mieleszko E, Stasky A. 1992. Olfactory Olfactory Sensory Neurons Are Trophically Dependent on the Bulb for Their Prolonged Survival. J Neurosci 12:3896–3919.
Schwob JE, Youngentob SL, Mezza RC. 1995. Reconstitution of the rat olfactory epithelium after methyl bromide-induced lesion. J Comp Neurol 359:15–37.
Schwob JE, Youngentob SL, Ring G, Iwema CL, Mezza RC. 1999. Reinnervation of the rat olfactory bulb after methyl bromide-induced lesion: timing and extent of reinnervation. J Comp Neurol 412:439–57.
Scolnick JA, Cui K, Duggan CD, Xuan S, Yuan X bing, Efstratiadis A, Ngai J. 2008. Role of IGF Signaling in Olfactory Sensory Map Formation and Axon Guidance. Neuron 57:847–857.
Serizawa S, Ishii T, Nakatani H, Tsuboi A, Nagawa F, Asano M, Sudo K, Sakagami J, Sakano H, Ijiri T, Matsuda Y, Suzuki M, Yamamori T, Iwakura Y, Sakano H. 2000. Mutually exclusive expression of odorant receptor transgenes. Nat Neurosci 3:687–93.
Serizawa S, Miyamichi K, Nakatani H, Suzuki M, Saito M, Yoshihara Y, Sakano H. 2003. Negative feedback regulation ensures the one receptor-one olfactory neuron rule in mouse. Science 302:2088–94.
Shi Y, Lan F, Matson C, Mulligan P, Whetstine JR, Cole PA, Casero RA, Shi Y. 2004. Histone demethylation mediated by the nuclear amine oxidase homolog LSD1. Cell 119:941–953.
Shi Y-JJY, Matson C, Lan F, Iwase S, Baba T, Shi Y-JJY. 2005. Regulation of LSD1 histone demethylase activity by its associated factors. Mol Cell 19:857–864.
Shi Y. 2007. Histone lysine demethylases: emerging roles in development, physiology and disease. Nat Rev Genet 8:829–33.
Shou J, Murray RC, Rim PC, Calof AL. 2000. Opposing effects of bone morphogenetic proteins on neuron production and survival in the olfactory receptor neuron lineage. Development 127:5403–5413.
Shykind BM, Rohani SC, O'Donnell S, Nemes A, Mendelsohn M, Sun Y, Axel R, Barnea G. 2004. Gene switching and the stability of odorant receptor gene choice. Cell 117:801–15.
Sklar PB, Anholt RR, Snyder SH. 1986. The odorant-sensitive adenylate cyclase of olfactory receptor cells. Differential stimulation by distinct classes of odorants. J Biol Chem 261:15538–43.
Smart IH. 1971. Location and orientation of mitotic figures in the developing mouse olfactory epithelium. J Anat 109:243–51.
Sosulski DL, Lissitsyna Bloom M, Cutforth T, Axel R, Datta SR, Bloom ML, Cutforth T, Axel R, Datta SR. 2011. Distinct representations of olfactory information in different cortical centres. Nature 472:213–6.
Stanger BZ. 2015. Cellular homeostasis and repair in the mammalian liver. Annu Rev Physiol 77:179–200.
Strahl BD, Allis CD. 2000. The language of covalent histone modifications. Nature

403:41–5.
Strahl BD, Ohba R, Cook RG, Allis CD. 1999. Methylation of histone H3 at lysine 4 is highly conserved and correlates with transcriptionally active nuclei in Tetrahymena. Proc Natl Acad Sci 96:14967–14972.
Strotmann J, Wanner I, Helfrich T, Beck A, Breer H. 1994. Rostro-caudal patterning of receptor-expressing olfactory neurones in the rat nasal cavity. Cell Tissue Res 278:11–20.
Sullivan SL, Bohm S, Ressler KJ, Horowitz LF, Buck LB. 1995. Target-independent pattern specification in the olfactory epithelium. Neuron 15:779–89.
Sun G, Alzayady K, Stewart R, Ye P, Yang S, Li W, Shi Y. 2010. Histone demethylase LSD1 regulates neural stem cell proliferation. Mol Cell Biol 30:1997–2005.
Suzuki Y, Takeda M, Farbman AI. 1996. Supporting cells as phagocytes in the olfactory epithelium after bulbectomy. J Comp Neurol 376:509–17.
Suzuki Y, Takeda M. 1991. Keratins in the developing olfactory epithelia. 59:171–178.
Takahashi K, Tanabe K, Ohnuki M, Narita M, Ichisaka T, Tomoda K, Yamanaka S. 2007. Induction of Pluripotent Stem Cells from Adult Human Fibroblasts by Defined Factors. Cell 131:861–872.
Takeuchi H, Inokuchi K, Aoki M, Suto F, Tsuboi A, Matsuda I, Suzuki M, Aiba A, Serizawa S, Yoshihara Y, Fujisawa H, Sakano H. 2010. Sequential arrival and graded secretion of Sema3F by olfactory neuron axons specify map topography at the bulb. Cell 141:1056–1067.
Tan L, Li Q, Xie XS. 2015. Olfactory sensory neurons transiently express multiple olfactory receptors during development. Mol Syst Biol 11:844.
Tan L, Zong C, Xie XS. 2013. Rare event of histone demethylation can initiate singular gene expression of olfactory receptors. Proc Natl Acad Sci 110:21148–21152.
Tata PR, Mou H, Pardo-Saganta A, Zhao R, Prabhu M, Law BM, Vinarsky V, Cho JL, Breton S, Sahay A, Medoff BD, Rajagopal J. 2013. Dedifferentiation of committed epithelial cells into stem cells in vivo. Nature 503:218–23.
Tetteh PW, Basak O, Farin HF, Wiebrands K, Kretzschmar K, Begthel H, van den Born M, Korving J, de Sauvage F, van Es JH, van Oudenaarden A, Clevers H. 2016. Replacement of Lost Lgr5-Positive Stem Cells through Plasticity of Their Enterocyte-Lineage Daughters. Cell Stem Cell 18:203–213.
Thornton-Manning JR, Nikula KJ, Hotchkiss JA, Avila KJ, Rohrbacher KD, Ding X, Dahl AR. 1997. Nasal cytochrome P450 2A: identification, regional localization, and metabolic activity toward hexamethylphosphoramide, a known nasal carcinogen. Toxicol Appl Pharmacol 142:22–30.
Tickle C, Alberts B, Wolpert L, Lee J. 1982. Local application of retinoic acid to the limb bond mimics the action of the polarizing region. Nature:564–6.
Tirindelli R, Dibattista M, Pifferi S, Menini A. 2009. From pheromones to behavior. Physiol Rev 89:921–956.
Treloar HB, Feinstein P, Mombaerts P, Greer C a. 2002. Specificity of glomerular targeting by olfactory sensory axons. J Neurosci 22:2469–2477.
Treloar HB, Gabeau D, Yoshihara Y, Mori K, Greer CA. 2003. Inverse expression of olfactory cell adhesion molecule in a subset of olfactory axons and a subset of mitral/tufted cells in the developing rat main olfactory bulb. J Comp Neurol

458:389–403.
Treloar HB, Miller AM, Ray A, Greer CA. 2010. Development of the Olfactory System. CRC Press/Taylor & Francis.
Treloar HB, Purcell a L, Greer C a. 1999. Glomerular formation in the developing rat olfactory bulb. J Comp Neurol 413:289–304.
Tsai L, Barnea G. 2014. A critical period defined by axon-targeting mechanisms in the murine olfactory bulb. Science 344:197–200.
Tsuboi A, Miyazaki T, Imai T, Sakano H. 2006. Olfactory sensory neurons expressing class I odorant receptors converge their axons on an antero-dorsal domain of the olfactory bulb in the mouse. Eur J Neurosci 23:1436–1444.
Valverde F, Santacana M, Heredia M. 1992. Formation of an olfactory glomerulus: Morphological aspects of development and organization. Neuroscience 49:255–275.
Vanderhaeghen P, Schurmans S, Vassart G, Parmentier M. 1997. Specific repertoire of olfactory receptor genes in the male germ cells of several mammalian species. Genomics 39:239–246.
Vassalli A, Feinstein P, Mombaerts P. 2011. Homeodomain binding motifs modulate the probability of odorant receptor gene choice in transgenic mice. Mol Cell Neurosci 46:381–396.
Vassalli A, Rothman A, Feinstein P, Zapotocky M, Mombaerts P. 2002. Minigenes impart odorant receptor-specific axon guidance in the olfactory bulb. Neuron 35:681–96.
Vassar R, Chao SK, Sitcheran R, Nuñez JM, Vosshall LB, Axel R. 1994. Topographic organization of sensory projections to the olfactory bulb. Cell 79:981–91.
Vassar R, Ngai J, Axel R. 1993. Spatial Segregation of Odorant Receptor Expression in the Mammalian Olfactory Epithelium. Cell 74:309–18.
Verhaagen J, Oestreicher a B, Gispen WH, Margolis FL. 1989. The expression of the growth associated protein B50/GAP43 in the olfactory system of neonatal and adult rats. J Neurosci 9:683–91.
Vincent AJ, Taylor JM, Choi-Lundberg DL, West AK, Chuah MI. 2005. Genetic expression profile of olfactory ensheathing cells is distinct from that of Schwann cells and astrocytes. Glia 51:132–147.
Voigt JM, Guengerich FP, Baron J. 1985. Localization of a cytochrome P-450 isozyme (cytochrome P-450 PB-B) and NADPH-cytochrome P-450 reductase in rat nasal mucosa. Cancer Lett 27:241–7.
Vukovic J, Blomster L V, Chinnery HR, Weninger W, Jung S, McMenamin PG, Ruitenberg MJ. 2010. Bone marrow chimeric mice reveal a role for CX3CR1 in maintenance of the monocyte-derived cell population in the olfactory neuroepithelium. J Leukoc Biol 88:645–54.
Walz A, Mombaerts P, Greer CA, Treloar HB. 2006. Disrupted compartmental organization of axons and dendrites within olfactory glomeruli of mice deficient in the olfactory cell adhesion molecule, OCAM. Mol Cell Neurosci 32:1–14.
Wang F, Nemes a, Mendelsohn M, Axel R. 1998. Odorant receptors govern the formation of a precise topographic map. Cell 93:47–60.
Wang J, Hevi S, Kurash JK, Lei H, Gay F, Bajko J, Su H, Sun W, Chang H, Xu G, Gaudet F, Li E, Chen T. 2009. The lysine demethylase LSD1 (KDM1) is required for maintenance of global DNA methylation. Nat Genet 41:125–9.

Wang J, Scully K, Zhu X, Cai L, Zhang J, Prefontaine GG, Krones A, Ohgi K a, Zhu P, Garcia-Bassets I, Liu F, Taylor H, Lozach J, Jayes FL, Korach KS, Glass CK, Fu X-D, Rosenfeld MG. 2007. Opposing LSD1 complexes function in developmental gene activation and repression programmes. Nature 446:882–7.

Wang X, Penzes P, Napoli JL, Chem JB, Wang X, Penzes P, Napoli JL. 1996. Cloning of a cDNA Encoding an Aldehyde Dehydrogenase and Its Expression in Escherichia coli. Biochem J 271:16288–16293.

Wang Y, Wu Q, Yang P, Wang C, Liu J, Ding W, Liu W, Bai Y, Yang Y, Wang H, Gao S, Wang X. 2016. LSD1 co-repressor Rcor2 orchestrates neurogenesis in the developing mouse brain. Nat Commun 7:10481.

Weiler E, Farbman AI. 2003. The septal organ of the rat during postnatal development. Chem Senses 28:581–593.

Whitesides J, Hall M, Anchan R, LaMantia AS. 1998. Retinoid signaling distinguishes a subpopulation of olfactory receptor neurons in the developing and adult mouse. J Comp Neurol 394:445–61.

Winther M, Berezin V, Walmod PS. 2012. NCAM2/OCAM/RNCAM: Cell adhesion molecule with a role in neuronal compartmentalization. Int J Biochem Cell Biol 44:441–446.

Wong ST, Trinh K, Hacker B, Chan GC, Lowe G, Gaggar a, Xia Z, Gold GH, Storm DR. 2000. Disruption of the type III adenylyl cyclase gene leads to peripheral and behavioral anosmia in transgenic mice. Neuron 27:487–497.

Yan H-J, Zhou S-Y, Li Y, Zhang H, Deng C-Y, Qi H, Li F-R. 2016. The effects of LSD1 inhibition on self-renewal and differentiation of human induced pluripotent stem cells. Exp Cell Res 340:227–237.

Yang J, Tang Y, Liu H, Guo F, Ni J, Le W. 2014. Suppression of histone deacetylation promotes the differentiation of human pluripotent stem cells towards neural progenitor cells. BMC Biol 12:95.

Yang J-Y, Wang Q, Wang W, Zeng L-F. 2015. Histone deacetylases and cardiovascular cell lineage commitment. World J Stem Cells 7:852–8.

Yanger K, Zong Y, Maggs LR, Shapira SN, Maddipati R, Aiello NM, Thung SN, Wells RG, Greenbaum LE, Stanger BZ. 2013a. Robust cellular reprogramming occurs spontaneously during liver regeneration. Genes Dev.

Yanger K, Zong Y, Maggs LR, Shapira SN, Maddipati R, Aiello NM, Thung SN, Wells RG, Greenbaum LE, Stanger BZ. 2013b. Robust cellular reprogramming occurs spontaneously during liver regeneration. Genes Dev 27:719–24.

Yoshihara Y, Kawasaki M, Tamada A, Fujita H, Hayashi H, Kagamiyama H, Mori K. 1997. OCAM : A New Member of the Neural Cell Adhesion Molecule Family Related to Zone-to-Zone Projection of Olfactory and Vomeronasal Axons. 17:5830–5842.

Youden WJ. 1950. Index for rating diagnostic tests. Cancer 3:32–35.

Zhang X, Firestein S. 2002. The olfactory receptor gene superfamily of the mouse. Nat Neurosci 5:124–133.

Zhang X, Lu F, Wang J, Yin F, Xu Z, Qi D, Wu X, Cao Y, Liang W, Liu Y, Sun H, Ye T, Zhang H. 2013. Pluripotent Stem Cell Protein Sox2 Confers Sensitivity to LSD1 Inhibition in Cancer Cells. Cell Rep 5:445–457.

Zhang X, Zhang X, Firestein S. 2007a. Comparative genomics of odorant and pheromone receptor genes in rodents. Genomics 89:441–50.
Zhang Y, Reinberg D. 2001. Transcription regulation by histone methylation: Interplay between different covalent modifications of the core histone tails. Genes Dev 15:2343–2360.
Zhang YQ, Breer H, Strotmann J. 2007b. Promotor elements governing the clustered expression pattern of odorant receptor genes. Mol Cell Neurosci 36:95–107.
Zhao D, McCaffery P, Ivins KJ, Neve RL, Hogan P, Chin WW, Dräger UC. 1996. Molecular identification of a major retinoic-acid-synthesizing enzyme, a retinaldehyde-specific dehydrogenase. Eur J Biochem 240:15–22.
Zhao H, Ivic L, Otaki JM, Hashimoto M, Mikoshiba K, Firestein S. 1998. Functional expression of a mammalian odorant receptor. Science 279:237–42.
Zhao R, Fallon TR, Saladi SV, Pardo-Saganta A, Villoria J, Mou H, Vinarsky V, Gonzalez-Celeiro M, Nunna N, Hariri LP, Camargo F, Ellisen LW, Rajagopal J. 2014. Yap Tunes Airway Epithelial Size and Architecture by Regulating the Identity, Maintenance, and Self-Renewal of Stem Cells. Dev Cell 30:151–165.
Zhao S, Tian H, Ma L, Yuan Y, Yu CR, Ma M. 2013a. Activity-Dependent Modulation of Odorant Receptor Gene Expression in the Mouse Olfactory Epithelium. PLoS One 8:1–9.
Zhao ZK, Dong P, Gu J, Chen L, Zhuang M, Lu WJ, Wang DR, Liu Y Bin. 2013b. Overexpression of LSD1 in hepatocellular carcinoma: A latent target for the diagnosis and therapy of hepatoma. Tumor Biol 34:173–180.
Zou J, Wang W, Pan Y-W, Lu S, Xia Z. 2015. Methods to Measure Olfactory Behavior in Mice. Curr Protoc Toxicol:11.18.1–11.18.21.
Zozulya S, Echeverri F, Nguyen T. 2001. The human olfactory receptor repertoire. Genome Biol 2.